



UvA-DARE (Digital Academic Repository)

Analytical and statistical approaches in the characterization of synthetic polymers

Dimzon, I.K.

Publication date

2015

Document Version

Final published version

[Link to publication](#)

Citation for published version (APA):

Dimzon, I. K. (2015). *Analytical and statistical approaches in the characterization of synthetic polymers*. [Thesis, fully internal, Universiteit van Amsterdam].

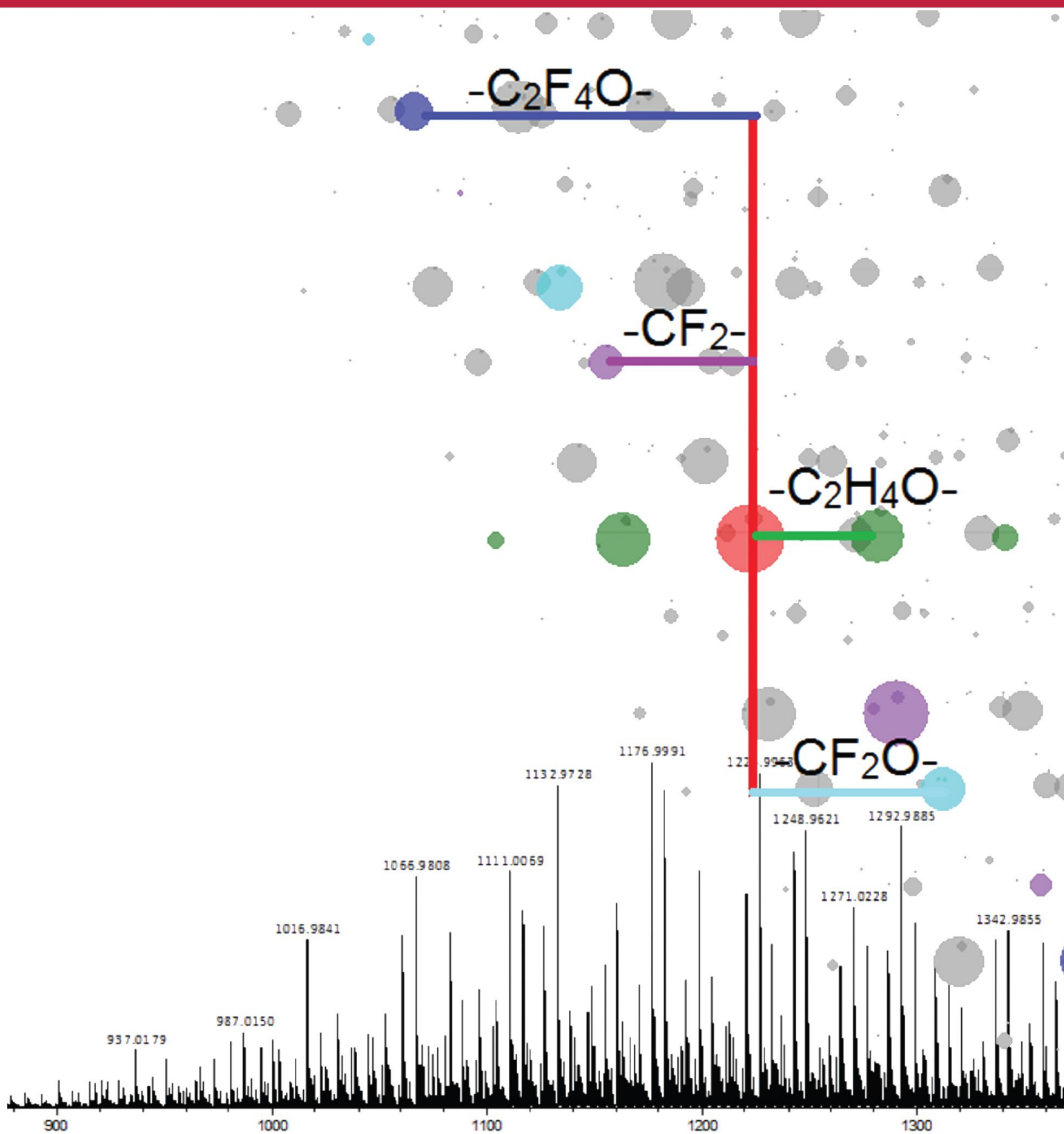
General rights

It is not permitted to download or to forward/distribute the text or part of it without the consent of the author(s) and/or copyright holder(s), other than for strictly personal, individual use, unless the work is under an open content license (like Creative Commons).

Disclaimer/Complaints regulations

If you believe that digital publication of certain material infringes any of your rights or (privacy) interests, please let the Library know, stating your reasons. In case of a legitimate complaint, the Library will make the material inaccessible and/or remove it from the website. Please Ask the Library: <https://uba.uva.nl/en/contact>, or a letter to: Library of the University of Amsterdam, Secretariat, Singel 425, 1012 WP Amsterdam, The Netherlands. You will be contacted as soon as possible.

Analytical and Statistical Approaches in the Characterization of Synthetic Polymers



Analytical and Statistical Approaches in the Characterization of Synthetic Polymers

Academisch Proefschrift

ter verkrijging van de graad van doctor
aan de Universiteit van Amsterdam
of gezag van de Rector Magnificus
prof. dr. D. C. van den Boom

ten overstaan van een door het college voor promoties
ingestelde commissie, in het openbaar te verdedigen in de
Agnietenkapel op vrijdag 22 mei 2015, te 10:00 uur

door

Ian Ken Dimzon

geboren te Iloilo, de Filippijnen

Promotiecommissie

Promotor: prof. dr. W.P. de Voogt
 prof. dr. T.P. Knepper

Overige leden: prof. dr. C.G. de Koster
 prof. dr. ir. P.J. Schoenmakers
 prof. dr. T. Hofe
 dr. J.R. Parsons
 dr. P.E.G. Leonards

Faculteit der Natuurwetenschappen, Wiskunde en Informatica

Cover by Geoffrey Matthew Tan

Printed by GVO - Ede, Netherlands

Analytical and statistical approaches in the characterization of synthetic polymers

by Ian Ken Dimzon

Proefschrift Universiteit van Amsterdam, FNWI, IBED, 2015

ISBN 978-94-91407-17-8

Copyright © 2015

This research work was done at the Institute for Analytical Research, Hochschule Fresenius in Idstein, Germany and at the Institute for Biodiversity and Ecosystem Dynamics, University of Amsterdam, in Amsterdam, The Netherlands. The thesis work was made possible through the project Environmental Chemoinformatics (ECO, ITN No. 238701) long term fellowship funded by the European Commission – Marie Curie Action – Initial Training Network. Also, the German Federal Environmental Agency (Umweltbundesamt, UBA) through the project PFAS Precursor Project (FKZ 3712 65 415/01) contributed to the accomplishment of some parts of this research. Certmedica GmbH is gratefully recognized for providing the chitosans and for the technical support.

To my parents, Terry and Delfin
and
To my siblings, Lester and Teresa

CONTENTS

List of Figures	10
List of Tables	13
Chapter 1. General Introduction	14
Polymers	14
Polymer Characterization	18
Objectives of this Research Work.....	22
Chapter 2. Characterization of Chitosan	25
A. Degree of Deacetylation of Chitosan by Infrared Spectroscopy and Partial Least Squares.....	25
Introduction	26
Materials and Methods	28
<i>Chitosan Samples and Reagents</i>	28
<i>Infrared Analysis</i>	28
<i>Partial Least Squares Modeling</i>	28
<i>Potentiometric Titration</i>	29
<i>Statistical Evaluation of Results</i>	29
Results and Discussion	30
<i>Infrared Spectrum of Chitosan</i>	30
<i>Partial Least Squares Modeling</i>	30
<i>Internal Validation</i>	34
<i>External Validation and Comparison to the Infrared-Absorbance Ratio Method</i>	35
<i>Robustness of the Infrared-Partial Least Squares Method</i>	38
Conclusion	38
B. The Interaction of Chitosan and Olive Oil: Effects of Degree of Deacetylation and Degree of Polymerization	39
Introduction	40
Materials and Methods	42
<i>Chitosan Samples and Reagents</i>	42
<i>Determination of Weight-Average Degree of Polymerization (DP_w)</i>	43
<i>Determination of Degree of Deacetylation</i>	44
<i>Oil-Binding Test</i>	44
<i>Statistical Analysis</i>	44
Results and Discussion	45
<i>Degree of Deacetylation and Weight-Average Degree of Polymerization of chitosan</i>	45
<i>Oil-Binding Capacity of Chitosan</i>	48
<i>Evaluation of the Results using Partial Least Squares</i>	50
<i>Interaction of Chitosan and Olive Oil</i>	52

Conclusion	56
Chapter 3. Review: Mass Spectrometry of Polymers	57
Introduction	58
Mass Spectrometry of Large Molecules.....	60
Matrix-Assisted Laser Desorption/Ionization Process	62
Sample Preparation.....	66
Hyphenation with Time-of-Flight Mass Analyzer	69
Matrix-Assisted Laser Desorption/Ionization Mass Spectrum	70
Electrospray Ionization – Quadrupole Mass Spectrometry as an Alternative Method.....	71
Chromatographic Separation prior to Mass Spectrometry.....	75
Future of MALDI-TOF in polymer analysis: Fate and Degradation Studies	77
Chapter 4. Characterization of Chitosan Oligosaccharide.....	80
Introduction	81
Methodology.....	82
<i>Sample and Reagents.....</i>	<i>82</i>
<i>Experimental Design.....</i>	<i>83</i>
<i>Matrix and Sample Spot Preparation Techniques</i>	<i>83</i>
<i>Matrix-Assisted Laser Desorption/Ionization-Time-of-Flight Analysis</i>	<i>84</i>
<i>Electrospray ionization - Quadrupole Analysis</i>	<i>84</i>
<i>Size-Exclusion Chromatography</i>	<i>84</i>
Results and discussion.....	84
<i>Choice of Matrix.....</i>	<i>84</i>
<i>Sample Preparation</i>	<i>85</i>
<i>Mass Spectrum.....</i>	<i>89</i>
<i>Size-Exclusion Chromatography</i>	<i>94</i>
Conclusion	96
Chapter 5. Characterization of 3-Aminopropyl Oligosilsesquioxane	97
Introduction	98
Methodology.....	99
<i>Silsesquioxane formulation</i>	<i>99</i>
<i>ESI-Q MS of the oligosilsesquioxane formulation.....</i>	<i>100</i>
<i>MALDI-ToF MS of the oligosilsesquioxane formulation</i>	<i>100</i>
<i>Fractionation of the oligosilsesquioxane.....</i>	<i>100</i>
<i>ICP-OES analysis of the fractions</i>	<i>101</i>
<i>Determination of the MWD of the oligosilsesquioxane formulation</i>	<i>101</i>
Results and Discussion	101
<i>MS of the 3-aminopropyl oligosilsesquioxane prior to fractionation</i>	<i>101</i>
<i>Fractionation of the 3-aminopropyl oligosilsesquioxane formulation.....</i>	<i>107</i>
<i>Determination of the silsesquioxane molar concentration by ICP-OES</i>	<i>108</i>

<i>Determination of the MWD of the oligosilsesquioxane by HPLC ESI-Q MS</i>	109
Conclusion	113
Chapter 6. High Resolution Mass Spectrometry of Polyfluorinated Polyether – based Formulation 114	
Introduction	115
Materials and Methods	118
<i>Unknown PFPE-based formulation and chemicals</i>	118
<i>High resolution MS</i>	118
<i>MS data processing and Kendrick mass defect analysis</i>	119
<i>Tandem Mass Spectrometry</i>	119
Results and Discussion	120
<i>MS Analysis of PFPE-based formulation</i>	120
<i>Analysis of Mass Defects</i>	121
<i>Tandem Mass Spectrometry</i>	126
<i>Reversed-phase HPLC</i>	127
<i>Comparison of the derived chemical structure to the published technical data</i>	129
<i>Chemical structure and physico-chemical properties of PFPE-based formulations</i>	129
Conclusion	130
Chapter 7. Synthesis and Outlook	132
Synthesis.....	132
Outlook.....	137
Summary	140
Samenvatting	142
Reference List	144
Acknowledgements	157

LIST OF FIGURES

Figure 1.1. Types of copolymerization: A. Random; B. Alternating; C. Block; and D. Graft .	15
Figure 2.1. IR absorption spectrum of a training set chitosan with 85% %DD. The assignment of absorption bands are based on literature data (Pearson, Marchessault et al. 1960; Shigemasa, Matsuura et al. 1996; Duarte, Ferreira et al. 2002). The baselines used to correct absorbances in this study are also shown (b1 to b3).....	31
Figure 2.2. The spectral region 1500 – 1800 cm ⁻¹ after baseline correction and data pre-treatments: A. normalized against highest absorbance; B. Normalized against the absorbance at 1660 cm ⁻¹ ; and C. normalized against the absorbance at 1600 cm ⁻¹ ..	32
Figure 2.3. x-loadings plot of the components of PLS Model A.....	36
Figure 2.4. Calculated %bias of the IR-PLS and IR area ratio methods compared to potentiometric titration.....	36
Figure 2.5. FT-IR absorption spectra (normalized to relative to the highest absorbance) at the wavenumber region 1800 to 1500 cm ⁻¹ of chitosan samples with known degree of deacetylation (73.6%, 94.3% and 84.7%) and of a chitosan sample with unknown degree of deacetylation (U2). The spectra were corrected for the baseline drawn from 1800 to 1500 cm ⁻¹ and were normalized relative to the highest corrected absorbance.	46
Figure 2.6. External validation of the partial least squares (PLS) model to predict the degree of deacetylation (DD) of chitosan. The dotted line represents: certified DD = PLS-predicted DD.....	47
Figure 2.7. Relationship between weight-average degree of polymerization (DP _w), degree of deacetylation (DD) and oil-binding capacity. Shown are: A. 3D-graph showing the combined effects of DP _w and DD on the oil-binding capacity; and B. the 2D graph representing the projection on the DD versus oil-binding capacity plane. The error bars represent ± 1 standard deviation.....	51
Figure 2.8. External validation of the partial least square (PLS) model to predict the oil-binding capacity of chitosan. The dotted line represents: experimental values = PLS-predicted values.....	52
Figure 2.9. Interaction of chitosan with olive oil. Shown is a representative triacylglyceride of olive oil with an oleic acid and two other fatty acids represented by R. A. Chitosan interacts directly with olive oil through the N-acetyl-D-glucosamine monomers; and B. Chitosan interacts indirectly with olive oil with the aid of free fatty acid (oleic acid) that is electrostatically bound to the amine group of the D-glucosamine monomer.....	55
Figure 3.1. Schematics of MALDI with reflector mode TOF MS.....	62
Figure 3.2. Mass Spectra of PEG 1000: a.) positive-mode MALDI-TOF using 2,5-DHB as matrix; b.) positive-mode ESI-q at declustering potential of 100 V.....	73
Figure 3.3. Positive-ESI-q mass spectrum of PEG at declustering potential of 40, 100	75
Figure 3.4. MALDI-TOF Spectra (positive ion mode) of PVP in FBBR after a) 0 h; b) 5 h; c) 8 days; and d) 16 days. (Trimpin, Eichhorn et al. 2001)	78
Figure 3.5. MALDI-TOF mass spectra (positive ion mode) of PEG in artificial seawater media from a) day 1 and b) day 14 sample. (Bernhard, Eubeler et al. 2008).....	79
Figure 4.1. Magnified view of the COS spots prepared using different spot preparation techniques and solvent system. The shown scale is based on rough estimates.....	87

Figure 4.2. Comparison of MALDI-TOF Spectra (positive ion mode) of COS obtained using different spot preparation techniques. The scaling was maintained constant to allow comparison of peak intensities.	88
Figure 4.3. Positive ion mode MALDI mass spectrum of COS with 2,5-DHB as matrix prepared in 1:5 ACN:H ₂ O solvent system. The sample spot was prepared using VD technique, 0.15 M NaCl is present.	89
Figure 4.4. Other ions in the positive ion mode MALDI mass spectrum of COS with 2,5-DHB as matrix at the region 600 < m/z < 1100.	90
Figure 4.5. Positive ion mode MALDI mass spectrum of COS with 2,5-DHB as matrix at the region 1500 < m/z < 3000.	91
Figure 4.6. Positive ion mode MALDI mass spectrum of COS with 2,5-DHB as matrix prepared in 1:1 MeOH:Milli-Q H ₂ O solvent system. The sample spot was prepared using VD technique. A. 0.15 M KCl and B. 0.15 M LiCl were added.	92
Figure 4.7. Positive ion mode ESI-Q mass spectrum of COS	93
Figure 4.8. Positive ion mode ESI-Q mass spectrum of COS in the region 230 < m/z < 35093	93
Figure 4.9. Size-exclusion chromatogram of COS in Novema 100 and Novema 1000 dual column with aqueous 0.3 M NaCl, 0.2% trifluoroacetic acid as mobile phase.....	94
Figure 4.10. MALDI-TOF spectra (positive ion mode) of the collected SEC fractions at specified collection times.	95
Figure 5.1. General reaction scheme in the formation of oligosilsesquioxane (n=4) from (3-aminopropyl)triethoxy silane and the formation of a fully condensed polyhedral silsesquioxane or a silene by intramolecular condensation.	103
Figure 5.2. Positive-mode mass spectra of 3-aminopropyl oligosilsesquioxane in methanol: A. ESI-Q at declustering potential of 160 V; and B. MALDI-TOF mass spectrum with 2,5-DHB as matrix. Inserts: Zoomed in region showing the ions with n=6.	104
Figure 5.3. Comparison of the degree of polymerization and degree of intramolecular condensation of the ions generated in: A. ESI and B. MALDI.....	106
Figure 5.4. Positive-mode ESI-Q mass spectra of fractions containing oligosilsesquioxanes of n= 5, 7 and 11 (A-C) respectively. The x represents the charge of the ions.....	108
Figure 5.5. Elution of the oligosilsesquioxane homologues in the C18 column and in the gradient of water and methanol with 5 mM PFHpA.	111
Figure 5.6. Degree of polymerization versus the slope of the calibration curve.....	112
Figure 5.7. MWD of oligosilsesquioxane obtained by HPLC-ESI-Q MS	112
Figure 6.1. Positive-mode QqTOF mass spectrum of the PFPE-based formulation. Insert: Magnified view of the peak with highest intensity	121
Figure 6.2. Molecular weight versus first-order Kendrick mass defect, MD1 (Generated using 'MassDef,'an R source code). The first-order mass transformation was done relative to the -C ₂ H ₄ O- repeating units. The values of the molecular weight used were from the positive-mode ESI-Orbitrap mass spectrum with relative intensities greater than 5%	123
Figure 6.3. First-order (MD1) versus second-order (MD2) Kendrick mass defect (Generated using 'MassDef,'an R source code). The second-order mass transformation was done relative to the -C ₂ F ₄ O- repeating units.....	124
Figure 6.4. Second-order (MD2) versus third-order (MD3) Kendrick mass defect (Generated using the 'MassDef,'an R source code). The third-order mass transformation was done relative to the CF ₂ O repeating units	125

Figure 6.5. A) Base peak chromatogram of the PFPE formulation and the Dissect chromatogram traces; and B) Chromatograms of selected ions that correspond to the indicated chemical formula..... 128

LIST OF TABLES

Table 1.1. Polymers used in this research work, their structure and some relevant chemical properties.....	16
Table 2.1. Performance Characteristics of the PLS models	34
Table 2.2. Comparison of the %DD values obtained by IR (PLS and absorbance ratio) to the %DD obtained by potentiometric titration. The values in parenthesis are the SDs of two trials.	37
Table 2.3. Degree of deacetylation and weight-average degree of polymerization of the chitosan samples. Data for the degree of deacetylation of S1 to S10 were directly lifted from the certificate of analysis while for U1 and U2 were obtained experimentally using FT-IR and partial least squares.	43
Table 2.4. Oil-binding capacity of the chitosan samples.....	49
Table 3.1. Some commonly used matrices for the MALDI of Polymers. The structures shown were drawn using ChemSketch (ACDLabs).	64
Table 3.2. Commonly used sample preparation techniques in MALDI of polymers. ^a	68
Table 4.1. Characterization of the different available matrices for their application to the MALDI-ToF MS analysis of COS.....	85
Table 5.1. Selected ions monitored in the HPLC ESI-Q MS. Aso shown in parenthesis are the degrees of charging (x).	110
Table 7.1. Polymers used in this research work.....	133

Chapter 1. GENERAL INTRODUCTION

Polymers

Polymers represent a broad class of macromolecules with a wide range of uses. Indeed, one would find it hard to imagine today's world without these compounds. Both natural and synthetic polymers are found in a variety of goods including drugs and cosmetics; household commodities; construction, building and electronic supplies; and packaging materials. Synthetic polymers are usually associated with plastic materials but their use is much more extensive. There are many other nontraditional uses of polymers in the industry and in research, for example, as highly surface active materials, unique drug delivery systems (Cammis, Suzuki et al. 1997; Alves and Mano 2008; Prabakaran 2008), biodegradable scaffolds in artificial tissues (Hutmacher 2000; Smith, Liu et al. 2009) and as highly specific stationary phases in chromatography. There are also polymeric nanomaterials (Cammis, Suzuki et al. 1997; Kietzke, Neher et al. 2003; Rao and Geckeler 2011). The growth in polymer science and engineering is driven by three factors: developments in the synthesis; optimization of properties by functionalization, coupling and copolymerization; and by discovery of new monomers.

Polymers are composed of covalently bonded, repeating structural units called monomers. The European Chemicals Agency (ECHA 2012) specifies that a polymer is a "sequence of at least three monomer units". In conventional usage, polymers refer only to the macromolecules with molecular weights greater than 1000 Da (Braun 2005). Oligomers, on the other hand refer to molecules with repeating structural units but with molecular weights less than 1000 Da. Polymers are often polydispersed and could be a mixture of structurally distinct species (Braun 2005). The diversity of the molecules of which polymers exist can be classified according to the influence these differences have on the polymer properties. These classifications which are the fundamental basis of characterization are the molecular weight distribution (MWD) and the chemical structure (Van Krevelen and Te Nijenhuis 2009).

Polymer substances due to the nature of synthesis, are mixtures of molecules that vary in size. The size of the polymer is expressed using average molecular weights. There are different ways to estimate the average molecular weights. The number-average molecular weight (M_n) is calculated based on the molar ratio while the weight-average molecular weight (M_w) is based on the weight ratio of the different species present in the mixture. The average molecular weights, while being useful descriptors of polymers, do not give a complete picture regarding the size of the polymer. The variability in the sizes of the individual species is also another important parameter. The polydispersity index (PDI) is a measure of how variable

the individual sizes of the polymer molecules are, or of the width of the MWD. The PDI is obtained by calculating the ratio of the M_w to M_n and is always greater than unity. The wider the MWD, the greater is the difference between the M_w and M_n , the greater is the PDI.

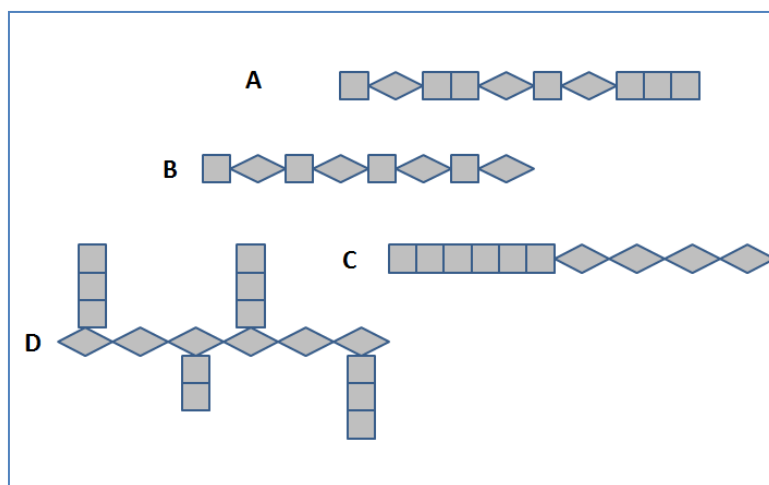


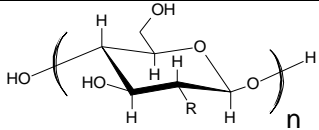
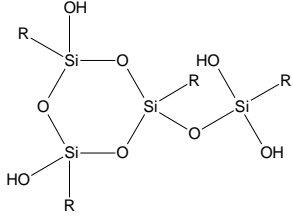
Figure 1.1. *Types of copolymerization: A. Random; B. Alternating; C. Block; and D. Graft*

Polymers are made up of either one (homopolymers) or more (copolymers) types of monomers that are covalently bonded to each other (Figure 1.1). The arrangement of the monomers in a copolymer can be random, alternating (or periodic) or blocked. Graft copolymers can also exist wherein a homopolymer is covalently bonded with one or more homopolymers (with different monomers) as side chain. Polymers can exist either as linear or branched molecules. Most often, extra chemical features like side chains or end groups are added to the polymer basic structure to add some functionality on the substance. Other polymers are cross-linked.

The diversity in the possible size and chemical structure of polymers is responsible for the wide ranging properties these polymers exhibit. This diversity, aside from the large sizes of individual molecules, makes polymers complex to analyze. First, there are many new monomers – some are charged, others have heteroatoms other than N and O, some are perfluorinated. Second, these polymers could be copolymers of two or three types of monomers. Third, the list of possible end groups and side chains has become longer. Lastly, their applications are no longer limited to the traditional use as bulk material.

Chitosan, oligo- and polysiloxanes, and perfluorinated polyethers (PFPE) are some examples of the growing list of widely-used polymers today. These polymers are the subjects of this research work. Table 1.1 highlights the diversity in structural characteristics and chemical properties of these polymers.

Table 1.1. *Polymers used in this research work, their structure and some relevant chemical properties.*

Polymer	Structure	Polymer Type	Chemical Properties
Chitosan/Chitin	 <p>R mostly NH₂: Chitosan R mostly NH(C=O)CH₃: Chitin</p>	Random or block copolymer of D-Glucosamine and N-acetyl-D-glucosamine	It is polycationic in acidic solution. Its solubility in acidic aqueous solution increases with the molar percentage of D-glucosamine.
Oligosilsesquioxane	 <p>R is -CH₂CH₂CH₂NH₂</p>	Homopolymer from (3-aminopropyl)triethoxy silane	It is polycationic in acidic solution. Intramolecular condensation occurs resulting to Si-O-Si bridges and to the formation of Si=C bonds.
Perfluorinated polyether	R-(CF ₂ O) _n -(C ₂ F ₄ O) _m -R ₁	Copolymer of perfluorinated and non-fluorinated blocks	Its composition is complex and diverse. It is soluble in water and in methanol. The fluorinated part renders hydrophobicity and oleophobicity to the molecule.

Chitosan is the deacetylated form of chitin, a natural polymer from the shells and exoskeletons of mollusks, crustaceans, insects and fungi (Kumar, Muzzarelli et al. 2004; Aranaz, Mengibar et al. 2009). Chitosan and chitin are both copolymers of N-acetyl-D-glucosamine and D-glucosamine connected via β -D-(1 \rightarrow 4) glycoside bond. Chitin becomes chitosan when the molar percent of the D-glucosamine is equal or greater than 60% (Aiba 1992). Chitosan is a unique biodegradable biopolymer that is soluble in acidic aqueous solutions (Sannan, Kurita et al. 1976). It has a wide range of modern applications especially in the biomedical field. It was shown in many studies that chitosan has unique biological properties including biodegradability, biocompatibility, hemostatic, analgesic and antimicrobial properties (Aranaz, Mengibar et al. 2009).

Chitosan has been used since the last five decades. Until now, chitosan is still subject to many new researches. What makes it important is its potential for functionalization, mostly at the -NH₂ functional group, by quarternization or by reaction with aldehydes via reductive amination (Rinaudo 2006). This is being done to further improve its aqueous solubility and to expand its uses (Alves and Mano 2008). Chitosan derivatives are found in medical and environmental applications (Alves and Mano 2008) such as in hydrogel drug carriers for the controlled release of difficult-to-release drugs (Prabaharan 2008), as a component in artificial

tissues (Riva, Ragelle et al. 2011), and as a metal sequestration agent in environmental clean-up (Miretzky and Cirelli 2009).

Polysiloxanes and polymeric silsesquioxanes refer in general to the polymers whose backbone structure is an alternating oxygen and silicon atom (Rahimi and Shokrolahi 2001). Polysiloxanes have repeat units of $[R_2SiO_2]$ whereas silsesquioxanes have $[RSiO_{2/3}]$ (Wallace, Guttman et al. 2000). These silicon-containing polymers are important surface active compounds. Polymeric silsesquioxanes are more thermally stable and have higher chemical resistance compared to the polysiloxanes because of the three-fold coordination of Si with O. One important parameter in silsesquioxanes is the degree of intramolecular condensation. Intramolecular condensation creates more Si-O-Si bridges within the molecule as opposed to unreacted silanols (Si-OH). This formation of Si-O-Si bridges creates an added stability within a molecule. The different R groups attached to the siloxanes can vary the surface tension reduction properties of the surfactant. The R groups that are charged, for example those that contain quarternary ammonium groups can reduce the surface tension of water at the critical micelle concentration. (Schmaucks, Sonnek et al. 1992).

PFPEs are also an important group of modern polymers with unique applications. These polymers have high thermal and chemical stabilities; and low surface energies, dielectric constants and vapor pressures (Karis and Jhon 1998; Howell, Shtarov et al. 2011). Because of their low wettabilities and coefficients of friction (Pilati, Toselli et al. 1992), PFPEs are widely used as high performance lubricating oils and greases. The surface properties of PFPEs are dependent on molecular structure and degree of polymerization (Karis and Jhon 1998). The different PFPE formulations in the market today have their backbone structures synthesized using manufacturer-specific processes based on a combination of techniques like anionic polymerization, hydrolysis, exhaustive fluorination and photo-induced oxidation polymerization from raw materials such as 2,2,3-trifluoro-3-(trifluoromethyl)oxirane, 2,2,3,3-tetrafluorooxetane, tetrafluoroethene and/or hexafluoropropene (Howell, Friesen et al. 2007; Howell, Shtarov et al. 2011). The differences in the synthetic processes results in a wide range of complex chemical structures of the PFPE base polymers. The unmodified PFPE bases can have $-CF_2O-$, $-C_2F_4O-$, $-C_3F_6O-$ or a random combination of these repeating units with molecular weights ranging from 500 to 15,000 Da (Howell, Shtarov et al. 2011).

Chitosan, silsesquioxanes and PFPEs have promising applications and are representative models of the various kinds of polymers today. The unique applications of these polymers result from the chemical nature of the polymers themselves. Slight alterations in the chemical structure of these polymers can lead to significant changes in their properties leading to failure in intended applications. This therefore calls for a development of

necessary MWD determination and chemical characterization tools apart from those that are currently being used. This task is an analytical challenge.

Polymer Characterization

Polymer characterization can be classified either as chemical or physical characterization. The traditional methods are often straightforward, standard and have general application. Chemical characterization involves studying the chemical structure of the polymers. Infrared (IR) Spectroscopy is the fastest and most widely used technique in identifying the monomer composition of the polymer. Each functional group in a repeating unit will have characteristic absorption bands. Infrared spectral libraries contain the IR spectra of the common homopolymers as well as block copolymers. In a standard IR analysis, the polymers are first extracted and dissolved using organic solvents like dichloromethane and chloroform. The solution is then spotted into a KBr plate and left to dry, then analyzed. The obtained IR spectrum is then compared to the ones in the IR spectral library. For polymeric films, direct transmission, attenuated total reflectance (ATR-IR) and reflection absorption (RA-IR) methods are used.

The IR method has many limitations. First, as the monomer composition becomes more complex, the less useful the IR analysis becomes. The presence of a functional group detected by the IR method does not necessarily translate unequivocally to a specific monomer. Second, IR is challenging when used for the polar, charged or hydrophilic polymers. The presence of water makes the IR spectrum noisy resulting in lower sensitivity of the instrument. Third, IR methods are not rugged for quantitative analysis, for example, determination of the relative amounts of each type of monomer in a copolymer. It must be noted though that IR methods are useful in studying polymer blends (Stevens 1990).

Nuclear magnetic resonance spectroscopy (NMR) gives more information about the chemical structure of the polymer than IR. Indeed, it is one of the most powerful tools available for chemists to study polymer structures (Stevens 1990). Like IR, NMR is used to identify the monomeric composition of the polymer. The integration of monomer-specific proton signals in ^1H NMR can be used to estimate the relative amounts of monomers in a copolymer with a certain degree of accuracy. One limitation in using NMR is the need to dissolve the polymers in deuterated solvents. For better sensitivity, the polymer in a solution must be of intermediate concentration. The concentration must be high enough to get acceptable sensitivity but not too high to avoid that the solution becomes very viscous. Polymer polydispersity can also be a limitation in NMR characterization. The more diverse

the polymer becomes, the lesser is the sensitivity of NMR to the individual, unique molecule and the longer the time required for the signal acquisition.

Various titration methods are also used as a chemical characterization tool for polymers. Potentiometric titration has been applied to copolymers if one of its monomer can donate or accept protons. For example, the molar ratio of the D-gluocosamine in chitosan can be determined using this technique (Kasaai 2009). Also, chemical behaviour of polymers in acidic or basic environments can be studied using potentiometric titration. The dependence of the self-assembly and the change in micelle size of poly(methacrylic acid-block-ethyl acrylate) in aqueous solution of varying pH was studied by potentiometric titration (Wang, Ravi et al. 2004). Titrations with detection using different methods have been applied: conductometry, spectrophotometry, radiometry and calorimetry (van den Hul and Vanderhoff 1970; Tōei and Kohara 1976; Fischer and Chiu 1983; Bloor, Holzwarth et al. 1995; Tan, Khor et al. 1998).

Physical characterizations are traditionally done independent of the chemical nature of the polymer. Average molecular weight and MWD are the most important properties that are characterized. Size-Exclusion Chromatography (SEC) is the often used method in determining the average molecular weights and the MWD of polymers. Size-exclusion columns are usually connected to refractive index (RI) and ultraviolet (UV) detectors. Larger polymers are partially secluded from the pores of the stationary phases and thus they travel shorter paths and elute faster. Smaller polymers on the other hand, permeate into the pores and thus elute at a later time. The retention times of the polymers determine their molecular weights when compared to the retention times of molecular weight standards. Accurate determinations of average molecular weights and MWD are only possible if the polymer has the same basic structure as the molecular weight standards used. The molecular size of polymers in a solution is determined not just by the molecular weight but also by the shape and the hydrodynamic volume of the molecule. Two very different polymers with the same molecular weights will have different shapes, conformations and hydrodynamic volumes in the solution resulting in differences in their retention times in SEC. In recent years, determination of molecular weight averages and MWD by SEC is often considered not enough. Detectors that allow estimation of molecular weights independent of retention times are often added to correct for the bias in calculations, for example, viscosity detectors. The average molecular weight can also be estimated by using a universal calibration that is corrected by the intrinsic viscosity of the polymer solution (Goedhart and Opschoor 1970). The radius-of-gyration distribution of the polymer can also be obtained from the SEC with viscosity detectors (Yau and Rementer 1990). However, there are also reports that indicate that the universal calibration does not work when the polymers have different shapes when

in solution. Flexible chains, spheroids, semiflexible rods and rigid rods elute at different retention times despite of having the same viscosity radius (Dubin and Principi 1989). In recent years, low-angle and multiangle light scattering detectors are used to determine absolute molecular weight values (Senak, Wu et al. 1987; Podzimek 1994; Podzimek, Vlcek et al. 2001) of polymers including the branched ones.

Bulk polymers are usually evaluated based on the physical properties they exhibit: thermophysical, optical, mechanical, magnetic and electrical properties. Classical techniques such as differential thermal analyzer (DTA), differential scanning calorimeter (DSC) and thermogravimetric analyzers (TGA) are used to determine the thermal properties of polymers such as melting point, glass transition temperatures and degradation temperatures. Mechanical properties like the modulus of elasticity are measured using dynamic mechanical analyzers (DMA). Surface properties like surface tension are determined by a variety of experiments such as contact angle measurements, electron microscopy and by ATR-IR spectroscopy. The information obtained from polymer characterization is used to determine the applicability of new materials and in the quality control of the manufacturing processes of the established ones (Stevens 1990; Braun 2005).

The three polymers in this study present an analytical challenge both in the accurate determination of MWD and in the chemical characterization. In SEC, there are no molecular weight standards that have the same basic structure as these polymers. Column selection would involve a thorough understanding of the polymer behavior in a specific mobile phase. And, classical detectors might be insensitive to these new classes of polymers. Spectroscopic tools in chemical characterization are as well limited. In chemical characterization, IR and NMR qualification of the functional groups will not be enough. It can be noted though that modern, fourier-transform, high resolution NMR techniques will have unique contributions as to the sequencing of the monomers. Two dimensional NMR spectra can provide additional information as to the conformation of the monomer side chains. Solid-state NMR provides a way of characterizing solid bulk polymers. However, as the polymer gets more complex and the concentration of a unique molecule becomes smaller, NMR become less effective due to its low sensitivity.

The use of mass spectrometry (MS) in polymer analysis has greatly increased at the onset of the 21st century. In general, the progress in MS in the last two decades has been overwhelmingly fast. Developments in electronics and instrumentations paved the way for mass analyzers with very high resolving power like the modern time-of-flight (TOF), Orbitrap® and fourier-transform ion cyclotron resonance (FT-ICR). These advancements were complemented by the development in the soft-ionization techniques like matrix-assisted laser desorption ionization (MALDI) and electrospray ionization (ESI). The growth in

the use of MS was observed in polymer research. Hart-Smith and Barner-Kowollik noted that after 1989, there was a rise in the number of publications drawn from *SciFinder Scholar* using the search terms 'mass spectrometry' and 'poly', year after year. This only attests to the increasing importance of MS in polymer characterization. However, the use of MS in polymer science "remains unduly limited" compared to other techniques, despite the numerous capabilities and possibilities that MS can offer (Hart-Smith and Barner-Kowollik 2010).

MS must not be regarded as an alternative to the existing methods of polymer characterization but rather a complementary method that gives additional information about the structure, absolute molecular weights, degree of polymerization and functionalization, and end groups of the polymer. MS offers a fast, robust, highly selective and sensitive method of detecting polymers. The capabilities of MS can be exploited to widen the scope of polymer analysis beyond the traditional ones. Physico-chemical information of the specific polymers can help control their proliferation in the environment especially if they serve as precursors to highly persistent and toxic smaller molecules upon degradation. Currently, the use of MS in polymer research is limited by the molecular weight of the polymer under study and the diversity and complexity of polymer mixtures. These limitations are addressed by careful selection of a better suited MS and sample preparation techniques.

With the advent of fast computers, the use of statistics and informatics in all fields of science has also dramatically increased. In the area of analytical chemistry, chemometrics is rapidly becoming popular. Chemometrics makes use of "mathematical, statistical and other methods of logic to determine (often by indirect means) the properties of substances" (Lavine 2000). Multivariate chemometric techniques make possible the characterization of difficult-to-analyze compounds and complex mixtures using data from simple instrumental techniques like spectroscopy. The developments in instrumentation and advancements in data gathering make way for higher-order calibrations (Booksh and Kowalski 1994), thus increase the necessity for chemometrics in processing the data. There are several advantages in using chemometrics, especially multivariate methods in analytical chemistry (Bro 2003). First, there is reduction in the noise and there is proper handling of interferences. Second, besides calibration, a number of other parameters become useful sources of information and can be tools for further exploration. Thirdly, there is a control for outliers. Chemometrics also support "green" analytical chemistry and toxicology by minimizing the "wet" experiments and animal testing (Armenta, Garrigues et al. 2008; Tetko, Schramm et al. 2014).

Partial least squares (PLS) is one of the basic and commonly used tools of chemometrics (Wold, Sjöström et al. 2001). PLS has been used with various infrared and near infrared spectroscopic techniques to simultaneously determine components of mixtures (Azzouz,

Puigdoménech et al. 2003; Maggio, Kaufman et al. 2009; Neves, de Araújo et al. 2012). In PLS, a set of dependent variables Y are modeled using a set of predictor variables derived from the reduction of X . What makes PLS different and more practical than the other tools is its ability to decrease the large number of X variables such as the absorbance at each wavenumber in IR (most of these variables are strongly correlated with each other, noisy and could be incomplete) to only a few variables that have the highest likelihood to predict Y (Wold, Sjöström et al. 2001). The availability of free statistical computing tools like the R, makes statistical methods even more accessible for analytical chemists. These tools can be exploited for polymer characterization as well.

The purpose of polymer characterization is not just about product development and quality control. Polymer characterization has been a way for authorities to regulate their production and distribution – establish toxicity and chemical properties; study their biodegradability and know their behavior when released into the environment. In 2006, the European Parliament and the Council of the European Union adopted the regulation on the registration, evaluation, authorization and restriction of chemicals (REACH) (The European Parliament and the Council of the European Union 2006). This regulation was adopted to protect human health and the environment. Under this regulation, unambiguous identification of the substances is necessary (ECHA). Polymers are exempted from registration and evaluation under the REACH framework (The European Parliament and the Council of the European Union 2006). Compared to other substances, the risk posed by polymers is minimal due to their high molecular weight (ECHA 2012). Specific polymers may however be subject to authorization and restriction after evaluation of the risk they pose to human health and to the environment. Polymer substances can “contain additives necessary to preserve the stability and impurities deriving from the manufacturing process” (ECHA 2012). Additives, monomers and intermediates are not exempted from registration and evaluation, thus, manufacturers of polymers are obliged to register these as part of one substance. In relation to the policy, polymer characterization must allow differentiation in a polymer sample the individual molecular species, including the unreacted monomer impurities, additives and degradation products.

Objectives of this Research Work

In this work, multi-technique but polymer-specific approaches are employed instead of the standard single-technique approaches for the characterization of polymers. To demonstrate the suitability of this type of approach three modern polymers were investigated: chitosan, oligomeric silsesquioxanes prepared in-house from (3-aminopropyl) triethoxysilane, and a

PFPE formulation. The MWD as well as the monomeric composition of the three polymers were studied using a combination of different instrumental and computational methods: SEC, IR, MS, partition chromatography and chemometrics. To demonstrate the importance of monomer composition on polymer properties, the oil-binding of chitosan is additionally presented. Specifically, this research work sought to answer the following questions:

1. How can the IR determination of the degree of deacetylation of chitosan be improved? What is the effect of the degree of deacetylation on the oil-binding property of chitosan?

Chapter 2 discusses the characterization of chitosan. Other than MW, DD is the most important chemical property of chitosan as it dictates the other properties and the activities of chitosan. There is a need to accurately determine DD. There are many ways to determine DD, for example NMR and titration. IR is a fast but often less precise alternative method in DD determination. In chapter 2A, PLS as a tool to improve the quantitative determination of the DD of chitosan using IR is recommended. In this sub-chapter, the results of PLS were compared to the older quantitative IR method using the absorbance ratios as well as to the absolute method of potentiometric titration. Chapter 2B presents the oil-binding activity of chitosan as affected by its DD. Also, PLS was used to study this relationship between DD and oil-binding activity.

2. How is MS used in polymer characterization? What are the main differences in the molecular weights obtained by MS to that by SEC?

Chapter 3 is a literature review on the use of MS in characterizing polymers. Chapter 4 serves as an illustration of the general ideas presented in the previous chapter. Chitosan oligosaccharide was analyzed using SEC, MALDI-TOF MS and ESI-MS. The differences in the derived MWD are discussed.

3. How can the accuracy of the MS determination of the MWD of oligomeric silsesquioxanes be improved?

Independent single-technique analysis of oligomeric silsesquioxane using ESI-Q and MALDI-TOF gave different MWD results. In chapter 5, the meticulous development of a method to determine, more accurately, the MWD of an in-house synthesized silsesquioxane is discussed. The use of an ion pair reagent enabled the separation of the different homologues of the silsesquioxane in a C18 column. Single homologue standards were prepared by fractionation and quantified by inductively coupled plasma – optical emission spectrophotometry (ICP-OES).

4. How can the high resolution MS information be used to study the chemical composition of the PFPE-based formulation?

High resolution MS proved to be important in the chemical characterization of polyfluorinated polymers like the PFPE shown in Chapter 6. Analysis of the difference patterns as well as the plots of the n^{th} -order mass defects can lead to some highly probable repeating units of the PFPE based formulation. Tandem mass spectrometry provided additional details as to the nature of the end group as well as a strong confirmation on the repeating units.

5. How can MS be a tool to study the environmental fate and degradation of polymers?

The review on Chapter 3 provides an opener on the potentials of MS in polymer characterization. In Chapter 5, it will be shown that absolute molecular weights derived from MS are useful in determining the exact degrees of polymerization (n) of the polymers that may be vital in their differentiation from monomers and dimers. This is especially important if the substance is made-up of oligomers with n between 3 to 10 monomer units. In Chapter 6, MS was used to identify the monomer units and end groups. This can be useful in predicting degradation products and their potential contribution to the environmental risks.

Chapter 2. CHARACTERIZATION OF CHITOSAN

A. Degree of Deacetylation of Chitosan by Infrared Spectroscopy and Partial Least Squares

ABSTRACT

The determination of the degree of deacetylation of highly deacetylated chitosan by infrared (IR) spectroscopy was significantly improved with the use of partial least squares (PLS). The IR spectral region from 1500 to 1800 cm^{-1} was taken as the dataset. Different PLS models resulting from various data pre-treatments were evaluated and compared. The PLS model that gave excellent internal and external validation performance came from the data that was corrected for the baseline and that was normalized relative to the maximum corrected absorbance. Analysis of the PLS loadings plot showed that the important variables in the spectral region came from the absorption maxima related to the amide bands at 1660 and 1550 cm^{-1} and amine band at 1600 cm^{-1} . IR-PLS results were comparable to the results obtained by potentiometric titration. IR-PLS results were found to be more precise and rugged compared to the usual IR absorbance ratio method. This is consistent with the fact that IR spectral resolution is not really high and that the absorption at a single wavelength is influenced by other factors like hydrogen bonding and the presence of water.

Keywords: chitosan, partial least square, degree of deacetylation

Published work

Dimzon, I.K.D. and Knepper, T.P. 2015. Degree of deacetylation of chitosan by infrared spectroscopy and partial least squares. *International Journal of Biological Macromolecules* **72**: 939 - 945

Introduction

Chitosan is an important polymer with a wide range of application. It is obtained from chitin, an abundant natural polymer composed mainly of N-acetyl-D-glucosamine monomer units (Kumar, Muzzarelli et al. 2004; Aranaz, Mengibar et al. 2009). Chitosan, which is mostly D-glucosamine monomer units, is a product of alkali- or enzymatic deacetylation of chitin. The degree of deacetylation (%DD) describes the extent of the transformation of N-acetyl-D-glucosamine to D-glucosamine. It is usually expressed as a molar percent of the D-glucosamine relative to the total D-glucosamine and N-acetyl-D-glucosamine. When %DD reaches 60%, chitosan is formed (Aiba 1992). Some papers refer to the degree of acetylation (%DA) instead of %DD. Both terms are related and add up to 100%.

The %DD is a key property of chitosan on which other properties like biological, physico-chemical and mechanical properties depend (Kasaai 2009), for example, solubility. The amine group of the D-glucosamine monomer gains a positive charge in the presence of excess protons (Sannan, Kurita et al. 1976). The interaction of chitosan in aqueous solution is an interplay between hydrophobic and electrostatic forces dictated by the relative number of D-glucosamine and the N-acetyl-D-glucosamine monomers present. This only suggests that the properties of chitosan in aqueous environment are related to the %DD. Among these properties are: refractive index and radius of gyration (Schatz, Viton et al. 2003); intrinsic viscosity and the ability to form aggregates (Philippova, Korchagina et al. 2012; Novoa-Carballal, Riguera et al. 2013); and oil-binding capacity (Dimzon, Ebert et al. 2013). A more accurate %DD determination, therefore, is significant in chitosan characterization as these polymers are being developed for some specific and novel applications ranging from nanoparticles to hydrogels, wound dressing materials, food and agriculture, and anti-obesity supplements (Ravi Kumar 2000; Khan, Kaushik et al. 2008; Kasaai 2009).

There are a number of classical and instrumental techniques used to determine %DD (Kasaai 2009), among them are the widely used potentiometric titration and proton nuclear magnetic resonance spectroscopy (^1H NMR). In potentiometric titration, known amount of dried, neutralized chitosan is dissolved in a known volume of standard solution of HCl. The molar amount of D-glucosamine can be determined by indirect titration of the excess H^+ with OH^- until the first equivalence point. Potentiometric titration method, aside from being time-consuming, are also labor intensive. In the case of chitosan samples, necessary sample preparations are done to eliminate the impurities as well as to make sure that the polymer is in the neutral form. Chitosan also precipitates at pH 7. In ^1H NMR, chitosan needs to be dissolved in a solution of DCl or CD_3COOD in D_2O . The areas under the curve of the different ^1H signals are used to estimate the relative amounts of the D-glucosamine and N-acetyl-D-glucosamine species. No matter how accurate ^1H NMR is in determining %DD, this

method is only useful for the samples that can be dissolved in the solvent system being used.

Infrared (IR) spectroscopy is being developed as fast and simple alternative to the potentiometric titration and ^1H NMR methods. It offers an advantage of having less sample preparation and having no need of dissolving the polymers. In the IR spectrum, the different absorption bands represent the different functional groups present in chitosan. It is usually the %DA that is determined first using IR. To determine the DA, two absorption bands are selected – a characteristic band (also known as probe band) representing the amide group of the N-acetyl-D-glucosamine and a reference band that represents a group that is present in both N-acetyl-D-glucosamine and D-glucosamine species. A linear function can be determined relating %DA and the absorbance ratio of the two bands. Generating a best fit calibration curve is a difficult task. There are numerous publications describing how the various ratios produced by combinations of characteristic and reference absorption bands produces highly variable coefficient of determinations (Baxter, Dillon et al. 1992; Sabnis and Block 1997; Brugnerotto, Lizardi et al. 2001; Duarte, Ferreira et al. 2002). The sources, isolation and preparation method of chitosan can introduce inaccuracies in the DA determination (Duarte, Ferreira et al. 2002).

Results from IR spectroscopy suffer from imprecision especially for chitosans with $\text{DA} < 10\%$ ($\text{DD} > 90\%$). This is due to the high noise signal and to the low absorption signal of the amide group. In this study, it is proposed that the IR determination of %DD (or %DA) can further be improved with the use of partial least squares (PLS) multivariate chemometric technique. Chemometrics deals with the use of statistics and informatics in chemistry. One of its aim is to provide chemical information from a chemical data, e.g. spectra (Massart, Vandeginste et al. 1998). Among the variety of chemometric techniques, PLS has found a wide application. PLS has been used with various infrared and near infrared spectroscopic techniques to simultaneously determine components of mixtures (Azzouz, Puigdoménech et al. 2003; Maggio, Kaufman et al. 2009; Neves, de Araújo et al. 2012). In PLS, a set of dependent variables \mathbf{Y} are modeled using a set of predictor variables derived from the reduction of \mathbf{X} . What makes PLS different and more practical than the other tools is its ability to decrease the large number of \mathbf{X} variables (most of these variables are strongly correlated with each other, noisy and could be incomplete) to only a few variables that has the highest likelihood to predict \mathbf{Y} (Wold, Sjöström et al. 2001).

This paper reports on the development a PLS model to determine more accurately the %DD of chitosan samples using the IR absorbances in the spectral region from $1500 - 1800 \text{ cm}^{-1}$ as raw data. The target samples studied were the chitosan within the %DD range of $75\% < \text{DD} < 95\%$. The paper describes the different data pre-treatments prior to PLS modeling

and the comparison of the %DD results obtained by IR-PLS to the results obtained by IR-absorbance ratio and potentiometric titration.

Materials and Methods

Chitosan Samples and Reagents

The different chitosans used in this study can be divided into two groups: the training set chitosans and the unknown chitosans. The training set chitosans from Hepe Medical Chitosan (HMC) GmbH (Halle an der Saale, Germany) were used to derive the chemometric model. These chitosans were from crab chitins. The %DD of these chitosans were known and were shown in the certificates of analysis. The chitosan standards have the following %DD: 94.3, 94.2, 93.4, 92.7, 91.8, 89.7, 89.4, 84.7, 78.1, and 73.6. The unknown chitosans (labeled U1 to U4), provided by Certmedica International GmbH (Aschaffenburg, Germany), were used to test the developed chemometric model. Sample U1 is of a fungal source while samples U2-U4 are of crab sources. The molecular weight of the training set and unknown chitosans were obtained by size-exclusion chromatography and were between the range of 77 to 235 kDa.

Infrared Analysis

The analysis was carried out in a Perkin Elmer Spectrum Bx FTIR System. The chitosans were previously dried for at least one hour in an oven at 105 – 110 °C and at atmospheric pressure condition. A 0.025 g chitosan was mixed with 0.475 g KBr and homogenized in a mortar and pestle. A 0.20 g aliquot of the mixture was then made into a pellet using a hydraulic press and was analyzed in the IR at the wavenumber region from 600 to 4000 cm^{-1} at an interval of 2 cm^{-1} . The resulting IR spectrum was the average of 20 determinations at a resolution of 4000.

Partial Least Squares Modeling

The data pre-treatments were done using Microsoft Excel™ (v. 2007). The absorbances within the wavenumber region 1500 to 1800 cm^{-1} were extracted. These absorbances were then corrected using a baseline drawn from 1500 to 1800 cm^{-1} (Figure 2.1, b1). Three data pre-treatments were then explored using the corrected absorbances: A. normalization relative to the highest absorbance; B. normalization relative to the absorbance at 1660 cm^{-1} ; C. normalization relative to the absorbance at 1600 cm^{-1} .

The free software 'R' (The R Foundation for Statistical Computing) was used in the generation of the PLS model through the 'pls' package (Bjorn-Helge and Wehrens 2007).

The 'pls' function was applied on the pre-treated training set chitosan datasets using the default kernel algorithm and with a maximum of six components. Internal validation was done using the leave-one-out (LOO) technique. The optimal number of components to be used in regressing %DD was chosen based on the calculated lowest root mean square error of prediction ($RMSEP_{LOO}$) and on the highest explained variance criteria.

Potentiometric Titration

To evaluate the accuracy of the IR-PLS method, potentiometric titration was employed on the unknown chitosan samples. The method is based on previous works (Azzouz, Puigdoménech et al. 2003). Prior to analysis, all samples were washed with deionized water and then dried overnight at 105 °C at normal air pressure condition. A 0.2 g portion of chitosan was accurately weighed and was dissolved in 25.00 mL of standard 0.1 M aqueous HCl solution. The total volume of the solution was increased to 100 mL with deionized water. The ionic strength of the solution was maintained at 0.1 using KCl. The pH of the solution was monitored using VWR pH meter (VWR International, USA) with glass electrode (Schott Instrument Blue Line Electrode, SI Analytics, Germany). A 0.1 M standard aqueous NaOH solution with 0.1 M KCl was used as titrant. The NaOH solution was standardized against reagent grade sodium carbonate to the methyl orange end point while the HCl solution was standardized against the NaOH solution to the phenolphthalein endpoint.

Statistical Evaluation of Results

Different statistical parameters were employed to describe and compare the results of the different methods. Both the Microsoft Excel and the 'pls' package of the 'R' software were used to generate the parameters. The coefficient of multiple determinations (R^2) is indicative of the goodness of fit of the regression model. A good R^2 however does not ensure that the model will have good prediction power. The correlation coefficient (Q^2) either from an internal or external validation gives a better overview of the model's robustness and ability to predict the %DD. In this study, only the internal validation correlation coefficient (Q^2_{LOO}) was reported. There was an error in the correction factors to calculate the external validation correlation coefficient (Q^2_{Ext}) resulting to negative values in some of the models. The $RMSEP$ is a good alternative to measure the prediction power of a model. The $RMSEP_{Ext}$ (external validation) were determined and were used as criteria to assess the model's performance.

Additionally, one tailed student's t-test with the assumption of equal variance was done to determine the effects of moisture and pellet thickness in the %DD of a chitosan sample.

Results and Discussion

Infrared Spectrum of Chitosan

The IR spectrum of a training set chitosan with a %DD of 84.7% is shown in Figure 2.1. Also shown are the assignments of the major infrared absorption bands that are mostly based on the work of Pearson, Marchessault and Liang (Pearson, Marchessault et al. 1960) on chitin. The spectral region between 1500 and 1800 cm^{-1} is a rich data source. For example, the amide I and amide II absorption bands at 1630 to 1660 cm^{-1} and 1560 cm^{-1} respectively are widely used characteristic bands. In the same region however, is the band at 1597 cm^{-1} due to primary amines and at 1640 cm^{-1} due to the OH group of polysaccharides (Shigemasa, Matsuura et al. 1996). Because the bands are broad and overlap each other, finding the most fit characteristic band or characteristic band combination that is linearly related to %DD in a wide range of sample has been a difficult task. Adding to the complexity is finding a good baseline and a good reference band. The presence of water causes an increase in the absorption band at 1640 cm^{-1} and can introduce a negative bias on the %DD. This can be corrected if the band at 3450 cm^{-1} is used as a reference peak because this also is increased proportionally with moisture (Domszy and Roberts 1985). In general, %DD determination using IR – absorbance ratio method has low to moderate accuracy and working on several absorbance ratios and applying statistical evaluations can improve the accuracy (Kasaai 2008).

Partial Least Squares Modeling

The whole spectral region from 1500 cm^{-1} to 1800 cm^{-1} can be taken as a single ‘super’ band whose shape is influenced by the %DD. In Figure 2.2, the IR spectra of chitosans with varying %DD in the region from 1500 cm^{-1} to 1800 cm^{-1} are plotted after three different data pre-treatments. In a closer examination of Figure 2.2A (where the data were normalized relative to the highest corrected absorbance), one can easily observe the changes in the shape of the band with %DD. It is of particular interest to point out that the three sub regions of the ‘super’ band with the highest variability with %DD are 1550, 1600 and 1660 cm^{-1} . This is expected because these are the characteristic bands of amide and amine groups. The differences were further highlighted when the data were normalized to the absorbance of a single wavenumber (Figure 2.2B and Figure 2.2C). The changes in the shape of the band can be used as an alternative to absorbance ratio in predicting the %DD of an unknown chitosan.

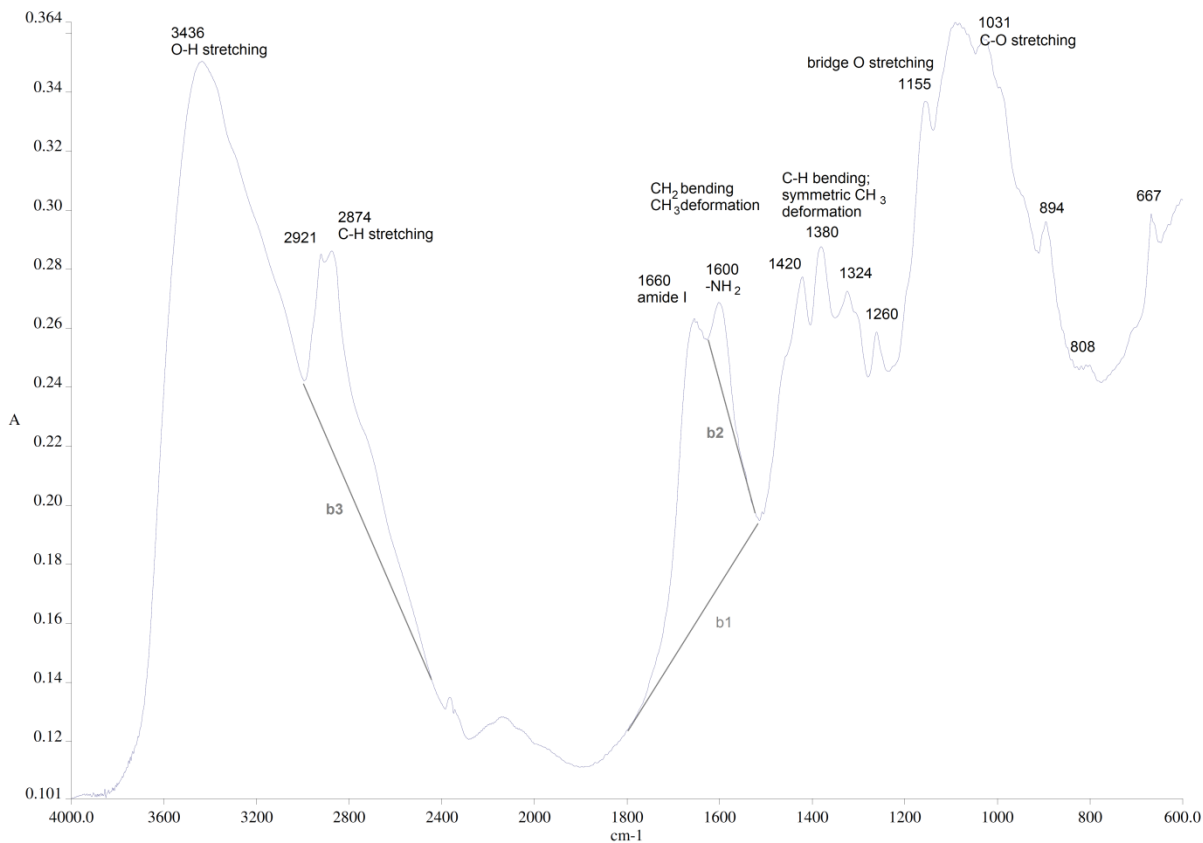


Figure 2.1. IR absorption spectrum of a training set chitosan with 85% %DD. The assignment of absorption bands are based on literature data (Pearson, Marchessault et al. 1960; Shigemasa, Matsuura et al. 1996; Duarte, Ferreira et al. 2002). The baselines used to correct absorbances in this study are also shown (b1 to b3).

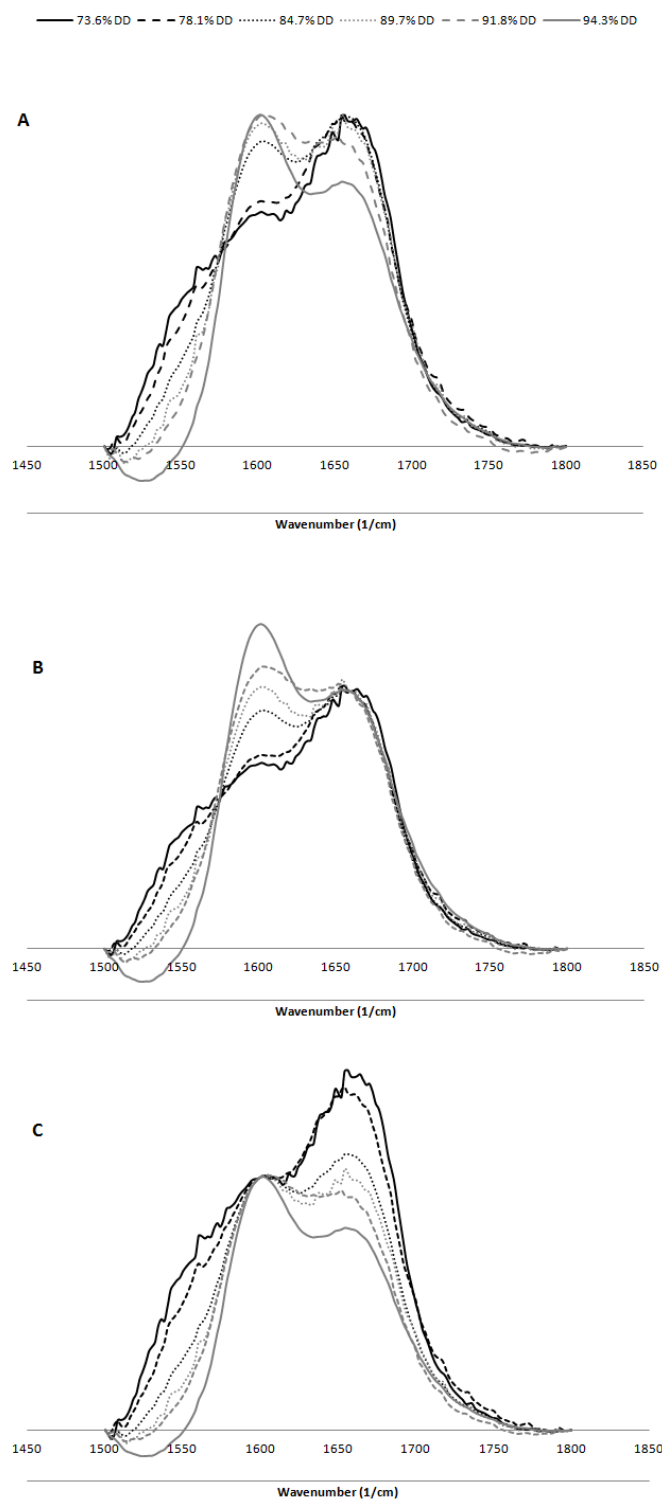


Figure 2.2. The spectral region 1500 – 1800 cm^{-1} after baseline correction and data pre-treatments: A. normalized against highest absorbance; B. Normalized against the absorbance at 1660 cm^{-1} ; and C. normalized against the absorbance at 1600 cm^{-1} .

Statistical treatment using PLS can model band shape changes and %DD. All the wavenumbers in the spectral region can be considered variables (\mathbf{X}) with some of them changing more significantly with the changes in %DD (\mathbf{Y}) than the others. The aim of PLS here is to efficiently reduce the \mathbf{X} to a few variables that can be used to predict \mathbf{Y} . The reduction or decomposition process is described by the matrix equation:

$$\mathbf{X} = \mathbf{TP}^T + \mathbf{E}$$

Equation 2.1

where \mathbf{T} , \mathbf{P} and \mathbf{E} are the score, loading and residual matrices respectively (The T is a matrix transposition symbol) (Maggio, Kaufman et al. 2009). In general, the PLS method can be viewed as a projection of the \mathbf{X} matrix on a hyperplane of A dimensions (A gives the number of coordinates). The coordinates of this hyperplane are the components of the PLS model. The elements of \mathbf{T} are referred to as the x -scores, t_a ($a=1,2,3...A$). PLS was specifically chosen from a number of other multivariate techniques like the principal components regression (PCR) because of its robustness to factors with high variance but are not at all correlated to the dependent variable (Vandeginste, Massart et al. 1998; Bjorn-Helge and Wehrens 2007). Like PCR, the first step in the reduction process involves finding a vector that can explain the largest variation in the data. However, unlike PCR, PLS also simultaneously reduce \mathbf{Y} and has an additional criterion that the vector of \mathbf{X} must have a maximum covariance with the vector of \mathbf{Y} (Massart, Vandeginste et al. 1998). The second criterion makes PLS unique and robust so that the effects of x -variables that are collinear but are not correlated to \mathbf{Y} are minimized. When the two criteria are met, the first component is found; and the loadings of the original variables can be assigned and the scores, t_1 , can be calculated. The vectors of the first component are then subtracted from the original \mathbf{X} and \mathbf{Y} and the process is repeated on the remaining data to find the second component. The reiteration continues to find the third, fourth, and so on components until the \mathbf{X} becomes a null matrix (Abdi 2010). The t_a 's, based on the order of generation, are arranged in a way that the explained variance is greatest in component 1 (t_1) and diminishes in every proceeding component (t_2, t_3, \dots). It also follows that t_1 will have the greatest correlation to \mathbf{Y} . The choice of algorithm to use in PLS modeling is "mainly of technical interest" and that the different variants were developed to further improve the model given different data shapes (Wold, Sjöström et al. 2001). The 'kernel' algorithm was designed for datasets with a large number of observations compared to the number of variables (Khan, Kaushik et al. 2008).

Three datasets were modeled and compared. The datasets came from the same raw spectra but were pre-treated in three ways as described in section the methodology. Table

2.1 shows the comparison of the performance characteristics of the three models. The code of the PLS models corresponds to the code of the data pre-treatment. The R^2 of the models were all greater than 0.94.

Table 2.1. Performance Characteristics of the PLS models

Validation Parameters	Model A		Model B		Model C	
	2 comp	3 comp	2 comp	3 comp	2 comp	3 comp
Explained Variance (%)	92.8	97.4	97	98.1	98.5	99.2
R^2	0.981	0.985	0.947	0.981	0.979	0.989
RMSEP _{LOO}	1.81	2.04	2.59	2.79	1.81	2.06
Q^2_{LOO}	0.930	0.911	0.856	0.832	0.929	0.908
RMSEP _{Ext}	1.82	2.70	3.40	13.07	3.49	4.29
Precision (RSD) of a 4-trial run	0.03	0.11	0.27	0.18	0.64	0.05

Internal Validation

To further assess the performance of the PLS models, two levels of validation were done. Internal validation using the LOO technique provided initial information on the quality of the models and on the optimum number of components to be used in the regression of %DD. In LOO, one sample in the training set is removed from the set and a model is created using the remaining elements. This model is used to predict the %DD of the removed element. The derived value is compared with the labeled value and the difference can be noted. The process is repeated by removing another random element from the original training set. The RMSEP_{LOO} represents the error difference between the PLS-derived %DD and the labeled values. Shown in Table 2.1, the RMSEP_{LOO} of all the models were below 3%. In model A, when only the first two components were used, the explained variance was 92.8% and the error was only 1.81. If another component is added in the regression, the explained variance jumped to 97.4% but the error is increased by approximately 0.2%. This only means that the additional variations that were introduced in the third component do not really add to the improvement of the regression. A two component model, in this case would already be enough to predict with less error the %DD but at the same time prevents overfitting. The Q^2_{LOO} of models 1 and 3 were greater than 0.9.

In terms of internal validation, model A had the best performance. This can be due to the fact that in models B and C, an important variable was forced to be constant by normalization. The initial step in PLS algorithms is assigning greater weights on variables with maximum

covariance with %DD. If an important variable is made constant, then that variable becomes less significant in that model and it will cause the variability in the other variables that are not as important and can result to bias in the predictions. This is obvious in model B where the amide I absorbance at 1660 cm^{-1} was forced to be constant.

Figure 2.3 shows the x-loadings plot of the first three components of model A. The x-loading is the weight given to each x-variable before they are linearly combined to give the x-score. The greater is the absolute value of the loading of a variable the greater is the contribution of that variable in the generation of the score and the more is its influence on the prediction of %DD. The sign of the value gives the direction of the influence. The x-loadings plot of the first component which accounts for 79.3% of the variance shows two minima (1546 and 1660 cm^{-1}) and a maximum (1600 cm^{-1}). This is consistent with the behavior of the amide and amine bands with increasing %DD. This alone already gives a good prediction of %DD with the $\text{RMSEP}_{\text{LOO}}$ value of 2.32. The loadings plot of the second component has a flat broad maximum from $1560 - 1670\text{ cm}^{-1}$. This can be attributed to the region of overlap between the amide and amine bands. The scores of the second component (t_1) when added to the scores of second component (t_2), provides a fine tuning that results to a better regression model and the $\text{RMSEP}_{\text{LOO}}$ is decreased to 1.81. The loadings plot of the third component, in contrast to the first two is noisy and appears to be having an inflection at 1600 cm^{-1} . There is no obvious basis to correlate this component with the %DD. This reinforces the previous observation that the $\text{RMSEP}_{\text{LOO}}$ increased by 0.2% when this component was added to the model.

External Validation and Comparison to the Infrared-Absorbance Ratio Method

The R^2 , Q^2_{LOO} and the $\text{RMSEP}_{\text{LOO}}$ provide essential information about the fitness of the PLS models. However, these are not enough to assess the predictive power of the latter (Ravi Kumar 2000; Golbraikh and Tropsha 2002; Roy and Roy 2008). To address this issue, external validation was done by analyzing chitosan samples of unknown %DD. Potentiometric titration was utilized as a standard method to compare the IR methods against. The summary of the %DD using the different methods is shown in Table 2.2. The precision of the IR-PLS results with the exception of model C with 2 components were less than 0.3%. The % biases of the results against potentiometric titration are shown in Figure 2.4. Calculated %bias of the IR-PLS and IR area ratio methods compared to potentiometric titration.. Among the models of the IR-PLS method, model A gave the least combined % bias. Model A has the lowest $\text{RMSEP}_{\text{Ext}}$ of only 1.8 (Table 2.1).

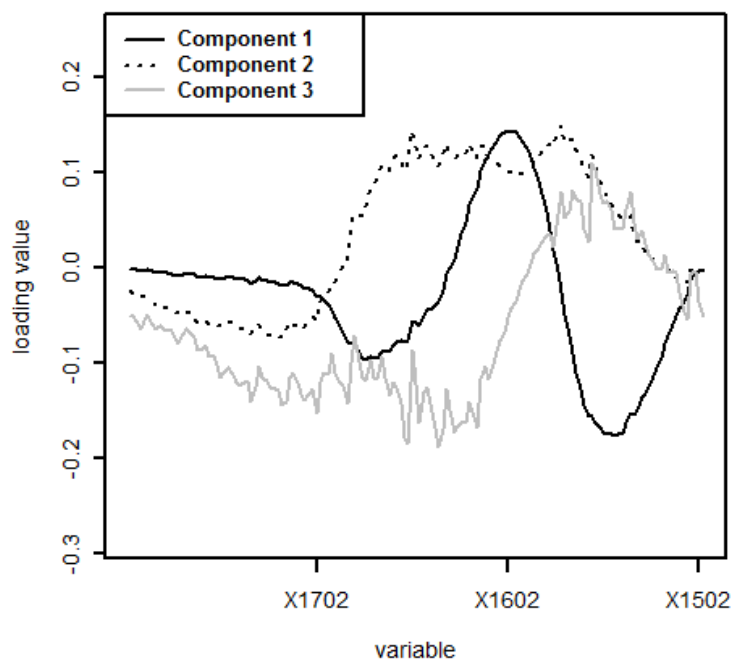


Figure 2.3. *x-loadings plot of the components of PLS Model A.*

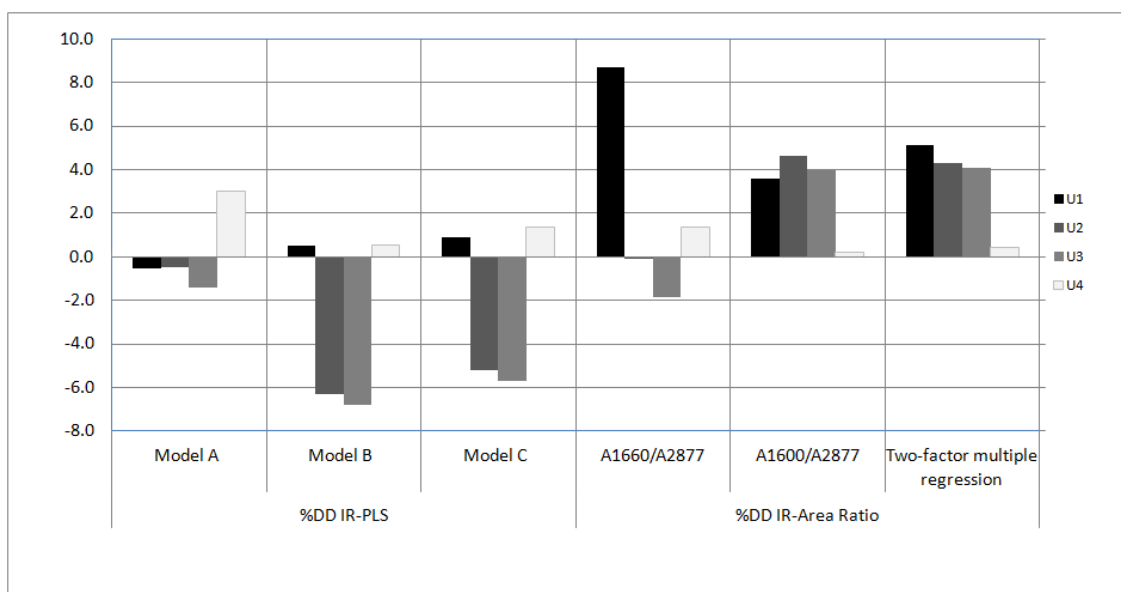


Figure 2.4. *Calculated %bias of the IR-PLS and IR area ratio methods compared to potentiometric titration.*

Table 2.2. Comparison of the %DD values obtained by IR (PLS and absorbance ratio) to the %DD obtained by potentiometric titration. The values in parenthesis are the SDs of two trials.

Sample	%DD IR-PLS			%DD IR-Area Ratio			%DD Potentiometric Titration
	Model A	Model B	Model C	A_{1660}/A_{2877}	A_{1600}/A_{2877}	Two-factor Multiple Regression $A_{1660}/A_{2877}, A_{1600}/A_{2877}$	
U1	77.8 (0.02)	78.6 (0.3)	78.9 (0.7)	85 (6)	81 (4)	82.2 (0.5)	78.2 (1.5)
U2	83.7 (0.2)	78.8 (0.4)	79.7 (0.6)	84 (17)	88 (8)	87.7 (2.7)	84.1 (0.2)
U3	84.4 (0.1)	79.8 (0.4)	80.7 (0.5)	84 (3)	89 (1)	89.1 (0.2)	85.6 (1.5)
U4	92.5 (0.1)	90.3 (0.04)	91.0 (0.01)	91 (5)	90 (6)	90.2 (1.4)	89.8 (1.0)

An attempt was made to obtain the %DD of the unknown samples using the same IR spectra but with area ratio method. Two characteristic bands, 1660 and 1600 cm^{-1} , and a reference band, 2870 cm^{-1} were tested. The absorbances at the mentioned wavenumbers were corrected according to the baselines as shown in Figure 2.1. The absorbance ratios from training set chitosan were used as calibration points. The calibration curves from A_{1660}/A_{2870} and A_{1600}/A_{2870} had negative and positive slopes respectively. Three out of ten points were eliminated because they were obvious outliers in the calibration curve. Monitoring of amide absorptions in chitosan with large %DD was inappropriate as the absorbances became no longer distinguishable from a noisy IR baseline and from the effects of the other overlapping absorption bands. This causes large imprecision in the results. The combined %bias of the area ratio method was also larger compared to the IR-PLS method (Figure 2.4). In particular, U1 deviated greatly when the absorbance at 1660 cm^{-1} was used while U2 and U3 were affected when the absorbance at 1600 cm^{-1} was used. U1 is a chitosan synthesized from fungal chitin while all the training set chitosan to generate the calibration curve were from crab chitin. It can be noted that the band at 1660 cm^{-1} is just one of the doublet (the other is at 1626 cm^{-1}) related to the amide absorption. The relative absorption of the doublet varies depending on the H-bonds in which the C=O group participates in different types of chitin/chitosan (Kasaai 2008). U1 having been synthesized from a chitin of fungal source can have a different H-bonding than the training set chitosans. The combination of the two absorbance ratios using two-factor multiple linear regression was also explored with the expectation that the one reference band can enhance the other. The precision and trueness were significantly increased but are still inferior compared to the IR-PLS.

Robustness of the Infrared-Partial Least Squares Method

The robustness of the IR-PLS method to the variations in the thickness of KBr pellet and to the presence of moisture was investigated. A thicker KBr pellet of U1 was prepared by doubling the amount of the KBr-chitosan mixture. The obtained value for %DD was 78.2 and an SD of 0.04. The mean is significantly higher (t-test, one tailed, $p=1.1 \times 10^{-4}$, $\alpha=0.05$) than the value obtained in thinner film which has a mean of 77.8 and an SD of 0.02. A U1 sample that was not dried in the oven was also analyzed and the obtained %DD was 76.9 and an SD of 0.3. The mean is significantly lower than that of the dried sample (one tailed t-test, $p=7.8 \times 10^{-9}$, $\alpha=0.05$). This is consistent with the earlier findings that moisture can introduce negative bias in the determination using A_{1660} if it is not compensated in a reference band (Domszy and Roberts 1985). The differences between the three means were all less than 1% yet these differences appeared to be significant because of the high precision of the PLS results making the variance between replicates small. All the three values were well within the confidence interval of the potentiometric titration results ($\pm 3\%$, 95% confidence).

Conclusion

Determination of the %DD of chitosan using IR absorbance ratio method becomes erroneous for chitosans with %DD greater than 90% since most of the characteristic bands used in the estimation are amide absorptions. The absorbances at these bands become indistinguishable from baseline noise leading to large bias and imprecision. In this paper, for chitosan with approximate %DD between 75% and 95%, PLS provides a robust and highly precise alternative in processing IR spectra to determine the %DD. The results obtained from IR-PLS are comparable to the results obtained using standard potentiometric titration. To ensure accuracy in the results, the spectral raw data needs to be pre-treated prior to PLS modeling. A good PLS model can be derived if the absorbances in the spectral region from 1500 to 1800 cm^{-1} are first corrected for the baseline and are then normalized against the highest corrected absorbance. The PLS method transformed the dataset of 151 x-variables to a matrix of only six components. The scores of the first two components can be used to regress and predict %DD. Examination of the loadings of the first two components revealed that the absorbances with greatest weights in the model are from the wavenumbers 1660, 1600 and 1546 cm^{-1} which are related to the amide I, NH and amide II absorption respectively. This attribution to known facts makes the PLS model more reliable and provides support to the validity of its prediction. Without these solid scientific basis, the PLS models are no more than mathematical correlations.

B. The Interaction of Chitosan and Olive Oil: Effects of Degree of Deacetylation and Degree of Polymerization

ABSTRACT

The combined effects of degree of deacetylation (DD) and degree of polymerization (DP) on the ability of chitosan to interact with olive oil was studied. The oil-binding test, a method that makes use of olive oil as a representative fat, was adopted as a measure of the interaction of chitosan and olive oil. The oil-binding capacities of twelve chitosan samples with DPs ranging from 470 to 1450 and DDs of 75 % to 95 % were determined. The oil-binding capacities were then correlated to the DD and DP using partial least squares (PLS) regression. The generated PLS model had a root mean square error of prediction (RMSEP) of 9.1%. Results indicated that oil-binding capacity is a function of DD more than of DP. For chitosan with DD at the interval 50 % < DD < 90%, a negatively sloped linear correlation was obtained for DD and oil-binding capacity suggesting that hydrophobic intermolecular forces of attraction dominates the interaction of chitosan with olive oil. For chitosan with DD > 90 %, the observed deviation from the linear correlation increased. In this interval, free fatty acid anions facilitate the interaction of chitosan and olive oil. Free fatty acids form a stable ionic interaction with the former and a strong hydrophobic interaction with the later.

Keywords: chitosan, degree of deacetylation, degree of polymerization, pls, chemometrics, oil-binding capacity

Published work

Dimzon, I.K.D., Ebert, J. and Knepper, T.P., 2013. The interaction of chitosan and olive oil: Effects of degree of deacetylation and degree of polymerization. *Carbohydrate Polymers* **92**: 564-570

Introduction

Chitosan has been widely used for a variety of purposes. Commercially available chitosan is mainly synthesized from chitin, a naturally abundant polymer in exoskeletons and support structures of crustaceans, mollusks and insects and in the cell wall of fungi (Kumar, Muzzarelli et al. 2004; Aranaz, Mengibar et al. 2009). Chitin is composed mainly of N-acetyl-D-glucosamine monomer units and the rest are D-glucosamine monomers linked by β -D-(1 \rightarrow 4) glycoside bonds. Alkali-catalyzed deacetylation of N-acetyl-D-glucosamine in chitin leads to the formation of more glucosamine monomers. The extent of this reaction of chitin is described by the property degree of deacetylation (DD). DD is the ratio (usually expressed in percent) of the amount (in moles) of D-glucosamine units to the total D-glucosamine and N-acetyl-D-glucosamine units. Chitosan is formed when the DD reaches a certain value (Kasaai 2009). For example, chitosan contains a minimum of 60% D-glucosamine units (Aiba 1992).

Chitosan is a mixture of homologues at a wide range of degree of polymerization (DP) and molecular weight (MW). Different average molecular weight parameters are often used to describe the average size of the polymer depending on the method used to estimate them. Weight-average molecular weight (Mw) and number-average molecular weight (Mn) are estimated using size-exclusion chromatography (SEC) while viscosity molecular weight (Mv) is derived from the measurement of the intrinsic viscosity of the polymer solution in a particular solvent. The use of SEC in polymer analysis especially for polycations like chitosan can be complex. A SEC method that uses neutral stationary phase and a high ionic strength, acidic mobile phase was shown to be robust for the determination of the molecular weight of chitosan (Bernhard, Flato et al.).

Both the DD and DP are basic physico-chemical properties from which the other properties of chitosan are functions of. For example, both the DP and DD influence the viscosity of chitosan solutions. The Mark – Houwink equation (Equation 2.2) shows that the intrinsic viscosity ($[\eta]$) of a polymer solution changes with the molecular weight. A study by Wang et al. (Wang, Bo et al. 1991) showed that for chitosan samples of the same DD, the logarithm of intrinsic viscosity is a linear function of the logarithm of Mw, consequently is directly proportional to the logarithm of DP. On the other hand, DD influenced the Mark – Houwink constants k and α (Wang, Bo et al. 1991) and the non-Newtonian flow properties of chitosan solutions (Wang and Xu 1994).

$$[\eta] = kM^\alpha$$

Equation 2.2

DD and DP also influence chitosan solubility in aqueous solutions. Chitosan solubility in water increases with the decrease in the DP and with the increase in DD. The ability of the amine group to gain a positive charge in acidic environment makes the deacetylated chitosan easily dissolve in aqueous acidic medium (Sannan, Kurita et al. 1976; Vårum, Ottøy et al. 1994; Qin, Li et al. 2006). It was also reported that chitosan behaviors in aqueous solutions of high ionic strength like refractive index and gyration radius are functions of DD. The interactions of chitosan in aqueous solutions can be divided into three domains based on the DD: 1) at $DD > 80\%$, electrostatic interaction predominates; 2) at $50\% < DD < 80\%$, hydrophobic and hydrophilic interactions are counter balanced; and 3) at $DD < 50\%$, stable aggregates are favored (Schatz, Viton et al. 2003). Additionally, chitosan in dilute aqueous solutions has a semi-flexible rod conformation (Morris, Castile et al. 2009). The rigidity in the structure of chitosan and chitin is mainly due to the interchain H bonds (Muzzarelli 2012).

The activity and uses of chitosan are directly linked to their physico-chemical properties. A review by Aranaz et al. (Aranaz, Mengibar et al. 2009), shows that many of the biological properties of chitosan like biodegradability, biocompatibility, hemostatic, analgesic and antimicrobial properties are particularly influenced by DD and molecular weight.

One of the recent uses of chitosan is as an active ingredient in “fat-binder” tablets or anti-obesity supplements (Woodgate and Conquer 2003). It is claimed that chitosan has the ability to “bind” with fatty substances in the intestines making them unavailable for metabolism. They are consequently excreted out of the body. Many studies substantiate these claims. *In vivo* studies show that chitosan has hypocholesterolemic effect in humans (Maezaki, Tsuji et al. 1993; Bokura and Kobayashi 2003) and in other animal subjects such as mice or rats (Gallaher, Munion et al. 2000; Bokura and Kobayashi 2003; Liu, Zhang et al. 2008). Chitosan was also associated with the increase in fecal fat (Deuchi, Kanauchi et al. 1994; Deuchi, Kanauchi et al. 1995; Kanauchi, Deuchi et al. 1995; Han, Kimura et al. 1999; Gallaher, Munion et al. 2000) and fecal bile acid (Gallaher, Munion et al. 2000) excretion. *In vitro* studies, on the other hand, reveal that the interaction of chitosan to triacylglycerides contained in olive oil, is highly influenced by the physico-chemical properties of the former. These studies rely mainly on measuring the oil-binding capacity (called fat-binding capacity in some papers) of chitosan. In the test, olive oil is made to form a stable complex with a test substance under a simulated gastrointestinal condition (Zhou, Xia et al. 2006). The unbound oil is separated from the stable complex and is measured. The difference between the initial amount of oil added and the measured amount of unbound oil gives the amount of the oil bound to the complex and is taken as a measure of the oil-binding capacity (Cho, No et al. 1998). It was shown that the oil-binding capacity of chitosan is negatively related to its bulk density and is directly related to viscosity (Cho, No et al. 1998). It was also shown that for a

series of chitosan with increasing MW but constant DD, highest oil binding was achieved in an optimal MW (No, Lee et al. 2003). Despite the efforts, however, only a number of significant correlations have been demonstrated (Aranaz, Mengibar et al. 2009). This can be due to the fact that the mechanism of interaction of triacylglyceride and chitosan is a complex process.

In this paper we investigate the effects of DD and DP on the interaction of chitosan with olive oil. To achieve this, DD, DP and oil-binding capacity of different chitosan samples should be determined. Partial least squares (PLS), novel chemometric technique, is used to elucidate the relationships.

Materials and Methods

Chitosan Samples and Reagents

The chitosan samples (labeled S1 to S10 in this paper) used to derive the chemometric model were from Heppe Medical Chitosan (HMC) GmbH (Halle an der Saale, Germany). The DD of the samples were known and were shown in the certificates of analysis (COA). DD ranged from 73.6% to 94.3% (see nTable 2.3). The MW of the chitosan samples written in the COA were approximate values. SEC was used to derive the M_w .

Two chitosan samples of unknown DP and DD from Certmedica International GmbH (Aschaffenburg, Germany) were also analyzed (labeled U1 and U2 in this paper). Fourier transform – infrared (FT-IR) spectroscopy with the Heppe chitosan samples as standards was used to determine the DD of the unknown. SEC was used to derive the M_w .

The extra virgin olive oil (Villa Gusto, Italy) used was purchased from a German supermarket. The oil was submitted to Prof. Dr. Georg Kurz GmbH (Cologne, Germany) for determination of fatty acid distribution and free fatty acids. Analytical reagent grade acetic acid, sodium acetate, sodium chloride, potassium chloride, potassium dihydrogenphosphate and trifluoroacetic acid (TFA) were from Carl Roth (Karlsruhe, Germany). The analytical reagent grade disodium hydrogenphosphate was from Riedel-de Haën (Seelze, Germany). Ultrapure water (Milli-Q water) was prepared by a Milli-Q system with Simpapak2 ion exchanger (Millipore, Milford, MA, USA).

Table 2.3. Degree of deacetylation and weight-average degree of polymerization of the chitosan samples. Data for the degree of deacetylation of S1 to S10 were directly lifted from the certificate of analysis while for U1 and U2 were obtained experimentally using FT-IR and partial least squares.

Sample Code	DD (%)	DP _w
S1	94.3	474
S2	73.6	589
S3	91.8	583
S4	89.7	802
S5	84.7	905
S6	94.2	912
S7	78.1	1076
S8	89.4	987
S9	93.4	1063
S10	92.7	1440
U1	83.8	542
U2	82.2	539

Determination of Weight-Average Degree of Polymerization (DP_w)

A robust SEC method was used to estimate the MW of the Heppe chitosan and unknown samples (Bernhard, Flato et al.). The polymers were previously dissolved (0.5% wt/v) in 0.3 M acetate buffer (0.2 M CH₃COOH and 0.1 M Na⁺CH₃COO⁻). Chromatographic separation was carried out in Novema 3000 Å and Novema 300 Å dual column (both columns have: internal diameter, 8 mm; length, 30 cm; particle size, 10 µm; material, OH-functionalized methacrylatecopolymer; Polymer Standards Service, Mainz, Germany) using 0.2% trifluoroacetic acid (TFA) v/v in 0.3 M aqueous sodium chloride (NaCl) solution as eluent. Detection of the polymers was done in a refractive index detector. The M_w's, were then estimated using the absolute retention time of polyvinyl pyridine (PVP) molecular weight standards (PSS, Mainz, Germany) dissolved in 0.5% TFA v/v in 0.3 M aqueous NaCl. The determinations were done in duplicates.

The DP_w was estimated from the M_w and DD using Equation 2.3:

$$DP_w = (M_w - 18)/[204 - (43 \times DD)] \quad \text{Equation 2.3}$$

Determination of Degree of Deacetylation

FT-IR spectroscopy was used to determine the DD of U1 and U2. Chitosan S1 to S10 were used as DD standards. The chitosan samples (S1 to S10, U1 and U2) were initially dried at 105 °C for at least one hour. Five to ten milligram portion of chitosan was mixed and homogenized with 100 mg KBr. The mixture was then made into a pellet using a hydraulic press. The IR spectrum at the wavenumber region 4000 to 600 cm^{-1} was then obtained using Perkin Elmer Spectrum Bx FTIR System. The IR spectrum of a blank KBr pellet was used as background. The resulting IR spectrum is the average of 10 scans at a resolution of 4000.

The IR data files of the absorbance spectra were extracted as ASCII files using the Spectrum v5.0.1 software. The absorbances within the region 1800 to 1500 cm^{-1} were used to generate a calibration and to determine the DD of the unknown using partial least squares (PLS). Prior to PLS, the absorbance data were corrected for the baseline and were normalized against the highest absorbance using Microsoft Excel™. The analysis using PLS is discussed in the statistical analysis section.

Oil-Binding Test

The oil-binding capacity of chitosan was determined using a commonly used technique (Zhou, Xia et al. 2006) with some modifications. A 0.125 to 0.250 g chitosan was dissolved in 25 mL 0.1 M HCl. Then, an aliquot was mixed with 11.67 g olive oil. The mixture was stabilized in a water bath for 2 hrs at 37 °C after pH adjustment to 2.0 using VWR pH 100 pH meter (VWR International, USA) with Schott Instrument Blueline electrode (SI Analytics, Germany). A 10 mM phosphate buffer saline solution was then added and the pH was adjusted to 7.0. The resulting mixture was stabilized in the water bath for 30 mins. at 37 oC. The mixture was then centrifuged at 2000 rpm speed and 25 oC for 20 mins. The amount of unbound oil is weighed and the oil-binding capacity is calculated in percentage relative to the initial amount of olive oil added. The determination was done two to eight times per sample for Hepepe chitosan and in duplicate for the unknown chitosan.

Statistical Analysis

The free software, 'R' (The R Foundation for Statistical Computing) was used in the statistical evaluation of the results. The 'pls' package was used to perform partial least

squares (PLS) analysis on the derived data (Bjorn-Helge and Wehrens 2007). PLS was used in two ways in this study.

First, PLS was used to determine the DD of U1 and U2. The 'pls' function was performed on the calibration dataset (absorbances of S1 to S10 at the region 1800 to 1500 cm^{-1}) using the default kernel algorithm and with the number of components set to a maximum of eight. Internal validation using the leave-one-out (LOO) technique was done. Based on the calculated root mean square error of prediction (RMSEP), PLS prediction was done with the optimal number of components.

Secondly, PLS was also used to investigate the interaction of chitosan and olive oil as affected by DD and DP. The oil-binding capacities of the chitosan samples were tabulated against the DD and DP. Ten datasets (S1 to S10) were initially selected to be the training set while the two remaining datasets (U1 and U2) were selected to be the test set. All datasets were scaled prior to analysis. The 'pls' function was performed on the training set using the default kernel algorithm and with the number of components set to a maximum of two. Internal validation using the LOO technique was done and results were evaluated by calculating the RMSEP.

The 'scatterplot3d' package, also from 'R' was used to generate the 3D plot to visualize the combined effects of DP and DD on the oil-binding of chitosan. All data pre-treatments were done using Microsoft Excel TM (v. 2007).

Results and Discussion

Degree of Deacetylation and Weight-Average Degree of Polymerization of chitosan

Chitosan samples S1 to S10 were pure chitosan samples with respective COA specifying the DD of the polymers. The DD values are summarized in Table 2.3. Chitosans S1 to S10 were also used as calibration standards to determine the DD of U1 and U2 with FT-IR in combination with PLS chemometric technique. Traditionally, in determining the DD using FT-IR, the absorbances of chitosan standards with known DD at two wavenumbers are selected. One is the characteristic wavenumber which is related to the amide vibrations and can be correlated to the number of the N-acetyl-D-glucosamine monomers. The other is the reference wavenumber which is related to either the hydroxyl groups or the bridge oxygen – carbon bond in the main pyranose ring and can be correlated to the total number of N-acetyl-D-glucosamine and D-glucosamine monomers. The absorbance ratio of the characteristic wavenumber to the reference wavenumber is plotted against DD generating a negatively-

sloped linear calibration curve that can be used to determine the DD of an unknown chitosan (Shigemasa, Matsuura et al. 1996; Brugnerotto, Lizardi et al. 2001).

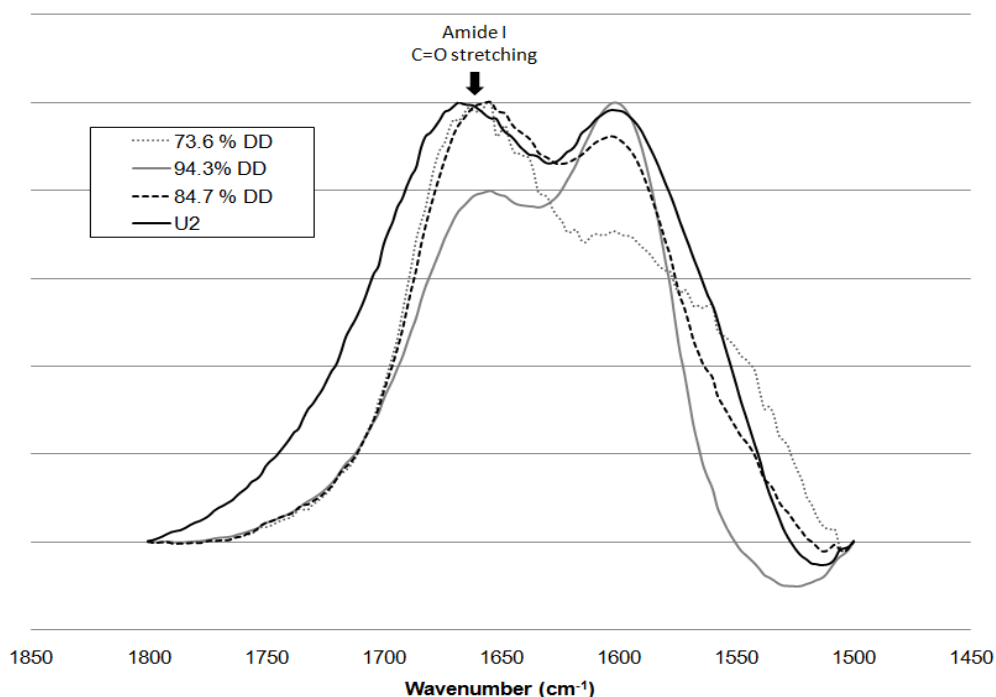


Figure 2.5. FT-IR absorption spectra (normalized to relative to the highest absorbance) at the wavenumber region 1800 to 1500 cm^{-1} of chitosan samples with known degree of deacetylation (73.6%, 94.3% and 84.7%) and of a chitosan sample with unknown degree of deacetylation (U2). The spectra were corrected for the baseline drawn from 1800 to 1500 cm^{-1} and were normalized relative to the highest corrected absorbance.

An alternative method is to consider the whole amide absorption band and correlate the changes in its shape with the change in DD. Figure 2.5 shows how the infrared absorption band shape in the wavenumber region 1800 to 1500 cm^{-1} varies with DD. The absorption at approximately 1660 cm^{-1} is due to the amide I bond vibrations (C=O stretching). Only the N-acetyl-D-glucosamine monomers will exhibit the absorption, thus, as DD is increased, the absorption at this wavenumber is decreased relative to the neighboring band. This creates a change in the shape of the normalized bands. By visual inspection, one can easily deduce that the U2 has a DD between 84.7% and 94.3%.

The PLS method provides a way of estimating more accurately the DD of the unknown samples. PLS was specifically chosen from a number of other multivariate regression techniques like the principal component regression (PCR) because of its robustness to

factors with high variance but not at all correlated to the dependent property (Vandeginste, Massart et al. 1998; Bjorn-Helge and Wehrens 2007). In this chemometric technique, the absorptions of the individual wavenumber within the infrared spectral region 1800 – 1500 cm^{-1} are taken as unique variables. Through the algorithm specified in the PLS package for R (the default Kernel algorithm was used (Bjorn-Helge and Wehrens 2007)), the number of original variables are reduced to only a few components (latent variables). Features reduction is done by linear combination of the original variables (Massart, Vandeginste et al. 1998)). Characteristic of any algorithm used in this family of techniques, the first component is always chosen so that it explains the greatest variation in the spread of data points, component 2 explains the 2nd greatest variation and so on. In the end all the components should be able to explain 100% of the variations in the data. One or more of these components can be used to generate the ‘scores’ that have a linear relationship with the property being predicted, thus can be used as x-variables in a regression model.

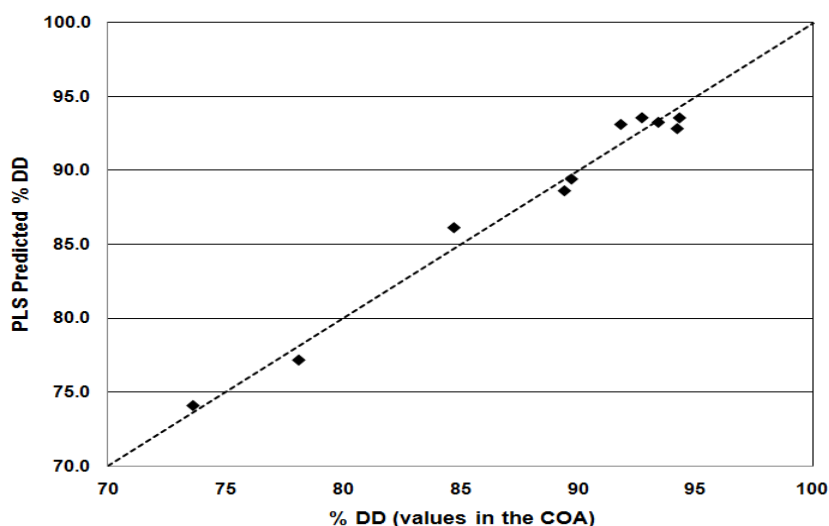


Figure 2.6. External validation of the partial least squares (PLS) model to predict the degree of deacetylation (DD) of chitosan. The dotted line represents: certified DD = PLS-predicted DD.

In the analysis, the ‘plsrf’ function generated a PLS model with 3 components. To find out which of the 3 components or their combinations have a linear relationship with DD, model validation was simultaneously performed using the LOO validation technique. In LOO, one sample is taken out and the model is generated using the remaining samples. The one taken out is then used as a test sample. This process is repeated until a substantial amount of validation points are gathered. The predicted values of the validation points are then compared to the experimental or labeled values. The RMSEP can be calculated based on the difference between the predicted and experimental values. In this study, results revealed

that if only the first component was taken into account in the prediction, the RMSEP was 2.35 %. This value was lowered to 1.81 % if the first and second components were taken. The value was increased again if the rest of the components were added. This implies that two is the optimum number of components in the regression to predict DD. Figure 2.6 shows the external validation using the PLS model with only two components. The low deviation from the dotted line (representing values in the COA = PLS-predicted values) is consistent with the computed RMSEP of 1.78 %. The model was thus used to predict the DD of U1 and U2. The results gave 83.8% and 82.2% DD for U1 and U2 respectively (also shown in Figure 2.6). The relative standard deviation was below 3% for the two to four trial runs.

The COA showed only approximate values for the M_w . It was thus necessary to determine experimentally the M_w by SEC. Most of the chitosan samples are only partially soluble in the mobile phase used. It was thus necessary to use another solvent system to dissolve the chitosan with. The use of 0.3 M acetate buffer as a solvent system for chitosan was shown to give an M_w that is not statistically different from the M_w if the mobile phase 0.2% TFA in 0.3 M NaCl in Milli-Q water is used (Bernhard, Flato et al.). From the M_w and DD data, the DP_w of S1 to S10 was calculated using Equation 2.3. The calculated DP_w of the samples are summarized in Table 2.3.

Oil-Binding Capacity of Chitosan

The oil-binding capacity measures the ability of chitosan to interact with oil. To do this, chitosan is made to form a stable emulsion complex with olive oil. The excess olive oil (unbound oil) is separated from the stable complex and is measured gravimetrically.

The CODEX standard for olive oils and olive pomace oils defines virgin olive oils as the “oils obtained from the fruit of the olive tree solely by mechanical or by physical means under conditions, particularly thermal conditions, that do not lead to alterations in the oil, and which have not undergone any treatment other than washing, decanting, centrifuging and filtration” (CODEX Alimentarius 1981). Results from Prof. Dr. Georg Kurz GmbH, a third party laboratory showed that the fatty acid content of the olive oil used in the study had the following distributions: palmitic acid, 9.9%; stearic acid, 3.3%; oleic acid, 79.1%; linoleic acid, 4.7%; and the rest of the fatty acids are less than 1%. The oil also contains 0.39% (expressed as % oleic acid) free fatty acid. These results are within the criteria set by CODEX Alimentarius (CODEX Alimentarius 1981). The sterol content of the olive oil was not determined although CODEX specifies that virgin olive oil can contain a minimum of 1000 $\mu\text{g/g}$ sterols composed mostly of β -sitosterol, δ -5-avenasterol, δ -5-23-stigmastadienol, clerosterol, sitostanol and δ -5-24-stigmastadienol (CODEX Alimentarius, 1981). In a separate study using phosphorus-31 nuclear magnetic resonance (^{31}P NMR) spectroscopy,

it was found out that olive oils can contain <0.20% 1-monoglycerides and <4.00% total 1,2- and 1,3-diglycerides (Spyros & Dais, 2000). Given these, it is safe to say that the olive oil used in this study is greater than 95% triacylglyceride with mostly C18 unsaturated and C16 saturated fatty acids.

Table 2.4. *Oil-binding capacity of the chitosan samples.*

Sample Code	Oil-binding capacity (%)	
	Value	RSD
S1	40.1	2
S2	86.5	7
S3	33.4	1
S4	38.3	10
S5	52.1	8
S6	22.7	16
S7	77.8	18
S8	35.7	8
S9	44.2	12
S10	27.1	10
U1	62.8	2
U2	69.0	1

The reported oil-binding capacity is expressed in percent. Based on its initial definition, oil-binding capacity does not consider the variable initial amount of chitosan used. To allow comparison, the results were normalized to 4.15 mg initial amount of chitosan and to 11.67 g olive oil used. The results of the oil-binding test are given in Table 2.4.

The oil-binding capacity values represent the means and relative standard deviation (RSD) of 2 to 8 trial runs. It can be observed that some of the RSD of the data is up to almost 20%. The relatively low precision of the oil-binding test results from the low ruggedness of the method used. The neutral pH to which the chitosan-olive oil complex is to be stabilized was difficult to control.

To study the relationship of DP_w and DD versus oil-binding capacity, the values for chitosan S1 to S10 were put in a graph shown in Figure 2.7. Figure 2.7A represents in a 3D graph the general relationship between the variables DP_w and DD versus oil-binding capacity. A regression plane was drawn to visualize the general trend of the data. It can be observed that DD has a greater effect on the oil-binding capacity than DP_w as indicated by the steepness and direction of the slope of the regression plane. This observation is highlighted in the 2D graph representing the projections of the points on the DD vs oil-binding capacity plane in Figure 2.7B. The error bars shown in the figure represent ± 1 standard deviation. There is a clear negatively-sloped linear relationship between DD and oil-binding capacity despite the samples having a wide range of DP.

Evaluation of the Results using Partial Least Squares

PLS was used to correlate DD and DP_w to oil-binding capacity. Initially, PLS was generated using the S1 to S10 as the training set. The kernel algorithm used with the 'pls' function fitted the training set with only two variables (DD and DP_w), and the data was pre-treated by scaling prior to analysis (Bjorn-Helge and Wehrens 2007). Cross-validation of the generated model using the LOO had 9.6 % RMSEP if only one component was used and 9.1% if two components were used. The sources of the large prediction errors were the data coming from samples with low oil-binding capacities. The model with two components can only explain 89.2 % of the variations in oil-binding capacity.

The ability of the regression model to predict the oil-binding of chitosan given only the information on its DD and DP was tested using U1 and U2. Figure 2.8 shows the correlation between the experimental oil-binding capacity and the predicted oil-binding capacity for both the training set and the test set using the PLS model. The data points are scattered around the line experimental oil-binding capacity = predicted oil-binding capacity. The model's prediction of the training set is consistent with the result of the internal validation. The calculated % residuals for the test sets were -4.5 % and -6.8 % for U1 and U2 respectively. The accuracy of the predicted value can only be as good as the precision of the experimental results used to derive the model.

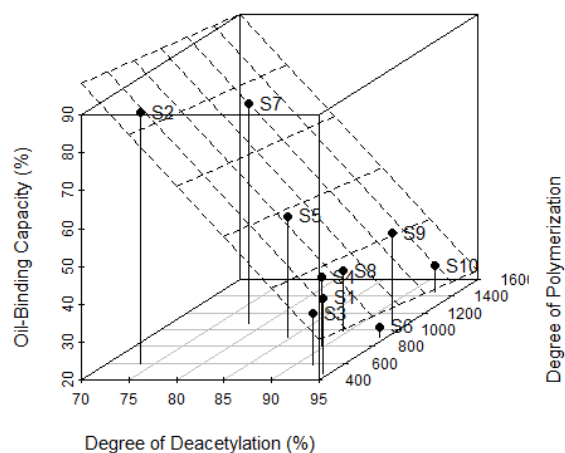
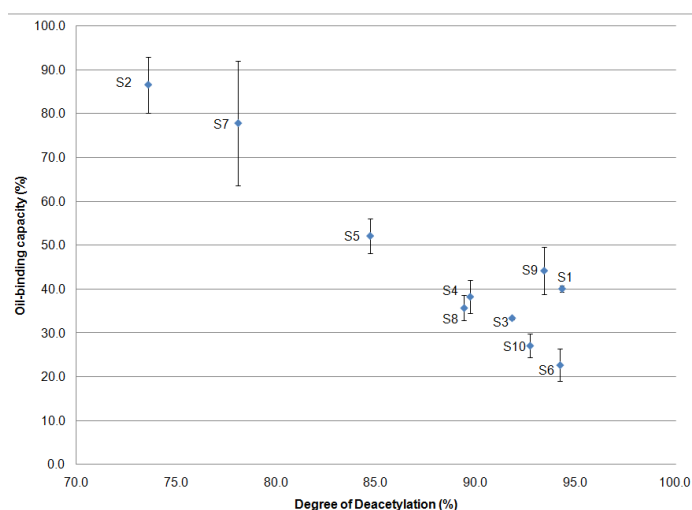
A**B**

Figure 2.7. Relationship between weight-average degree of polymerization (DP_w), degree of deacetylation (DD) and oil-binding capacity. Shown are: A. 3D-graph showing the combined effects of DP_w and DD on the oil-binding capacity; and B. the 2D graph representing the projection on the DD versus oil-binding capacity plane. The error bars represent ± 1 standard deviation.

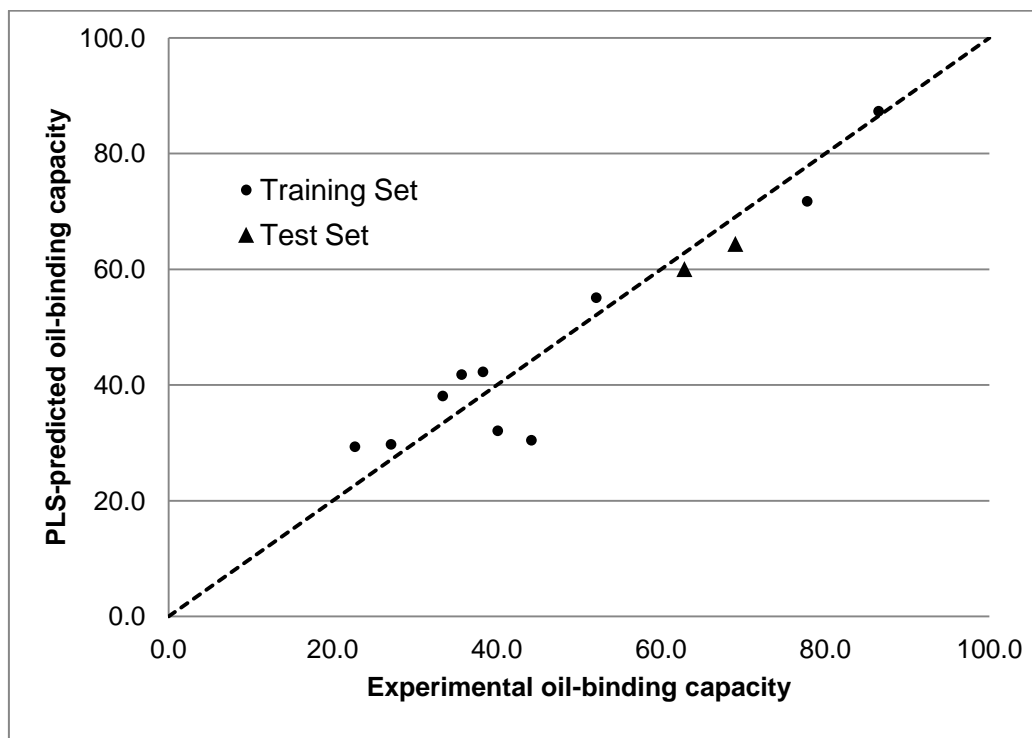


Figure 2.8. External validation of the partial least square (PLS) model to predict the oil-binding capacity of chitosan. The dotted line represents: experimental values = PLS-predicted values.

Interaction of Chitosan and Olive Oil

The oil-binding capacity can be taken as a measure of the stability of emulsion of chitosan and olive oil in an aqueous environment at neutral pH. The olive oil used in the study is a mixture of at least 95% triacylglycerides (based on estimation) and the rest are diacylglycerides, monoacylglycerides and free fatty acids. The behavior of chitosan of a specific DD and DP under the conditions stated dictates its interaction with the glycerides and fatty acids. This can be explained by a number of mechanisms proposed in the literature (Aranaz, Mengibar et al. 2009).

It was shown that chitosan is capable of direct hydrophobic interaction with nonpolar molecules like cholesterol in the air-water interface and can directly eliminate them from aqueous solution. Simulation studies indicated that there are specific sites for interactions between chitosan and stearic acid or cholesterol. Results from a number of experiments shows that cholesterol in aqueous (Liu, Zhang et al. 2008) and in nonpolar solvents such as chloroform (Parra-Barraza, Burboa et al. 2005) can interact with chitosan. The increase in

chain length (greater DP) increases the capacity of the chitosan for van der Waals interaction and thus the ability to bind with fat. However, for large polymers, conformation and folding in a complex aqueous system can decrease the interactions. It was shown in an *in vitro* study that at constant DD, high molecular weight chitosan adsorbed less cholesterol. In the same study, however, the effect of DD was unclear (Liu, Zhang et al. 2008). Zhou et al. also found the same trend for molecular size and the adsorption of olive oil by chitosan. They however have not found significant correlations between physico-chemical properties like DD and oil-binding capacity (Zhou, Xia et al. 2006). The hydrophobic interaction of chitosan with oil need not be a one-to-one interaction. Chitosan was shown to act as an emulsifier providing mechanical and electrostatic stability to the oil droplets resulting to a stable water-oil-water multiple emulsions (Schulz, Rodríguez et al. 1998; Payet and Terentjev 2008; Pereda, Amica et al. 2012).

A different mechanism suggests that chitosan, through the amino group of the glucosamine units, forms an insoluble salt by ionic interaction with bile acid anions (Muzzarelli, Orlandini et al. 2006). These anions are characterized by an ionic end on one side a hydrophobic region on the other. The resulting insoluble salt is hydrophobic and can trap fats like cholesterol and triacylglycerides. A similar mechanism suggests the formation of micelle-like structure with bile salts that can trap fats in the inside. This is made possible with the amino and hydroxyl groups of chitosan acting as an interface between the bile acid anion and the aqueous environment respectively (Thongngam and McClements 2004). Like the bile acids, the free fatty acids in the oil can also interact with chitosan. A study on chitosan-lipid interactions in Langmuir monolayers suggests that fatty acids interact with chitosan in two steps: first is for the fatty acid to anchor in chitosan via electrostatic forces, then second hydrophobic interactions occur between the lipid tail of the fatty acid and chitosan forming the complex. The study noted that the bulkiness and saturation of the fatty acid can influence the interactions (Wydro, Krajewska et al. 2007). This resulting complex of free fatty acid and chitosan can further interact with oils.

At first look, there seems to be a contradiction between the two mechanisms discussed above in explaining the interaction of chitosan and olive oil. However, after considering that chitosan behave differently in aqueous environment depending on its DD (Schatz, Viton et al. 2003), one can conclude that the two mechanisms in reality, complement each other. Chitosan in the domain $50\% < DD < 80\%$ behave in such a way that the hydrophobic and hydrophilic interaction in aqueous environment are counterbalanced. This domain is the interface between the highly electrostatic domain and the hydrophobic domain (Schatz, Viton et al. 2003). In this context, the first mechanism is favored. Chitosan without any need for additional surfactant can act as an emulsifier and interact directly with the triacylglycerides in

olive oil. Based on the PLS model in the previous section, DD has a negatively sloped linear correlation with oil-binding capacity suggesting that the chitosan – triacylglyceride interaction becomes stronger as the chitosan becomes acetylated and less polar. This model is consistent with the results of the study by Muzzarelli et al., where they percolated the olive oil in a column bed with chitin, chitosan or a chitosan derivative. The group found out that chitosan allowed more oil to be percolated through, while chitin on the contrary retained more of the olive oil. The authors also noted that the concentration of diacylglycerides (34 carbon and 36 carbon diacylglycerides) in the olive oil percolated in chitosan decreased compared with the original oil. On the other hand, the concentration of diacylglyceride was enriched in the percolated olive oil in chitin (Muzzarelli, Frega et al. 2000). The trend of oil-binding capacity decreasing with DD can be extended up to DD of 90 % based on the PLS model. The PLS model points to hydrophobic interaction as the dominant intermolecular force of attraction that “binds” chitosan via the N-acetyl-D-glucosamine monomers and olive oil triacylglycerides (Figure 2.9A).

At the region of very high DD (DD > 90 %) the negatively sloped linear correlation tends to be diminished. The amount of N-acetyl-D-glucosamine monomers limits the direct hydrophobic interaction of chitosan to olive oil triacylglycerides. It is inferred that on this region, the 2nd mechanism is favored. The free oleic acid interacts electrostatically with the amine group of the D-glucosamine monomers while at the same time also interacts via hydrophobic forces with olive oil (Figure 2.9B). Under this mechanism, it is expected that as DD is increased, oil-binding capacity should increase. However, in the results of this study (see Figure 2.8B), some points were off the line. In the oil-binding test, no additional oleic acid was added and the olive oil contained only 0.39 % free oleic acid. This paucity of free fatty acids could be a limiting factor in the interaction of excess chitosan and the olive oil triacylglycerides.

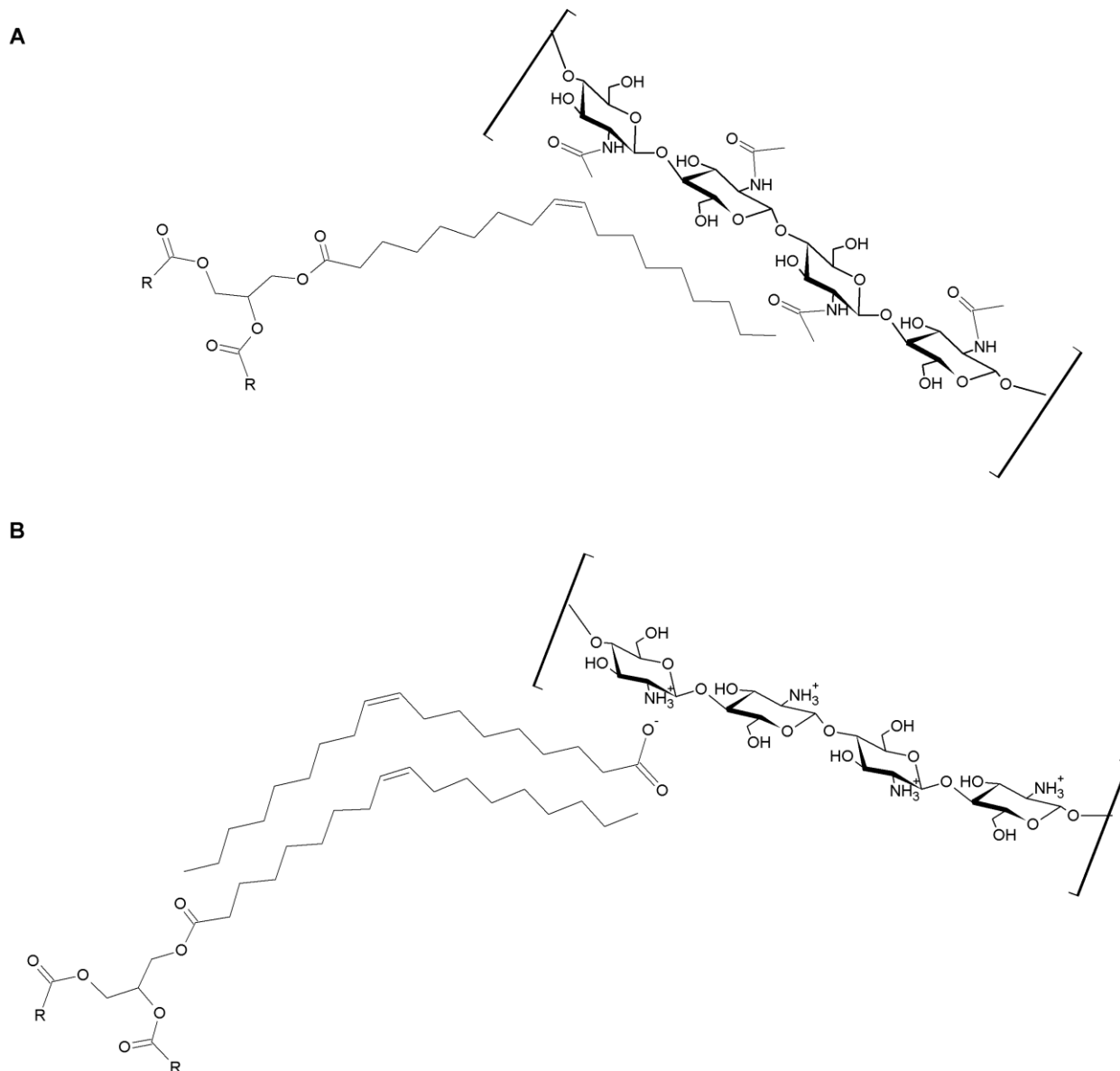


Figure 2.9. Interaction of chitosan with olive oil. Shown is a representative triacylglyceride of olive oil with an oleic acid and two other fatty acids represented by R. A. Chitosan interacts directly with olive oil through the N-acetyl-D-glucosamine monomers; and B. Chitosan interacts indirectly with olive oil with the aid of free fatty acid (oleic acid) that is electrostatically bound to the amine group of the D-glucosamine monomer.

Conclusion

The behavior of chitosan in aqueous solutions of high ionic strength governs its interaction with olive oil. In this study, the oil-binding capacity was taken as a measure of the strength of the interaction of chitosan and olive oil. PLS was used to study how the interaction is affected by the basic properties of chitosan as a polymer namely its DD and DP. It was found that DP and DD influence the polymer's capacity to interact with olive oil; with DD having the greater effect. For chitosan with DD in the interval $50\% < DD < 90\%$, oil-binding capacity increased with the increasing hydrophobicity of chitosan with the decrease in its DD. For chitosan with $DD > 90\%$, electrostatic forces dominates the interaction. Free fatty acid anions assist in the chitosan and olive oil by forming a stable ionic interaction with the former and a strong hydrophobic interaction with the later.

Chapter 3. REVIEW: MASS SPECTROMETRY OF POLYMERS

ABSTRACT

Polymers are large molecules composed of repeating monomer units. Variations in the composition and number of monomers, average size, distribution, microstructure and the functional groups attached to the basic units create thousands of different polymer substances with a wide range of physico-chemical properties and suit a variety of uses. In the recent years, time-of-flight mass spectrometry (TOF MS), especially the tandem with matrix-assisted laser desorption ionization (MALDI), plays a complimentary but vital role in polymer characterization. The mass spectrum provides a wealth of data regarding the structure, composition and functionality of the individual polymer specie. This unique information from MS is necessary in elucidating structure-property-activity relations. The use of MALDI-TOF MS in polymer analysis can be extended to study the fate and degradation of the large molecules in aqueous environment.

Keywords: MALDI-TOF MS, matrix, ESI, polymer, average molecular weights, degradation

Published as part of a book chapter in:

“TOF MS within Food and Environmental Analysis.” A.R. Fernandez Alba (ed.). *Comprehensive Analytical Chemistry* **58**: 307 – 338. Elsevier: Amsterdam, The Netherlands

Dimzon, I.K.D., Knepper, T.P. 2012. MALDI-TOF MS for characterization of synthetic polymers in aqueous environment

Introduction

Polymers are composed of repeating structural units called monomers. A polymer can be made-up of one (homopolymer) or more (copolymer) type of monomers linked together by a covalent bond. The European Chemicals Agency (ECHA) specifies that a polymer is a “sequence of at least three monomer units” bound to “at least one other monomer unit or other reactant” (ECHA 2012). The degree of polymerization (DP) refers to the total number of basic structural units including the end group. DP is related to both the chain length and to the molecular weight (Stevens 1990). Polymers are usually distributed over a range of molecular weights. The polydispersity index, calculated as the ratio of the weight average molecular weight (M_w) to the number average molecular weight (M_n), describes the size distribution of the polymer. Polymers vary in the way one or more monomer units are arranged in a microstructure. They can be linear, branched or cyclic. Many polymers are functionalized in the monomers or in the end group to enhance their properties.

By varying the monomer composition, average size, distribution, microstructure and the functional groups attached to the monomer, materials scientists and engineers are able to synthesize thousands of different polymer substances with a wide range of physico-chemical properties to suit a variety of uses. Indeed, many of the things being used today - from pharmaceuticals, cosmetics and household items; to construction and building supplies; to packaging and electronics contain polymer components.

Polymers are exempted from registration and evaluation under the European Registration, Evaluation, Authorization and Restriction of Chemicals (REACH) framework (The European Parliament and the Council of the European Union 2006). Compared to other substances, the risk posed by polymers is minimal due to their high molecular weight (ECHA 2012). Specific polymers may however be subject to authorization and restriction after evaluation of the risk they pose to human health and to the environment. On the other hand, monomers and intermediates are not exempted from registration and evaluation. In relation to the policy, there is a need to differentiate in a polymer sample the individual molecular specie, including the unreacted monomer impurities.

Because of their wide range of applications, polymers have become ubiquitous in the environment. Soluble, polar polymers readily enter the aqueous environment as part of effluents. Many of the synthetic polymers degrade very slowly making them proliferate in the ecosystems. Researches on the fate and degradation of polymers are necessary to better understand the long-term effects of these compounds in the environment. A highly selective but more robust and sensitive analytical method is indispensable to understand the transformations of these substances during the degradation process.

A number of techniques are currently used to characterize polymers. Infrared (IR), raman, UV-visible and nuclear magnetic resonance (NMR) spectroscopy are used to determine and confirm monomer composition and degree of functionalization. Size-exclusion chromatography (SEC) with refractive index, viscosity and light scattering detectors is used to estimate the average molecular weight and the polydispersity index. These techniques along with others like x-ray crystallography, differential scanning calorimetry, and dynamic mechanical analysis are used to test the physico-chemical properties of the raw or bulk polymers. These techniques, however, may not be fit-for-purpose in other areas of polymer research like in the structure elucidation of the individual components and in structure-property-activity relationship studies.

The use of mass spectrometry (MS) in polymer analysis has greatly increased at the onset of the 21st century. This trend was primarily driven by the development in the soft-ionization techniques like matrix-assisted laser desorption ionization (MALDI) and electrospray ionization (ESI) and by the improvements in the time-of-flight (TOF) mass analyzers. MS is not regarded as an alternative to the existing methods of polymer characterization but rather a complimentary method that gives additional information about the structure, absolute molecular weights, and degree of polymerization and functionalization, and end groups of the polymer. In contrast to NMR that is a widely used method to gain insight on the monomer composition and the general polymer structure, MS provides information on the identity and the relative amounts of every component present in a polymer sample including unreacted monomers.

MS offers a fast, robust, highly selective and sensitive method of detecting polymers. The capabilities of MS can be exploited to widen the scope of polymer analysis beyond the realm of materials science to other areas like environmental science, pollution control and sustainable development. Currently, the use of MS in polymer research is limited by the molecular weight of the polymer under study and the diversity and complexity of polymer mixtures. These limitations are addressed by careful selection of a better suited MS and sample preparation techniques.

In the MS of polymers, MALDI and ESI are the usual modes of ionization while TOF, quadrupole and fourier-transform ion cyclotron resonance (FT-ICR) are the preferred mass analyzers. The unique tandem of MALDI and TOF is of particular interest as it has become one of the routine (Montaudo, Samperi et al. 2006) but most powerful tools in polymer analysis today.

This paper reports on the current trends in the TOF MS analysis of polymers. It specifically highlights the use of MALDI-TOF MS. In the later part, examples on the use of MS in polymer characterization and degradation studies are given.

Mass Spectrometry of Large Molecules

Koichi Tanaka and coworkers, reported in 1987 during the 2nd Japan-China Joint Symposium on Mass Spectrometry the detection of different proteins with molecular weight between 10 to 100 kDa. The protein was mixed with ultrafine metal powder and glycerol and was analyzed in an MS equipped with pulsed N₂ laser and TOF mass analyzer (Tanaka 1987; Tanaka, Waki et al. 1988). This was the first reported detection of a high molecular weight compound using MS. Prior to this, in 1985, Michael Karas, Doris Bachmann and Franz Hillenkamp of Germany, were already developing a method that makes use of light-absorbing substances to aid in the desorption of the analyte leading to a more efficient ionization of organic molecules (Karas, Bachmann et al. 1985). They later demonstrated, in 1989, that the technique can be extended to desorb nonvolatile compounds and protein macromolecules of the mass range greater than 10 kDa. They coined the terms “matrix” to refer to the light-absorbing substance and “matrix-assisted laser desorption ionization” or MALDI to describe the new found technique (Karas, Bachmann et al. 1987; Karas and Hillenkamp 1988).

At about the same time, at the other side of the globe, John Fenn and coworkers were working on the necessary modification in the ESI instrumentation initially developed by Dole to make it better suited for MS. They reported in 1989 the detection of oligonucleotides and proteins having molecular weight of up to 130 kDa (Fenn, Mann et al. 1989). They noted the prevalence of multiply-charged ions enabling the detection of large molecules in a quadrupole mass analyzer with a mass range of up to only 1500 Da.

There is no doubt that the development of MALDI and ESI had been one of the major catalysts in the growth of the “omics” sciences and modern biochemistry. In 2002, because of their important contributions in the analysis of biological macromolecules, Tanaka and Fenn shared the Nobel Prize in Chemistry with Kurt Wüthrich. Wüthrich was credited for his work on the structure elucidation of proteins using 2D nuclear magnetic resonance (NMR) spectroscopy (The Royal Swedish Academy of Sciences).

Two most important parameters used to evaluate the performance of MS methods are mass resolution and mass accuracy. Mass resolution is defined as the ratio of a specific mass to the difference in mass (Δm). The Δm can be estimated from the width of a single peak at a defined height. The related term, mass-resolving power refers to the ability of the MS to

separate two neighboring peaks. Instruments with greater mass resolution are capable of separating two narrowly separated peaks and so have high resolving power (Gross 2004; Marshall and Hendrickson 2008). A high resolution MS is needed for accurate mass determination. Mass accuracy, refers to the difference between the mass measured by the instrument and the calculated exact mass. Mass accuracy can be expressed relative to the mass for which it is determined and is usually reported in parts per million ($\times 10^6$, ppm). Highly accurate mass improves the specificity of MS and thus is an important requirement in identifying unknown substances. In proteomics, for example, the number of proteolytic fragment masses needed to identify or confirm a protein decreases with increasing mass accuracy (Easterling, Mize et al. 1998; Mann and Kelleher 2008).

The progress in MS in the last two decades has been overwhelmingly fast. Developments in electronics and instrumentations paved way for mass analyzers with very high resolving power like the modern TOF and FT-ICR. These mass analyzers are easily interfaced with MALDI and ESI for the accurate determination of molecular weights of large molecules.

Although not as dramatic as in biochemistry, a growth in the use of MS was also observed in polymer research. Hart-Smith and Barner-Kowollik noted that after 1989, there was a rise in the number of publications drawn from *SciFinder Scholar* using the search terms 'mass spectrometry' and 'poly', year after year. This only attests to the increasing importance of MS in polymer characterization. They noticed, however, that the use of MS in polymer science "remains unduly limited" compared to other techniques, despite the numerous capabilities and possibilities that MS can offer (Hart-Smith and Barner-Kowollik 2010). Among the various MS techniques available for polymer analysis, MALDI-TOF MS have gained the most attention. Compared to other high resolution techniques, MALDI-TOF MS is less expensive, more rugged, faster and simpler to operate. That of the MALDI and TOF is a unique combination that is especially fit for polymer analysis.

Matrix-Assisted Laser Desorption/Ionization Process

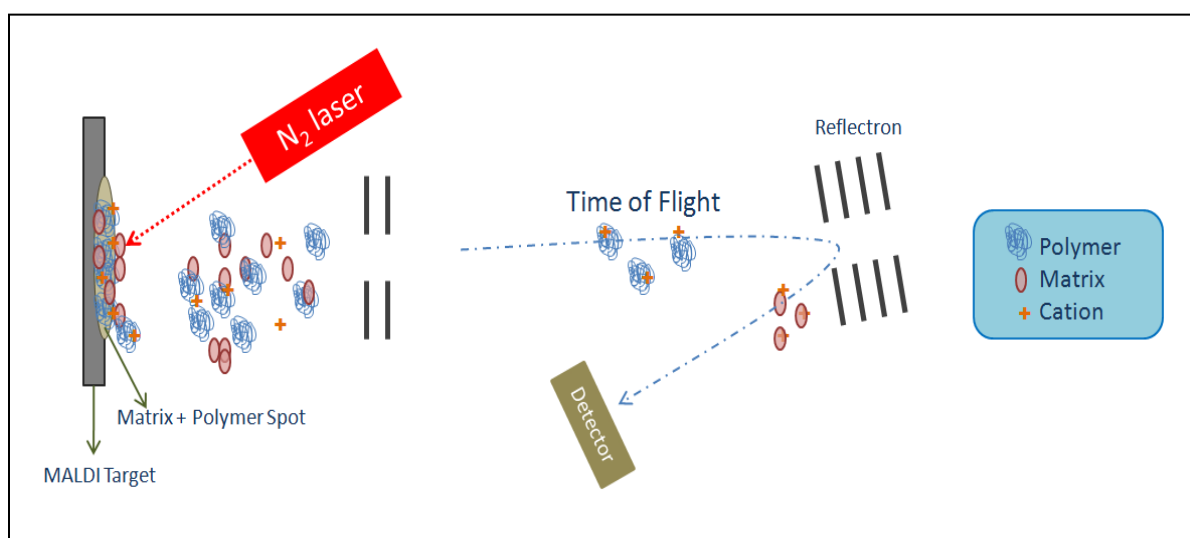


Figure 3.1. Schematics of MALDI with reflector mode TOF MS.

Figure 3.1 illustrates the MALDI-TOF process. The analyte (in this case the polymer), mixed with matrix, is spotted into a MALDI target. The solvent is usually allowed to evaporate leaving the spot dry. A laser is then fired into the spot at a very fast pulse time inside a vacuum chamber. The matrix absorbs the radiation and transfers the energy to the polymer molecules causing the latter to be desorbed and ionized.

The laser provides the energy needed for the ionization of the analytes. Different ultraviolet (UV) and infrared (IR) lasers are available for use in MALDI. The lasers are capable of very short pulses causing the rapid desorption but not the thermal degradation of the sample (Gross 2004). Prevention of thermal degradation is an important feature of soft-ionization techniques that make possible the MS analysis of large molecules. The desorption process is affected by the energy density reaching the sample rather than the rate of energy flow (Zenobi and Knochenmuss 1998). To limit the amount of energy reaching the sample, the laser signal is lessened by putting a rotating radiation filter that controls the amount of transmitted light (Gross 2004). The laser attenuation can be adjusted so as there is enough energy for analyte desorption and ionization but not too much to initiate fragmentation. The N₂ UV- laser (337 nm) is the most commonly used laser source.

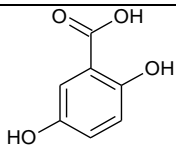
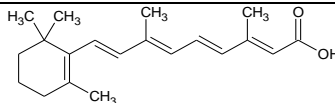
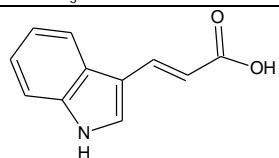
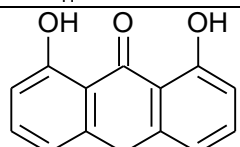
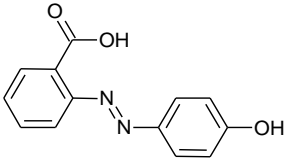
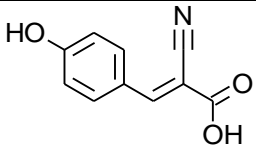
Matrix substances are compounds added to the analyte to aid in the laser desorption of the later. To qualify as a matrix, the compound must have a high molar extinction coefficient at the wavelength emitted by the laser; is stable under vacuum and not reactive with other components; and is compatible with the solvent used to dissolve the analyte (Macha and

Limbach 2002; Hart-Smith and Barner-Kowollik 2010). There is no established rule yet as to the choice of matrix in a specific MALDI run. Trial and error is employed to determine the best matrix for a specific analyte (Macha and Limbach 2002; Hart-Smith and Barner-Kowollik 2010), yielding surprising results in some cases. Choosing the matrix that has a polarity close to that of the analyte is a good starting point (Macha and Limbach 2002). Montaudo et al. suggest a two-step process of selecting a matrix for a particular polymer. The first step is to consider the backbone structure of the polymer and search the literature for matrices that have been applied for a similar backbone. There are some databases available that tabulates various matrix and backbone combinations. The second step is to try experimentally the top three or four matrices found in step one and determine which matrix gives the highest quality spectrum (Montaudo, Samperi et al. 2006). Other methods of finding a suitable matrix involve the use of reverse-phase high performance liquid chromatography (Hoteling, Erb et al. 2004) and chemometric calculations using principal components analysis (Meier, Adams et al. 2006) to compare the polarity of the analyte and the matrix.

Aside from absorbing the radiation, the matrix dilutes the analyte molecules preventing analyte-analyte and analyte-surface interactions. A good matrix must therefore be able to isolate the individual analyte molecules and allow a more efficient desorption and ionization (Hart-Smith and Barner-Kowollik 2010). In polymer characterization, an inhomogeneous mixture of analyte and matrix in a spot can not only lead to a decrease in signal intensity and reproducibility but also can result to a bias against the detection of certain specific polymer chain components (Hart-Smith and Barner-Kowollik 2010). If the matrix and polymer are not compatible, they crystallize separately. The polymer is not desorbed and ionized as in the case of polystyrene mixed with 2,5-dihydrobenzoic acid matrix (2,5-DHB) (Bahr, Deppe et al. 1992). Some matrices have been found to induce fragmentation of analytes (Karas, Bahr et al. 1995). Fragmentation due to matrix effects alters the molecular weight distribution of polymers as seen in the mass spectrum (Wetzel, Guttman et al. 2004).

Table 3.1 shows some of the commonly used matrices for polymers. The 2,5-DHB matrix is used for a wide range of polymers. The table is not complete but nonetheless gives a broad idea of what matrix to use for some common polymers. In some instances, a combination of matrices can give better desorption and ionization of the analytes. For example, the combination of DHB and 1-hydroxyisoquinoline gives better signal in the MALDI-TOF MS of oligosaccharides (Mohr, OlafBörnson et al. 1995). The combined matrix improves the co-crystallization (Zenobi and Knochenmuss 1998) and the distribution of the analyte in the spot.

Table 3.1. Some commonly used matrices for the MALDI of Polymers. The structures shown were drawn using ChemSketch (ACDLabs).

Matrix	Structure	Polymer analyzed	References
2,5-dihydroxybenzoic acid (DHB)		ethoxylates oligosaccharides poly(methyl methacrylate) poly(vinylpyrrolidone) polystyrene	(Lee, Rumbelow et al. 2009) (Mohr, OlafBörnsen et al. 1995) (Jackson, Larsen et al. 1996; Larsen, Simonsick et al. 1996) (Trimpin, Eichhorn et al. 2001) (Wetzel, Guttman et al. 2004)
all- <i>trans</i> retinoic acid (trans-RTA)		polydienes polystyrene	(Yalcin, Schriemer et al. 1997) (Schriemer and Li 1996; Wetzel, Guttman et al. 2004)
Trans-3-indoleacrylic acid (IAA)		polyesters poly(vinylpyrrolidone) poly(methyl methacrylate)	(Williams, Gusev et al. 1997) (Trimpin, Eichhorn et al. 2001) (Larsen, Simonsick et al. 1996)
Dithranol		Low MW polydienes polystyrene	(Yalcin, Schriemer et al. 1997) (Wetzel, Guttman et al. 2004)
2-(4-hydroxyphenylazo)-benzoic acid (HABA)		polystyrene poly(methyl methacrylate)	(Montaudo, Montaudo et al. 1994) (Larsen, Simonsick et al. 1996)
α -cyano-4-hydroxycinnamic acid (4-HCCA)		Polyethylene glycol	(Bernhard, Eubeler et al. 2008)

When the laser hits the surface of the analyte-matrix spot, a rapid solid to gas phase transition occurs releasing single molecules and ions as well as aggregates. There are a variety of ions present in the plume. Some ions like metal cations and polymers with ionic end group are already preformed. These ions are then just desorbed into the plume during the explosive expansion of matrix. Most of the ions, however, are formed during and after the laser irradiation. Ion formation is complex and no single mechanism can explain and account for the many different ions formed during the MALDI process. Zenobi and Knochenmuss classified the different mechanisms under two categories namely primary and secondary. Primary ionization involves the generation of ions from the neutral molecules upon irradiation. The generated ions are usually coming from the matrix molecules upon absorption of radiation and can be in many forms depending on the preferred mechanistic route. The ions can be radical cations; protonated and deprotonated adducts; and matrix aggregates (Zenobi and Knochenmuss 1998).

Secondary ionization involves generation of ions in the MALDI plume after irradiation. Gas-phase diagnostics and laser-induced fluorescence imaging revealed that the MALDI plume is dense and multicomponent, mostly of intact matrix molecules (Poretzky and Geohegan 1998). This suggests high frequency of collision and that the reactions continue in the plume even after irradiation via secondary processes. Secondary ions are usually analyte ions and can also be in many forms: radical cations, protonated and deprotonated products and metal cation adducts (Zenobi and Knochenmuss 1998).

Polymer ions produced via MALDI are predominantly cation adducts. These ions are either pre-formed or are formed via secondary processes (Knochenmuss, Lehmann et al. 1998). Relatively polar polymers with heteroatoms like oxygen and nitrogen can form metal ion complexes through their lone pairs. Nonpolar, unsaturated polymers form metal ion complexes through the π -bonds (Macha and Limbach 2002). The metal ion - polymer complex can be pre-formed in the MALDI sample spot and then are just desorbed during plume formation. In this mechanism, a substantial amount of cation is needed since matrix molecules compete with the polymer for the free metal (Knochenmuss, Lehmann et al. 1998). Polymer and cations can also combine via a secondary process in the plume. The polymer molecules and cations are first separately desorbed into the plume. They then combine to form the polymer ions in the gas phase. In this mechanism, even a small amount of cation can readily react with polymer molecules. Evidences from experiments suggest that the second is more likely than the first mechanism. For instance, improved analyte signal was observed for the poly (methyl methacrylate) – dithranol mixture that was spotted on top of a previously spotted salt layer compared to if everything was mixed together before spotting. This means that by separately spotting the salt solution and the analyte-matrix mixture, the likelihood of forming metal-polymer complex prior to irradiation is decreased. Yet, this gives better signal than if everything were mixed together. It follows that complex formation happens after irradiation (Hobert and Haddleton 1997). It is also important to note that unlike in the ionization of biomolecules, protonation is not readily observed for polymer analytes (Knochenmuss, Lehmann et al. 1998).

Energy calculations for NaCl showed that the the Na^+ would require large energy for it to be released from its ionic interactions in a crystal structure. This energy however is decreased significantly for the Na^+ in the surface or in the crystal defect site (Knochenmuss, Lehmann et al. 1998). This gives a hint that the formation of highly ordered crystal structure in the sample spot preparation will decrease the ion intensity of the polymers.

Polar, synthetic polymers are speedily ionized by alkali metal cations using standard MALDI protocols initially developed for proteins. Nonpolar polymers, on the other hand, do not ionize with alkali metal cations and require a different approach using silver and copper ions

(Macha and Limbach 2002). This can be attributed to the low binding energy of the alkali metal cation to the nonpolar polymers. *Ab initio* quantum calculations, for example, revealed that sodium – polyolefin complexes have low binding energy causing the complex not to form or survive the high collision environment in the plume (Reinhold, Meier et al. 1998; Macha and Limbach 2002).

Sample Preparation

The quality of the polymer-matrix spot is an important concern that must be addressed to get a highly reproducible mass spectrum. Generally, the ideal spot for MALDI is thin, less crystalline and evenly spread. The polymer and the matrix molecules must be homogeneously distributed in the spot (Sigma-Aldrich 2001). Choosing the right matrix and employing a better suited sample preparation technique are critical in MALDI analysis (Gruending, Weidner et al. 2010).

MALDI spot preparation involves the following key steps: dissolving the polymer and the matrix in a proper solvent, spotting the analyte and matrix solutions into the MALDI target and evaporating the solvent.

A good solvent for MALDI must be able to dissolve both the polymer and matrix. For polymers in aqueous environment, the choice of solvent is not much of a problem since most matrices available are water-soluble. The choice of solvent is quite problematic for nonpolar polymers in organic solvents that need to be combined with a matrix and cationizing agents in aqueous media. Yalcin et al. discussed the idea of polymer nonsolvent and its effect on MALDI results. A polymer nonsolvent is a solvent in which the polymer is insoluble at any temperature at atmospheric pressure (1 atm). Solvent mixtures containing substantial amount of a polymer nonsolvent cause poor reproducibility and erroneous average weight results (Yalcin, Dai et al. 1998). In choosing the solvent, volatility must also be weighed in. Fast evaporation of solvent promotes the formation of a less crystalline but more homogeneous analyte-matrix spot, thus, an ideal solvent to use must be reasonably volatile.

Another consideration in choosing a solvent is the spreading of the solution in the stainless steel MALDI target. The combination of surface tension and viscosity in overcoming the applied inertia during dropping gives rise to dynamic contact angles (Vadillo, Soucemarianadin et al. 2009). A solution with less surface tension, when dropped into the stainless steel target tends to have low dynamic contact angle and tends to spread. The resulting MALDI spot, although thinner, has a wider diameter. The distribution of analyte molecules in the matrix becomes more dispersed, diluted and nonhomogeneous. On the other hand, a drop with greater surface tension tends to have higher dynamic contact angle

in the metal surface and tends to stay compact. The resulting spot is thick and with narrower diameter.

After establishing what matrix and solvent to use, the next step is to form the MALDI spot. Table 3.2 enumerates some of the sample spot preparation techniques used for polymer samples. The table includes a brief description on how the technique is done. The variations in the techniques are due to any of the following: 1.) whether to apply the analyte and matrix together as one mixture or separately, one after the other; 2.) speed of evaporating the solvent; and/or 3.) necessity for separation of components by forming layers.

The dried droplet method is the oldest and the most widely used method of preparing the sample spot. All the components are first mixed together forming a single solution. A drop of the solution is then spotted into a MALDI target and air-dried. The dried droplet method was found to be inadequate in some applications. For one, the process of evaporating the solvent at normal room conditions (25 °C, 1 atm pressure) takes a while promoting slow crystallization and segregation of analyte and matrix (Montaudo, Samperi et al. 2006). Moreover, if cationization salt is added, slow crystallization favors the formation of highly ordered crystalline structure which is undesirable during desorption and ionization process. To promote the rapid crystallization, vacuum drying and spin coating techniques were employed and were proven to work better than dried droplet in some polymers. In the quick and dirty method, the analyte is spotted first into the MALDI target. This allows for some on-target modification of the analyte prior to the addition of the matrix solution. Layered deposition is done if the effect of a certain component in the mixture is to be magnified or to be decreased.

The diameter of the sample spot produced by dried droplet or by other methods that involve directly spotting 0.5 - 1.0 μL of the solution unto the target is 1 – 4 mm. This is comparatively large compared to the spot of laser irradiation which has a diameter between 0.05 – 0.20 mm. Ion generation is limited only in a small area where the laser hits the spot. As a consequence, mass sensitivity and reproducibility are not that good. High signals are obtained at random and only if the laser happens to hit a hot spot (or sweet spot). A hot spot is a small area where there is a large concentration of analyte resulting from uneven distribution of analyte and matrix (Wei, Nolkrantz et al. 2004; Gruending, Weidner et al. 2010).

Table 3.2. *Commonly used sample preparation techniques in MALDI of polymers.^a*

Technique	Description
Dried-Droplet	The polymer (analyte) solution is mixed with matrix solution. A drop of the mixture is spotted into the MALDI target and air dried.
Vacuum-Drying	The polymer solution is mixed with matrix solution. A drop of the mixture is spotted into the MALDI target and vacuum-dried.
Fast Evaporation	A drop of matrix solution is spotted into the MALDI target and dried. The polymer solution is then applied over the matrix and dried.
Quick and Dirty	A drop of matrix solution is placed over the drop of polymer solution. The spot is allowed to dry.
Overlayer	The mixture of polymer and matrix solutions is spotted over the first layer of small crystals.
Spin-Coating	The mixture of polymer and matrix solutions is spotted on top of a rotating target.
Electrospray	The mixture of polymer and analyte solution is introduced into the MALDI target by aspiration in an electrospray needle.

^aThe names and descriptions of the techniques are based on the “Analytix” guide provided by Fluka (Sigma Aldrich) (Sigma-Aldrich 2001). The only exception is the electrospray technique which is a more recent addition.

Mass sensitivity and reproducibility are greatly improved if the sample spot is reduced to the size of laser irradiation. The electrospray technique (this MALDI sample preparation technique must not be confused with the ESI) gives a significantly smaller sample spot. In this method, the mixture of analyte and matrix is passed through a needle with applied high voltage. The charged solution is then sprayed into a MALDI target via a capillary electrospray emitter. The sample spot produced using this method has a diameter of 0.2 -0.3 mm and is comparable to the size of the laser irradiation spot (Wei, Nolkranz et al. 2004). Using polystyrene, dithranol as matrix and silver trifluoroacetate as ionization reagent, Hanton et al. studied the morphology of the spots prepared by dried droplet and by electrospray techniques. Scanning electron microscopy (SEM) reveal that the dried droplet sample is crystalline and highly heterogeneous with a wide variety of crystal sizes and sites. Electrospray sample, on the other hand, is composed of individual, small and highly uniformed spheres resulting to excellent precision in determining the molecular weight

distribution of polymers (Hanton, Hyder et al. 2004). Using the Bradykinin neuropeptide, it was demonstrated that the electrospray method gave better figures of merit than the dried droplet technique: more linear response ($R^2 > 0.99$) at a defined concentration range (35 – 345 amol); high reproducibility; and limit of detection at attomole range (Wei, Nolkrantz et al. 2004). These figures are promising signs that point to the development of quantitative MALDI-TOF MS in the future. Unlike in samples prepared by other techniques, electrospray samples can also produce multiply charged ions by MALDI (Kononikhin, Nikolaev et al. 2005) provided that the molar ratio of analyte, matrix and cationizing agent is optimized.

Hyphenation with Time-of-Flight Mass Analyzer

TOF is the ideal mass analyzer for MALDI. The ions formed from MALDI are easily directed towards the entrance of the TOF mass analyzer where a uniform accelerating potential is applied on the ions. The ions fly in the flight tube at a velocity inversely proportional to $(m/z)^{1/2}$. Since the distance travelled by the ions is constant, the m/z can be estimated by monitoring the time the ions reaches the detector. In principle, there is no upper limit in the m/z that TOF can separate and analyze. The high mass limitation can be due to other factors such as ion formation and ion detection.

During laser irradiation, ions of varying initial kinetic energy are formed. The initial kinetic energy adds to the accelerating potential applied to the ions at the entrance of TOF making the total kinetic energy of the ions slightly variable (Cotter 1992). As a consequence, ions with the same m/z travel at slightly different velocity and do not reach the detector at the same time. The resulting mass spectrum exhibits broadening of signal peaks and diminishing of mass resolution (Gross 2004).

To correct for the slight differences in initial kinetic energy, a reflectron is added at the end of the flight tube (Figure 3.1). The reflectron is made up of a series of rings with increasing voltage. As the ions of the same m/z but different kinetic energies approach it, the ions with larger energies penetrate more deeply taking a longer flight path than the ions with less energy. The ions will reach the detector at almost the same time. The generated mass spectrum shows narrower signal peaks and a significant increase in mass resolution (Cotter 1992). The reflectron mode, however, has some limitations in the high mass region (greater than 10 kDa) because large molecules have shorter flight paths (Belu, DeSimone et al. 1996). Both the linear mode and the reflector mode are used in polymer characterization.

From the analytical viewpoint, the unlimited mass range of linear TOF compliments MALDI's production of singly-charged ions. This is especially vital in the analysis of complex high molecular weight polymers. From the instrumentation viewpoint, both TOF and MALDI are pulsed methods. Fewer adjustments will be necessary to interface the two together.

MALDI can also be interfaced with a more powerful mass analyzer like the FT-ICR. In FT-ICR, the ions with low kinetic energy are trapped in a high magnetic field. The ions oscillate upon exposure to the oscillating radio frequency electric field in a frequency (ion cyclotron frequency) proportional to their m/z . The resulting overall signal is converted into a mass spectrum by Fourier-transform (Hart-Smith and Barner-Kowollik 2010). FT-ICR instruments have the greatest mass-resolving power from among the modern mass spectrometers but up to a limited mass range only. The high mass limit of FT-ICR is dependent on the strength of the magnetic field applied to maintain the oscillating ions inside the trap and on the trapping potential. Molecules with masses above the high mass limit will not be detected in the FT-ICR (Marshall, Hendrickson et al. 1998). Also, the FT-ICR cells can contain only a limited number of ions above which ion-ion repulsions occur causing the ions with nearly the same mass to charge ratio to coalesce. Large molecules show higher tendency to coalesce (Easterling, Mize et al. 1998; Marshall, Hendrickson et al. 1998).

While MALDI can be interfaced with FT-ICR, this combination will have limited applicability in polymer analysis. First, MALDI produces singly-charged ions. The ions coming from large molecular weight polymers will not be detected in the FT-ICR due to inherent mass limitation of the cell. Secondly, if polymer ions are detected, the best resolution known for FT-ICR will not be met because of peak coalescence. And thirdly, polymer ions unlike proteins are not composed of only one type of molecule. Given the limitation in the number of ions that FT-ICR cells can contain, the sensitivity of the method is greatly reduced with the increase in the number of different types of ions present.

Matrix-Assisted Laser Desorption/Ionization Mass Spectrum

Figure 3.2a shows a sample mass spectrum generated using MALDI-TOF MS. Polyethylene glycol (PEG) was dissolved in deionized water. A portion of the PEG solution was mixed with 2,5-dihydroxybenzoic acid matrix and was spotted in a MALDI target. The analysis was then carried out in Ultraflex III™ Bruker Daltonics MALDI-TOF/TOF MS. Ion separation was done in the reflector mode. The obtained mass spectrum was the sum spectrum of 4000 laser shots (10 different points in the spot x 400 shots per point).

Two apparent distributions can be seen from the MALDI mass spectrum of PEG but closer examination suggests that there is only one polymer distribution but two different cationization routes. The major series (*) is due to the attachment of a Na^+ to the PEG. For instance, the peak with m/z 1009.533 Da in the spectrum corresponds to $[\text{H}(\text{OCH}_2\text{CH}_2)_{22}\text{OH} + \text{Na}]^+$ ion with calculated monoisotopic mass of 1009.577 Da. The calculated mass accuracy was 44 ppm. The resolution was shown to be 4900. The minor series (x) is due to

the attachment of K^+ . The peaks are separated by 44.0 Da corresponding to the PEG monomer unit ($-OCH_2CH_2-$). The area below 400 Da (not shown in the spectrum) included ions produced from DHB matrix. It was suggested to use the term modal molecular weight (M_m) to refer to the molecular weight with highest intensity in the mass spectrum of polymer samples. In Figure 3.2a, the peaks with highest intensities are 1056 Da and 1070 Da corresponding to the Na^+ and K^+ adducts respectively of the chain consisting of 23 PEG repeating units. Thus, M_m can be shown to be 1032 Da. In MALDI mass spectrum, where the signals mostly come from singly-charged ions, the highest peak also gives the M_m .

The signals in the MALDI mass spectrum of polymers are often from singly-charged ions only. The presence of multiply-charged polymer ions is seldom observed. This is an important advantage of MALDI over other ionization techniques in polymer analysis. Polymers unlike proteins and other large biomolecules are not composed of only one kind of molecule but rather a distribution of molecules within a range of molecular weights and degree of polymerization. Also, a polymer can be a complex mixture of molecules with the same monomer unit but with different end groups and degree of functionalization. The presence of multiply-charged ions gives additional signals making the mass spectrum complicated and difficult to interpret.

Electrospray Ionization – Quadrupole Mass Spectrometry as an Alternative Method

An alternative ionization method used in MS of polymers is the ESI. In this technique, the analyte solution is nebulized into tiny charged droplets using an electrospray needle. As the droplets travel from the tip of the needle to the skimmer, the solvent evaporates and the charge density at the surface continuously increases. The droplet begins to disintegrate to smaller droplets when the electrostatic repulsion becomes large enough to overcome the surface tension of the droplet. Currently, there are two theories that explain how the droplets collapse. In the coulombic fission model, the droplet with a very high charge density undergoes a series of explosion forming smaller droplets and eventually the analyte ion (Fenn, Mann et al. 1990). On the other hand, in the droplet jet fission model, the droplets initially produced from the Taylor cone tip of the ESI needle have elongated ends called jets. As the droplets travel from the tip of the ESI needle to the skimmer, smaller droplets are ejected as the jets break up (Gross 2004; Kebarle and Verkerk 2009).

From the tiny charged droplets, the ions begin to form via two routes (Gross 2004). In the charge residue model, the analyte ion is the end result of a series of solvent evaporation and droplet disintegration (Kearle and Verkerk 2009). In the ion evaporation model, the analyte ions are directly evaporated from the highly charged surface of the droplets (Fenn, Mann et al. 1990). Any of the two routes presented favors the production of multiply-charged ions.

ESI can easily be interfaced to most mass analyzers like the quadrupole. The capability of the ESI to produce multiply-charged ions offset the mass range limitations of the mass analyzers, however, the continuous nature of ion production in ESI, makes it difficult to combine directly with the pulsed mass analyzers like the TOF. The tandem of ESI to TOF is made possible with the introduction of orthogonal acceleration technology. In this set-up, the ions from ESI source travel in the x-direction into an orthogonal accelerator. The orthogonal accelerator then applies an accelerating voltage on the ions towards the y-direction into the flight tube where the ions are separated based on their m/z (Dawson and Guilhaus 1989; Coles and Guilhaus 1993).

Figure 3.2b shows a sample mass spectrum of PEG generated using ESI with quadrupole mass analyzer (ESI-q). The same PEG standard was used in the generation of MALDI-TOF spectrum in Figure 3.2a. A solution of PEG in deionized water was introduced via a syringe pump into the APi 2000 MS-MS equipped with an electrospray chamber and triple quadrupole mass analyzer (Applied Biosystems). The analysis was carried out in q1 using the following ESI parameters: 5500 V ion spray voltage, 25 V cluster gas and 10 V ion source gas 1. The declustering potential (DCP) was set 100 V while the focusing and entrance potentials were at 400 V and 10 V respectively.

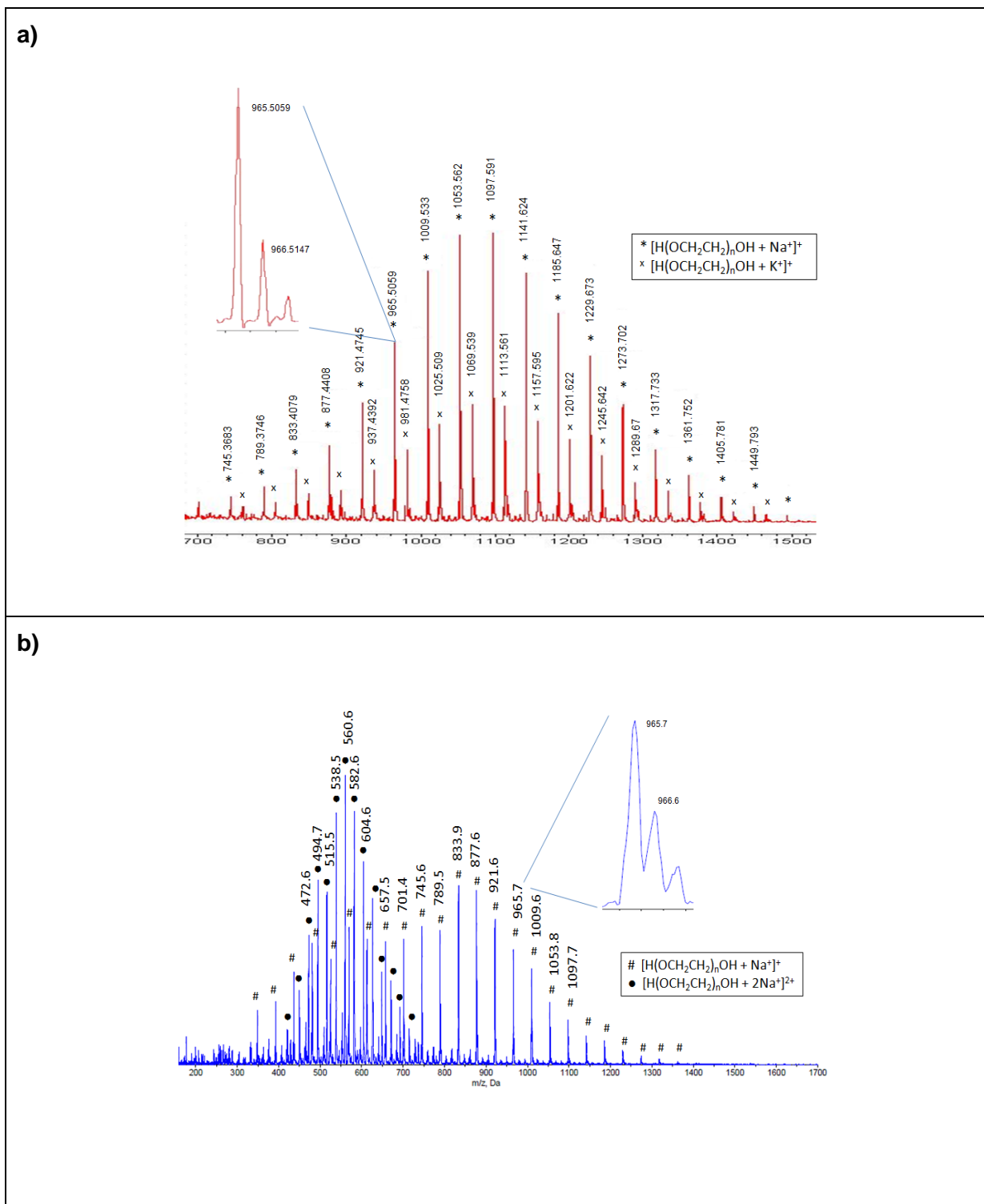


Figure 3.2. Mass Spectra of PEG 1000: a.) positive-mode MALDI-TOF using 2,5-DHB as matrix; b.) positive-mode ESI-q at declustering potential of 100 V.

The ESI mass spectrum consists of doubly- and singly-charged Na^+ adducts. Distributions resulting from the attachment of a proton or other cations were not observed. For the singly charged polymer distribution (#), the highest signal came from m/z 833.7 Da. This corresponds to the adduct $[\text{H}(\text{OCH}_2\text{CH}_2)_{18}\text{OH} + \text{Na}^+]^+$. For comparison, the doubly-charged distribution (•) has m/z 560 Da as its highest signal. This corresponds to $[\text{H}(\text{OCH}_2\text{CH}_2)_{24}\text{OH}$

+ 2Na]²⁺. Multiple charging is favored for larger molecules. The signal intensities of peaks with different charges do not have the same ion response making it difficult to predict the M_n and to picture the molecular weight distribution. This limits the applicability of ESI in polymer characterization.

DCP is a compound-dependent parameter in the operations of APi 2000 MS. Applied Biosystems define DCP as the potential applied between the ground (or skimmer) and the orifice plate. This potential is used to decrease the solvent cluster ions which may attach to the sample. However, a very high DCP can cause fragmentation of the sample (Applied Biosystems 2005).

The formation of multiply-charged PEG in the ESI-q MS at various DCP was studied. Figure 3.3 shows the generated mass spectrum at DP 40 V, 100 V and 160 V. The formation of singly-charged (Δ) ions is favored as DCP is increased. The spectrum generated at DP 160 V shows mostly singly-charged polymer ions. The high DCP caused not only the dispersion of solvent cluster ions but the elimination of the excess cation bound to the polymer.

Comparing the ESI-q mass spectrum generated with DP 160 V with the MALDI-TOF mass spectrum, noticeable differences in mass distribution can readily be observed even if the two are both made up of only singly-charged ions from the same polymer. The apparent bimodal appearance of the ESI spectrum is a result of incomplete elimination of single cations from the multiply-charged large polymers. Residues of multiply-charged PEG can be observed from the mass spectrum. This results to bias in favor of the smaller polymers. The complexity of the ESI process makes it less rugged and more difficult to reproduce.

The two mass spectra in Figure 3.2 shed light on the main difference between quadrupole and TOF mass analyzers. In terms of resolution, at the specified mass range, the quadrupole only provides unit mass resolution. This means that it can only separate masses that are 1 Da apart (see inlets). On the other hand TOF can provide a lot better mass resolution and can separate masses that are 0.1 Da apart. In terms of mass range, quadrupoles have limited mass range (up to 1800 Da). This implies that for large polymers to be analyzed in quadrupole, the polymers must be multiply charged and thus must be ionized accordingly. While the combination of ESI and TOF works with polymers, the combination of MALDI and quadrupole will find only few applications in polymer analysis.

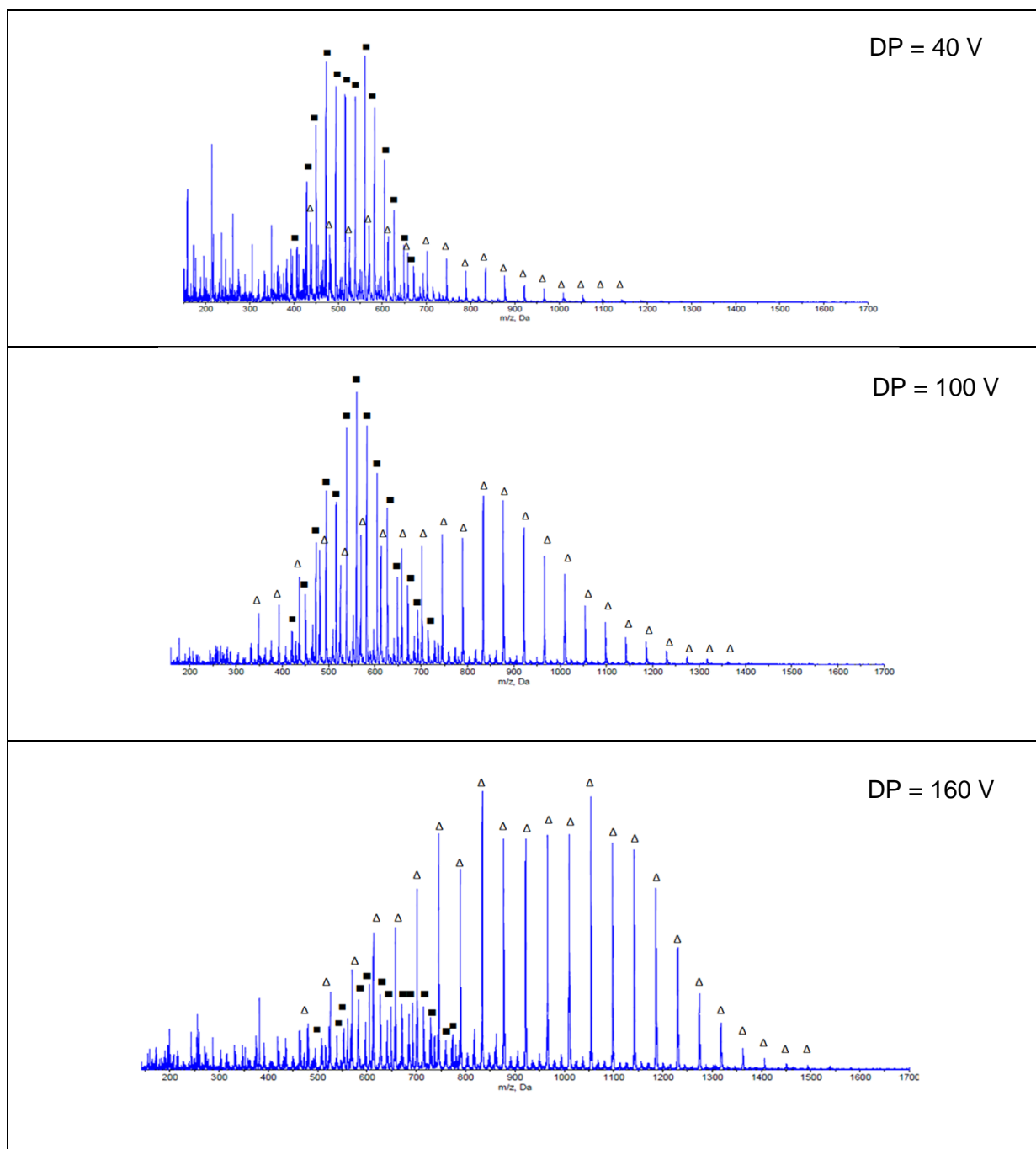


Figure 3.3. Positive-ESI-q mass spectrum of PEG at declustering potential of 40, 100 and 160 V. The Δ and \blacksquare represent the distribution with singly- and doubly-charged polymer ions respectively.

Chromatographic Separation prior to Mass Spectrometry

Liquid chromatography (LC) is used in tandem with MS for polymer characterization in two ways: 1.) to separate highly polydispersed polymers by their molecular weights using SEC; and/or 2.) to separate polymer mixtures by their overall polarity through partitioning. Online coupling of LC with ESI and/or MALDI are possible.

Average molecular weight data obtained by SEC does not often agree with the ones obtained from the mass spectrum. Peak-average molecular weight (M_p) is a SEC-derived parameter associated with the peak maximum in the chromatogram. Ideally, M_p is similar to the M_m in a mass spectrum. The main difference between the two is that M_p is an estimated value while M_m is an absolute value that describes a specific molecule component. In MALDI-TOF MS, it was observed that for polymers with lower polydispersity, the M_p values are 2 monomer units higher than the M_m . The discrepancy becomes even larger for more polydispersed polymers (Jackson, Larsen et al. 1996). For narrowly distributed polymers, the disparity in M_p and M_m is mainly due to the difference in the scales used to generate the chromatogram and the mass spectrum. SEC with either refractive index or UV detector makes use of weight fraction intensity while the TOF MS makes use of number-fraction intensities (Jackson, Larsen et al. 1996). For widely distributed polymers, the discrepancy is mainly due to bias of MS measurements against high molecular weight species. Large molecules easily get entangled and can form ordered microcrystalline state. To overcome this barrier for desorption into the gas phase, the polymer must be diluted to lower molar concentration and the amount of matrix must be increased (Schriemer and Li 1996). To characterize highly polydispersed polymers in the MALDI-TOF, there is a need to first separate the large molecules from the smaller ones. This is achieved by fractionation in a SEC column prior to MS analysis (Hanton and Liu 2000).

Polymers can be mixture of molecules with the same backbone structure but different end groups. Direct MS analysis of polymer mixtures can be a difficult task. First, there could be ionization bias depending on the nature of the end group. Secondly, the mass spectrum of a polymer mixture is complex and difficult to interpret. Partition chromatography can be employed to separate the polymer components firsts based on the polarity of the end group prior to analysis by MS.

In their study, Lee et al. used partition chromatography to separate the trace polymer impurities in fatty alcohol ethoxylates prior to MS. These impurities are the unreacted PEG and the ethoxylates with the undesired end group. The undesirable end group varies from the desirable ones only with the length of the fatty acid chain. The trace impurities cannot be determined directly by MALDI-TOF MS because the signal of the major components will shelve that of the trace impurities. Separation of impurities and the major components was done in an octadecyl (C18) column based on the polarity of the end group (Lee, Rumbelow et al. 2009).

LC can easily be coupled online to ESI. It is also possible to couple online or offline the LC to MALDI. For complex polymer mixtures, two dimensional LC can be employed prior to MS. In this set-up, the components in the mixture are first separated based on size using a SEC

column and then based on end group functionality in a reverse-phase column (Murgasova and Hercules 2002).

Future of MALDI-TOF in polymer analysis: Fate and Degradation Studies

In the previous sections of this chapter, it was shown how MS, specifically MALDI-TOF has become an important tool to characterize polymers. It has presented the important developments as well as current limitations and challenges as well as important developments in MS to accurately estimate molecular weight distributions and identify major components in complex polymer mixtures. Indeed, MALDI-TOF is becoming popular among polymer scientists.

The mass spectrum is a rich source of information and can further be exploited to include other areas of polymer research. Perhaps, one of those direct beneficiaries in the modern developments in MS of polymers is environmental science. The proliferation of polymers and their degradation products in water and in soil have been an important concern. Their high molecular weight, their diversity and the complexity of their degradation routes make polymers difficult to be determined in the environment. Nonetheless, MALDI-TOF MS offers a fast and reliable method to study these compounds in aqueous environment.

Trimpin et al. studied the fate of poly(vinylpyrrolidone) (PVP) in water. This was the first report on the use of a fixed-bed bioreactor (FBBR) in combination with MALDI-TOF MS to study polymer fate. Prior to the degradation study, a thorough method optimization of the MALDI sample preparation technique was done. This is always a necessary step to demonstrate the reliability of the derived results and to estimate the instrumental limitations. The researchers initially observed that while there was no shift in the molecular weight distribution of PVP after 16 days of exposure in FBBR chamber there is a slow decrease in the signal of high molecular weight PVP (Figure 3.4). With the use of an optimized MALDI-TOF procedure, they proved that the slow disappearance of large PVP molecules is neither due to microbial nor physico-chemical degradation but to adsorption in FBBR (Trimpin, Eichhorn et al. 2001).

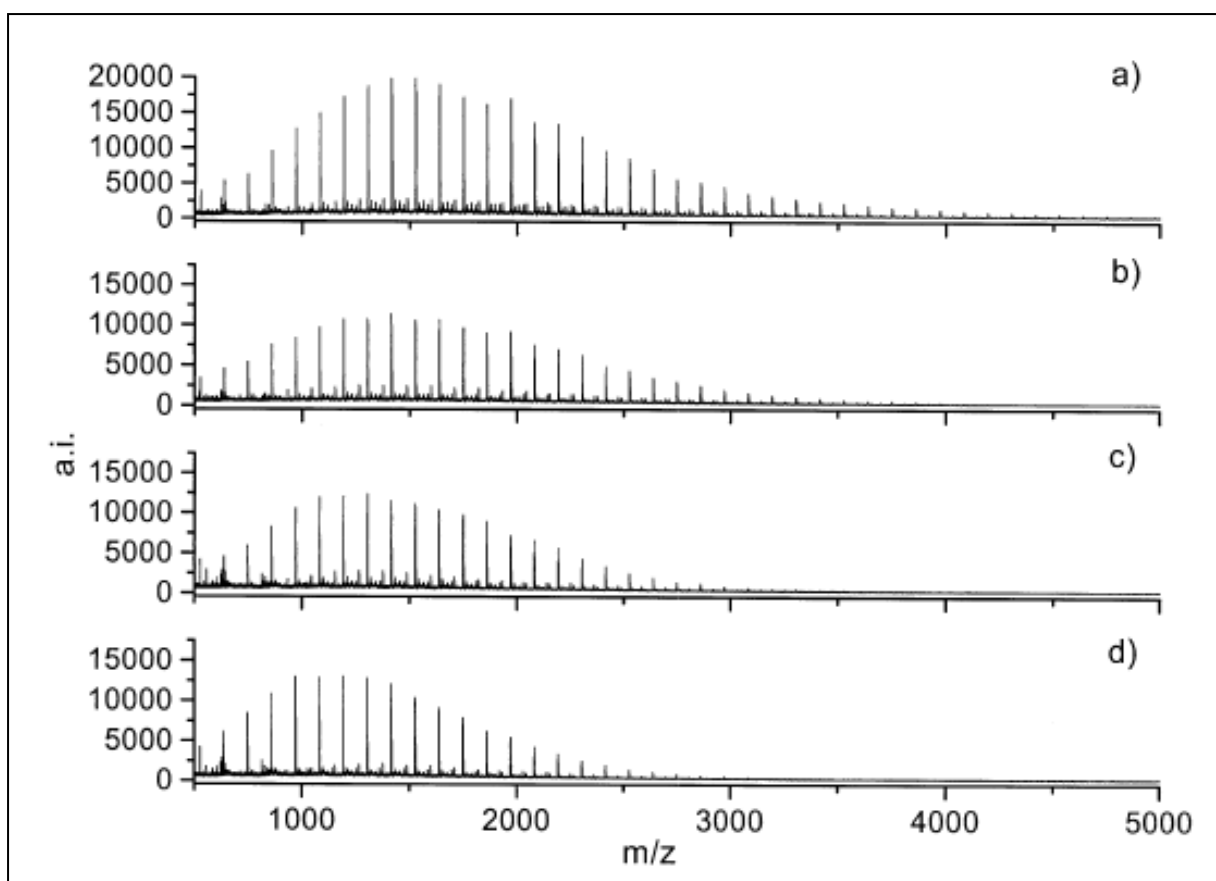


Figure 3.4. MALDI-TOF Spectra (positive ion mode) of PVP in FBBR after a) 0 h; b) 5 h; c) 8 days; and d) 16 days. (Trimpin, Eichhorn et al. 2001)

MALDI-TOF MS along with the classical carbon dioxide production test (CO_2 test) and dissolved organic carbon (DOC) test were used to study the aerobic degradation of PEG in wastewater and seawater. The CO_2 and DOC tests only tell in a general way the degradation of PEG and its kinetics. MALDI-TOF MS confirmed and gave additional information as to how the degradation proceeded. In this case the difference in the degradation of PEG in fresh water and in seawater environment was elucidated. The researchers found out by comparing the MALDI spectra of day 1 and day 14 PEG in an artificial seawater media, only short and medium-chain PEG are preferably degraded (Figure 3.5). The larger PEG remained intact (Bernhard, Eubeler et al. 2008).

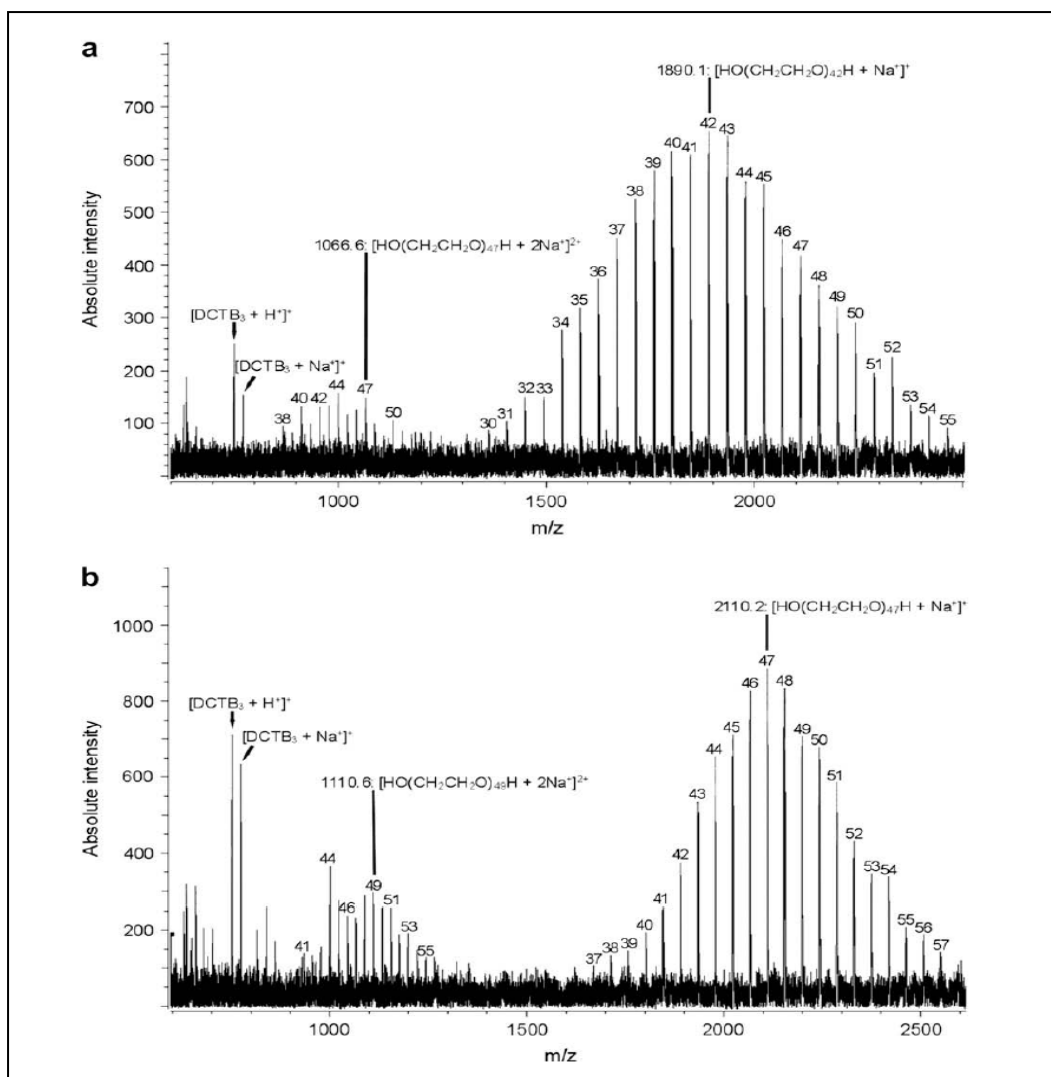


Figure 3.5. MALDI-TOF mass spectra (positive ion mode) of PEG in artificial seawater media from a) day 1 and b) day 14 sample. (Bernhard, Eubeler et al. 2008)

The role of MALDI-TOF MS in polymer analysis has greatly increased in the recent years. From being a characterization tool, MALDI-TOF MS can also be used to gain insight on polymer degradation and behavior in the environment. The future challenge is to be able to develop a highly reproducible MALDI process that is capable of accurate quantitative determination of polymer compounds and their degradation products, even with the limited availability of chemical standards that cater to the diversity of polymer components.

Chapter 4. CHARACTERIZATION OF CHITOSAN OLIGOSACCHARIDE

ABSTRACT

Matrix-assisted laser desorption/ionization time-of-flight mass spectrometry (MALDI-ToF MS) offers a fast and robust way of determining the molecular weight distribution of oligomers like chitosan oligosaccharide (COS). In this study, the parameters in the MALDI-ToF MS analysis of COS were optimized to improve the sensitivity and accuracy of the method. Three parameters were tested namely: the matrix, the sample spotting technique, and the presence of cations. A reproducible mass spectrum with high intensity of the COS homologue ions and with decreased interference from matrix ions was obtained from a desalted sample mixed with 2,5-dihydroxybenzoic acid matrix and prepared using the vacuum drying technique. Sodium adducts were the most predominant form of the COS ions. Lowering of the COS polydispersity by fractionation in a size-exclusion chromatographic (SEC) column improved the signal of the higher molecular weight chitosan and provided a confirmation about the molecular weight distribution of COS.

Keywords: MALDI-ToF MS, Chitosan oligosaccharide, SEC fractionation

Part of this chapter is published in the book chapter:

“TOF MS within Food and Environmental Analysis.” A.R. Fernandez Alba (ed.). *Comprehensive Analytical Chemistry* **58**: 307 – 338. Elsevier: Amsterdam, The Netherlands
Dimzon, I.K.D., Knepper, T.P. 2012. MALDI-TOF MS for characterization of synthetic polymers in aqueous environment

Introduction

Researches relating structure and activity have been applied to polymers especially to the polar oligomers that exhibit biological activities like the chitosan oligosaccharide (COS) (Mao, Shuai et al. 2004). COS is a short chain polymer composed mostly of D-glucosamine monomers linked by β -D-(1 \rightarrow 4) glycoside bonds and the rest are N-acetyl-D-glucosamine monomers. COS is synthesized via either acid-catalyzed; enzyme-catalyzed hydrolysis; or by oxidation of the much larger chitosan (Allan and Peyron 1995; Jia and Shen 2002; Vishu Kumar and Tharanathan 2004; Cabrera and Van Cutsem 2005; Kim and Rajapakse 2005). The degree of polymerization (DP) describes the number of monomer units in a single polymer molecule. For COS and chitosan, DP refers to the total D-glucosamine and N-acetyl-D-glucosamine monomers. COS and chitosan are a mixture of homologues and contains molecules at a range of DP. The chitosan raw material used to produce the COS is synthesized by deacetylation of chitin, a biopolymer composed mainly of N-acetyl-D-glucosamine monomers. Since the deacetylation process is not always complete, the degree of deacetylation (DD) describes the extent of the removal of the N-acetyl group. Both the DP and DD are important indicators of the other physico-chemical properties as well as the activities of COS (Rabea, Badawy et al. 2003). Because of its low molecular weight, COS is readily dissolved in aqueous solvents with neutral pH giving a solution with low viscosity (Kim and Rajapakse 2005). These properties make COS more interesting than chitosan especially in food and pharmaceuticals research. A number of studies suggest that COS has antibacterial (Rabea, Badawy et al. 2003; Moon, Kim et al. 2007), antifungal (Seyfarth, Schliemann et al. 2008), anti-inflammatory (Yoon, Moon et al. 2007) and other biological activities (Xia, Liu et al. 2011). These biological activities of COS are strongly dependent not on the bulk characteristic of the COS but on structural properties of the individual COS molecule present like degree of polymerization, degree of deacetylation and molecular weight (Moon, Kim et al. 2007; Seyfarth, Schliemann et al. 2008). Variety is expected in the molecular distribution of COS available or that can be produced. This is a result of several factors in the synthesis that includes: chitin source to produce the chitosan; the resulting chitosan degree and distribution of deacetylation; and the hydrolysis route used to produce the COS. In evaluating COS for a certain structure-dependent activity, average molecular weight data and polydispersity index would not be substantial. In this case, mass spectrometry (MS) can aptly be applied to determine the individual COS molecule present.

Of the various available MS methods, matrix-assisted laser desorption ionization (MALDI) with time-of-flight (ToF) mass analyzer has been the most widely used technique to characterize polymers (Montaudo, Samperi et al. 2006; Dimzon and Knepper 2012). The main challenges in MALDI-ToF MS of polymers come from three contributing factors:

complexity of the MALDI process, the large sizes of the molecules, and the polydispersity of the polymer samples. To obtain highly reliable molecular weight information from the MALDI-ToF mass spectrum, the challenges need to be adequately addressed by developing polymer specific sample preparation methodologies that includes: choosing the correct matrix, using the most appropriate sample spotting technique, controlling the cation content of the solution and addressing the polydispersity of the sample (Dimzon and Knepper 2012).

In the MALDI-ToF MS analysis of polymers with lower polydispersity, it was observed that peak-average molecular weight (M_p) derived from SEC are two monomer units higher than the molecular weight with the highest intensity in the mass spectrum (usually designated as modal molecular weight or M_m). The discrepancy becomes even larger for more polydispersed polymers (Jackson, Larsen et al. 1996). This discrepancy is mainly due to bias of MS measurements against high molecular weight species. Large molecules easily get entangled and can form ordered microcrystalline state. To overcome this barrier for desorption into the gas phase, the polymer must be diluted to lower molar concentration and the amount of matrix must be increased (Schriemer and Li 1996). To characterize highly polydispersed polymers in the MALDI-TOF, there is a need to first separate the large molecules from the smaller ones. This is achieved by fractionation in a SEC column prior to MS analysis (Hanton and Liu 2000).

This paper reports on a general strategy in developing a polymer-specific sample preparation technique for MALDI-ToF MS. COS was used as the sample polymer to demonstrate the strategy that was outlined in four major steps: choosing the correct matrix, using the most appropriate sample spotting technique, controlling the cation content of the solution and addressing the polydispersity of the sample. The molecular weight distribution obtained using MALDI-TOF MS was also compared with that using electrospray ionization - quadrupole (ESI-Q) MS and SEC.

Methodology

Sample and Reagents

The COS with lactic acid was from Sigma-Aldrich (Buchs, Switzerland). The MALDI matrices used in this study were: dithranol, sinapinic acid (SA) and α -cyano-4-hydroxycinnamic acid (4-HCCA) from Bruker Daltonics (Bremen, Germany); 2,5-dihydroxybenzoic acid (2,5-DHB) from Sigma-Aldrich; and 2,4,6-Trihydroxyacetophenone (THAP) and trans-2-[3-(4-tert-Butylphenyl)-2-methyl-2-propenylidene]malononitrile (DCTB) from Fluka (Sigma-Aldrich). The COS and matrix solutions were prepared from the following solvents, reagents and

materials: methanol suprasolv from Merck (Darmstadt, Germany); trifluoroacetic acid, sodium chloride, potassium chloride, lithium acetate and Amberlite mixed-bed resin from Carl Roth (Karlsruhe, Germany); and sodium trifluoroacetate and potassium trifluoroacetate from Fluka. Milli-Q water was produced using the Milli-Q system with Simpapak2 ion exchanger (Millipore, Milford, MA, USA). Polyethylene glycol used to calibrate the MALDI-ToF MS was from Sigma-Aldrich.

Experimental Design

Development of a MALDI-ToF MS method for the characterization of COS was carried-out by testing four factors namely: the matrix, the sample preparation technique, the presence of cations and the polymer polydispersity. Six matrices were tested for their applicability to the COS analysis. The matrices were initially dissolved in methanol. The second step was to know which sample preparation technique is appropriate to a given COS and matrix mixture and is able to give better signals in the MS. The effect of the presence of alkali cations on the intensity of the MS signal was studied by spiking the solution with known amount of sodium, potassium or lithium cations so that their final concentration was 0.15 M. The effect of polymer polydispersity was studied by fractionating the COS in a SEC column and analyzing the fraction in the MALDI-ToF MS. The obtained mass spectra of the fractions were compared to the mass spectrum of the unfractionated COS.

Matrix and Sample Spot Preparation Techniques

The COS working solution was prepared by dissolving the oligosaccharide at a concentration of 0.5% (w/v) in either 0.5% (v/v) trifluoroacetic acid (TFA), 0.3 M sodium chloride (NaCl) in Milli-Q water or in 100% Milli-Q water. The matrices were dissolved at a concentration of 1.0 % (w/v) in two solvent systems namely: methanol (MeOH); and/or in 1:2 acetonitrile (ACN): Milli-Q water.

The MALDI sample spots were prepared using three techniques. In the dried droplet (DD) technique, equal volumes of the COS working solution and the matrix solutions were initially mixed. One microliter of the resulting mixture was then spotted into the MALDI target and was left to dry in the air at normal room conditions (approx. 25 °C, 760 mmHg). In the quick and dirty (QD) technique, 0.5 µL of the COS working solution was first spotted into the MALDI target. Before the COS dried out, 0.5 µL was added into the COS spot. The mixture was then left to dry in the air at normal room conditions. In the vacuum drying (VD) technique, equal volumes of the COS working solution and the matrix solutions were initially mixed. One microliter of the resulting mixture was then spotted into the MALDI target and was left to dry under vacuum (~250 mmHg) at room temperature.

Matrix-Assisted Laser Desorption/Ionization-Time-of-Flight Analysis

MALDI-ToF MS analysis was carried out using Briflex™ III Bruker Daltonics MALDI-TOF-MS equipped with a nitrogen laser emitting at 337 nm. The system was set in reflector mode and pulsed at 3 ns. The signals monitored were from positive ions at the $0 \leq m/z \leq 3000$ range. Otherwise stated, the spectra shown were the sum of 300 shots (10 points x 30 shots/point) at 20-40 % laser attenuation. The instrument was externally calibrated using the generated mass spectrum of polyethylene glycol standard ($M_p = 1000$ Da) with 2,5-DHB as matrix at 26% laser attenuation. Ions with m/z below 350 were deflected. The samples and standards were spotted in a Scout 26 target (stainless steel).

Electrospray ionization - Quadrupole Analysis

A working solution was prepared by diluting the COS stock solution to 1/100 in MilliQ water. The working solution was introduced directly to the AB Sciex API 2000 in the ESI mode interfaced to a triple quadrupole mass analyzer, through a syringe pump at the rate of 10 $\mu\text{L}/\text{min}$. The ESI was operated in the positive ion mode with the following parameters: ion spray voltage, 5500 V; cluster gas, 25 psi; ion source gas 1, 10 psi; declustering potential, 40 V (max); focusing potential, 400 V; and entrance potential, 10 V. The mass spectrum was acquired at the quadrupole 1 (Q1), within the m/z 100 – 1800 mass range and 2 s cycle time.

Size-Exclusion Chromatography

SEC was used to determine the average MW and PDI of the COS. SEC was also used to partially separate the COS homologues. A 100 μL portion of the COS working solution was introduced into the SEC system with Novema 3000 Å and Novema 300 Å dual column (both columns have: internal diameter, 8 mm; length, 30 cm; particle size, 10 μm ; material, OH-functionalized methacrylatecopolymer; Polymer Standards Service, Mainz, Germany) using 0.2% trifluoroacetic acid (TFA) v/v in 0.3 M aqueous sodium chloride (NaCl) solution as eluent. Prior to collection of the fractions, the detection of the polymers was done in a refractive index detector. The average MW of COS was estimated using the absolute retention time of polyvinyl pyridine (PVP) molecular weight standards (PSS, Mainz, Germany) dissolved in 0.5% TFA v/v in 0.3 M aqueous NaCl. The fractions were collected from retention time 19 min. to 23 min. at an interval of 0.5 minutes per vial.

Results and discussion

Choice of Matrix

The first step done was to determine the appropriate matrix to use. COS is a polar molecule and it dissolves well in polar solvent systems like water and/or methanol. The best matrix for COS must also be soluble in polar solvent systems. Table 4.1 gives the summary of the

results of the preliminary experiments done on six possible matrices. Of the matrices tested for solubility in methanol, only 2,5-DHB, THAP and DCTB were completely soluble at a concentration of 10 µg/mL. Moreover, when the matrix solutions in methanol were mixed with the COS stock solution in a 1:1 v:v ratio, precipitation was observed in the solutions of dithranol and DCTB. Since the COS stock solution was prepared using an aqueous solvent system with 0.3 M NaCl and 0.5 % TFA, the resulting methanol-COS stock solution mixture was more polar than methanol and caused the precipitation of DCTB and dithranol.

Of the matrices tested only THAP and 2,5-DHB were able to ionize COS. This result confirms that solubility is an important property to consider in choosing the right matrix. In addition, 2,5-DHB was found to be a better suited matrix than THAP because it was able to generate more intense signal. In the literature, 2,5-DHB is often used for chitosan and other oligosaccharides (Mohr, OlafBörnsen et al. 1995; Trombotto, Ladavière et al. 2008; Chen, Zhu et al. 2010).

Table 4.1. *Characterization of the different available matrices for their application to the MALDI-ToF MS analysis of COS.*

Matrix	Solubility in methanol at a concentration of 10 µg/mL	Precipitation when the solution in methanol was mixed with the COS stock solution at a ratio of 1:1.	COS signal in the MALDI-ToF mass spectrum
2,5-DHB	Soluble	None	yes
Dithranol	Sparingly soluble	Some precipitation	no
SA	Sparingly soluble	None	no
4-HCCA	Sparingly soluble	None	no
DCTB	Soluble	Some precipitation	no
THAP	Soluble	None	yes

Sample Preparation

In this study, two solvent systems, namely 1:1 MeOH : H₂O and 1:5 ACN : H₂O were tested with 2,5-DHB as matrix. The COS was dissolved in 0.5% TFA in 0.3 M aqueous NaCl while the matrices were dissolved in either MeOH or 1:2 ACN:H₂O. A 1:1 mixture of the COS stock solution and matrix solution results to either of the two solvent systems mentioned above. The sample spot was prepared on the target using three different techniques, namely DD, QD and VD.

Figure 4.1 shows the magnified view of the sample spots prepared with the different combinations of solvent system and spot preparation techniques. By visual inspection, it can readily be observed that DD (Figure 4.1A and Figure 4.1B) produced the largest crystals while VD (Figure 4.1E and Figure 4.1F) had finer crystals. Evaporation in ambient conditions (normal room temperature and pressure) results to slow crystallization promoting the crystal growth than nucleation. On the other hand, evaporation in vacuum is a fast process giving less time for crystal growth.

Inhomogeneity of the sample spot is readily visible on sample spots dried under atmospheric pressure. One form of inhomogeneity that is apparent is the accumulation of dried solids in the periphery of the spots. This appearance of the spot resembles the drying of a drop of coffee that produces a ring stain instead of an even spot. During vacuum drying, the evaporation of solvent is fast so that all the solvent is gone before a capillary flow produces an observable accumulation of solute particles at the periphery of the spot.

Spots prepared from solutions with 1:1 MeOH:H₂O were generally thinner and more spread than the corresponding spots with 1:5 ACN:H₂O. Because the 1:1 MeOH:H₂O solvent system is less polar compared to the 1:5 ACN:H₂O, the resulting solution with MeOH had less surface tension and tends to spread than the mixture with ACN. While thinner sample spots are preferred, the wide spread makes the spot less homogeneous.

To compare the intensity of the analyte signals produced from the different sample spots, the laser is beamed on 10 random points in the spots. At each point, the laser shots 30 times. The resulting spectrum generated was the sum of 300 shots. Figure 4.2 shows the mass spectra of the sample prepared using the different spot preparation techniques.

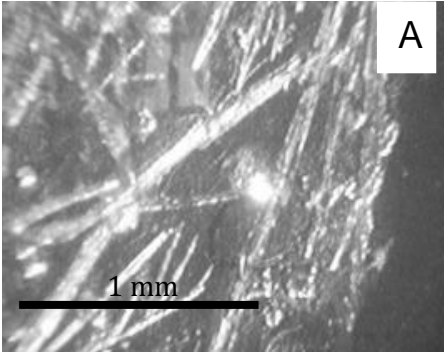
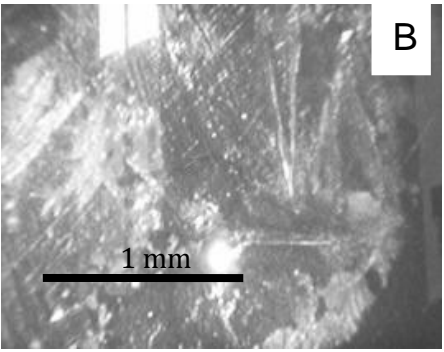
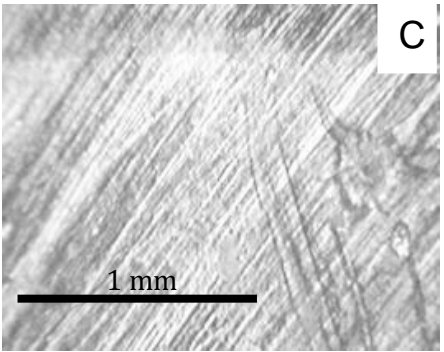
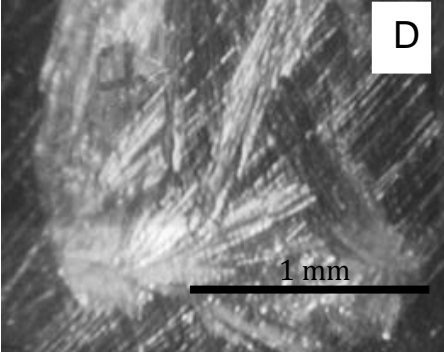
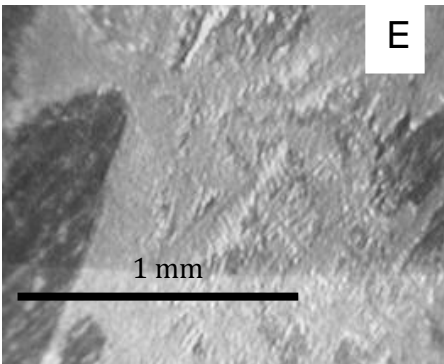
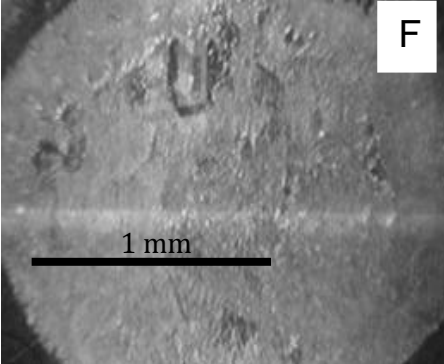
Spot Preparation	In 1:1 MeOH:H ₂ O Solvent	In 1:5 ACN:H ₂ O Solvent
Dried Droplet	 A	 B
Quick and Dirty	 C	 D
Vacuum Drying	 E	 F

Figure 4.1. Magnified view of the COS spots prepared using different spot preparation techniques and solvent system. The shown scale is based on rough estimates.

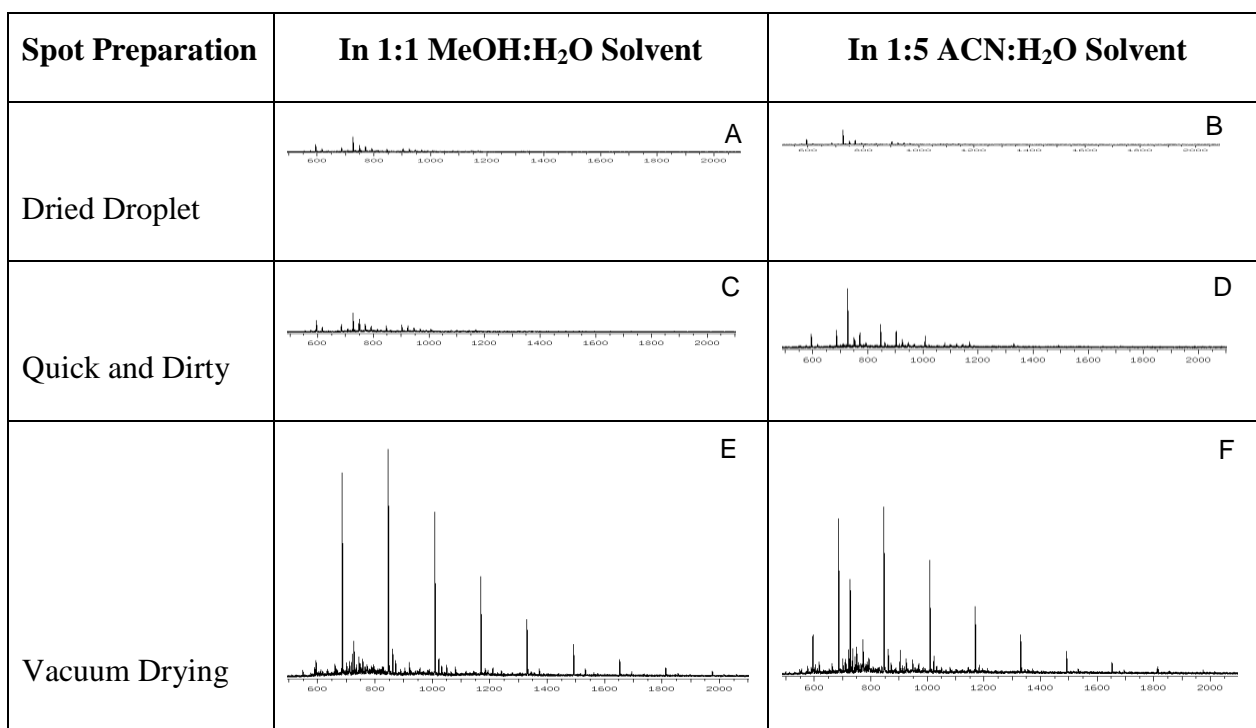


Figure 4.2. Comparison of MALDI-TOF Spectra (positive ion mode) of COS obtained using different spot preparation techniques. The scaling was maintained constant to allow comparison of peak intensities.

Sample spots prepared using VD (Figure 4.2E and Figure 4.2F) produced the most intense analyte signals (more than 10 times greater than from the other sample spots). The probability of getting a signal at any point within the sample was high. The signal from the spots prepared by DD and QD were less intense. The generation of an analyte signal in a random point in the sample spot is unpredictable. The presence of narrow hot spots with very intense signals was observed in the samples prepared particularly using DD. A hot spot (or sweet spot) is a small area where there is a large concentration of analyte. This is a result of an uneven distribution of analyte and matrix molecules in a sample (Gruending, Weidner et al. 2010). As a consequence, the analyst must try several random shots at different locations within the MALDI sample until the hot spot is found. A common practice when a hot spot is located is to shoot at the site several times until no more ions is detected from that hot spot. If the number of required shots is not met yet, another hot spot is searched again in random at a different location within the same MALDI sample. This ambiguity in the process of generating the mass spectrum presents a challenge in demonstrating the validity of the derived molecular weight data. Moreover, the reproducibility

of the method is sacrificed putting doubts whether a valid quantitative technique can be developed from this procedure. Additionally, the spectra from sample prepared by DD and QD were dominated by matrix signals.

Mass Spectrum

Shown in Figure 4.3 is the positive ion mode MALDI mass spectrum of COS with 2,5-DHB prepared by vacuum drying. The ions with most intense signal detected were that of the sodium (Na^+) adducts of the homologues of COS. The sodium ions came from the 0.15 M NaCl present in the COS-DHB mixture. The formation of cation adducts is expected for polymer molecules (Hart-Smith and Barner-Kowollik 2010). It was also reported in the literature that some polymers with amine group like poly(vinylpyridine) can also form proton adducts (Wong, So et al. 1998) although this was not always observed for COS under the experimental conditions of this study. Polar polymers like COS in particular, are readily ionized by alkali metal cations (Macha and Limbach 2002) like sodium and potassium. COS forms metal ion complex through the lone pairs of oxygen and nitrogen (Macha and Limbach 2002).

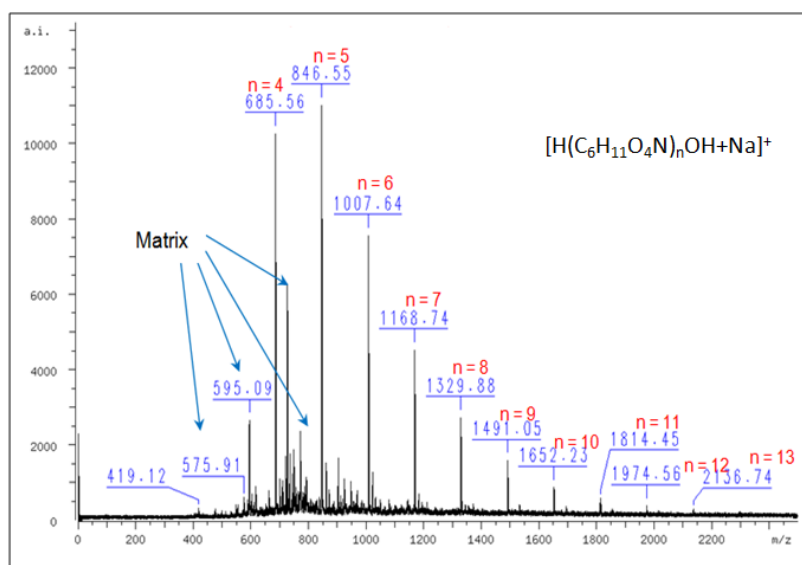


Figure 4.3. Positive ion mode MALDI mass spectrum of COS with 2,5-DHB as matrix prepared in 1:5 ACN:H₂O solvent system. The sample spot was prepared using VD technique, 0.15 M NaCl is present.

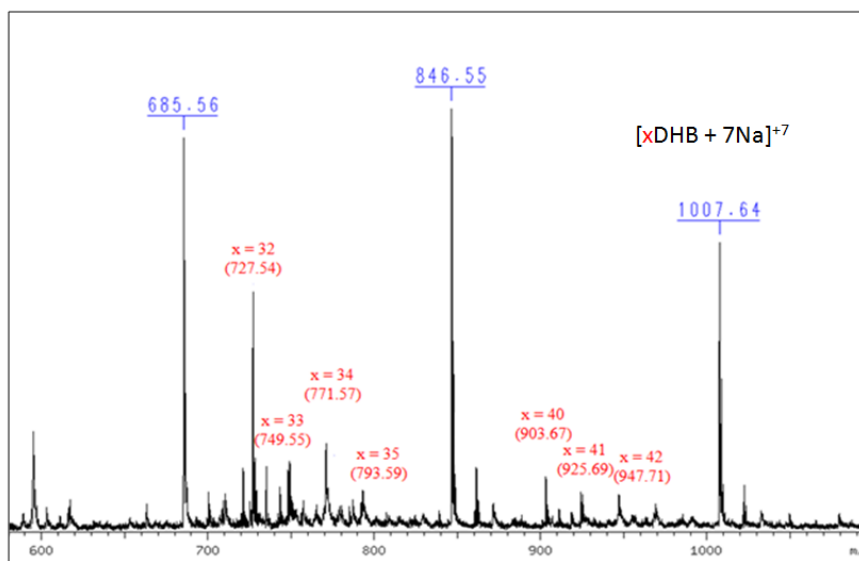


Figure 4.4. Other ions in the positive ion mode MALDI mass spectrum of COS with 2,5-DHB as matrix at the region $600 < m/z < 1100$.

The lowest mass that can be attributed to the sodium adduct of the oligosaccharide is the m/z 686 (sodium adduct of the oligosaccharide with 4 D-glucosamine monomer units). The m/z difference of 161 corresponds to the mass of the repeating D-glucosamine monomer unit. Potassium adducts of the chitosan oligosaccharide were also detected in the MALDI spectrum. Potassium can be an impurity of the sodium chloride used to prepare the solvent system to dissolve the chitosan. No ion with m/z less than 350 was shown in the mass spectrum because these were deflected prior to analysis in the ToF.

Signals coming from the matrix ions are unavoidable in MALDI analysis. These signals are usually prevalent in the region of the MALDI mass spectrum below m/z 1000. Figure 4 shows the positive ion mode MALDI mass spectrum of COS with 2,5-DHB as matrix in the region $600 < m/z < 1100$. Two ion groups that are not related to the COS can readily be seen: group 1: m/z 727, 749, 771 and 793; group 2 m/z 903, 925 and 947. For each ion group, the m/z difference between consecutive ions is 22. This can be due to multiply charged matrix and cation (C^+) cluster. For example, the m/z 727 can be the cluster of 32 molecules of 2,5-DHB and 7 sodium ions. This observation is consistent with the findings of Krutchinsky and Chait that the matrix cluster has the composition $[(DHB)_nXC]^{+x}$ where X is the number of C^+ (Krutchinsky and Chait 2002). In this study, the number of C^+ attached to the cluster can be multiple. The formation of matrix cluster ions is aided by the presence of cations (Dubois, Knochenmuss et al. 1996). Formation of matrix clusters is well studied. In

fact, these matrix clusters were also thought to aid in the ionization of nonpolymer analytes like peptides (Karas and Krüger 2003).

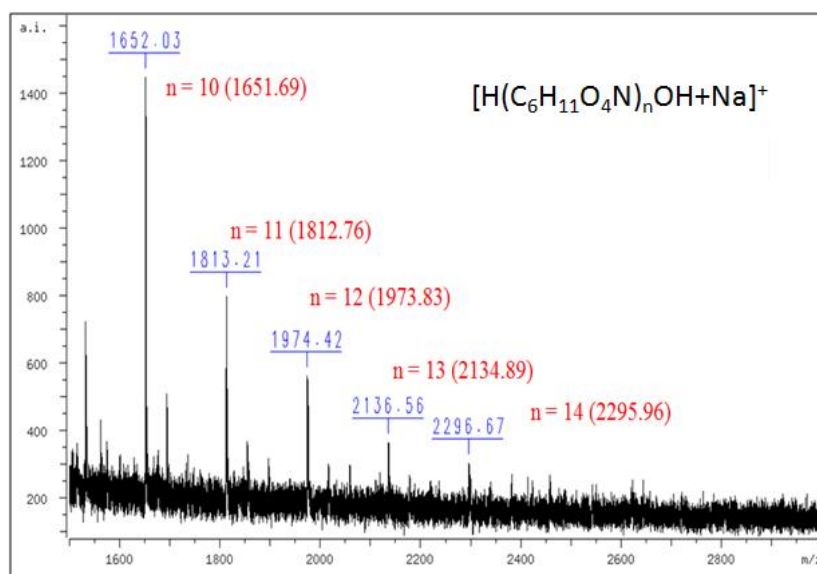


Figure 4.5. Positive ion mode MALDI mass spectrum of COS with 2,5-DHB as matrix at the region $1500 < m/z < 3000$.

Higher molecular weight COS were observed only in vacuum dried samples. Figure 4.5 shows the portion at $1500 \leq m/z \leq 3000$ of the MALDI spectrum of a spot prepared by vacuum drying. The COS of up to 14 monomer units (m/z 2296) was detected. In contrast, only up to 8 chitosan monomer unit (m/z 1330) was detected on the spots prepared using the other techniques. Also shown in Figure 4.5 are the calculated monoisotopic masses of the sodium adduct of COS from 10 – 14 monomer units. The mass differences between the experimental and the corresponding theoretical values are all less than 0.08%.

Even without the added NaCl, MALDI-TOF still yielded the sodium adducts of the COS homologues. The sodium ions are present as impurities both the COS and 2,5-DHB. Only a small amount of alkali metal cations would be necessary for the ionization of COS. In another experiment, the solutions with 0.15 M NaCl were desalted at various degrees using Amberlite® mixed bed ion exchange resins. Solutions exposed to excess resin at long period of time yielded no signal in the MS. Partially desalted solutions, however, yielded better mass spectra than the one with 0.15 M NaCl.

The capability of potassium and lithium ions to ionize the COS was also tested. Figure 4.6 shows the positive ion mode MALDI mass spectrum of COS with 2,5-DHB as matrix and dissolved in 1:1 MeOH : H₂O with 0.15 M K⁺ ions and 0.15 M Li⁺ ions added. Potassium

adducts of the COS homologues, like that of sodium, were also readily observed. The mass spectrum of COS with Li^+ ions showed peaks with drastic decrease in resolution. This change is due to the increase in the complexity of ion – polymer interaction.

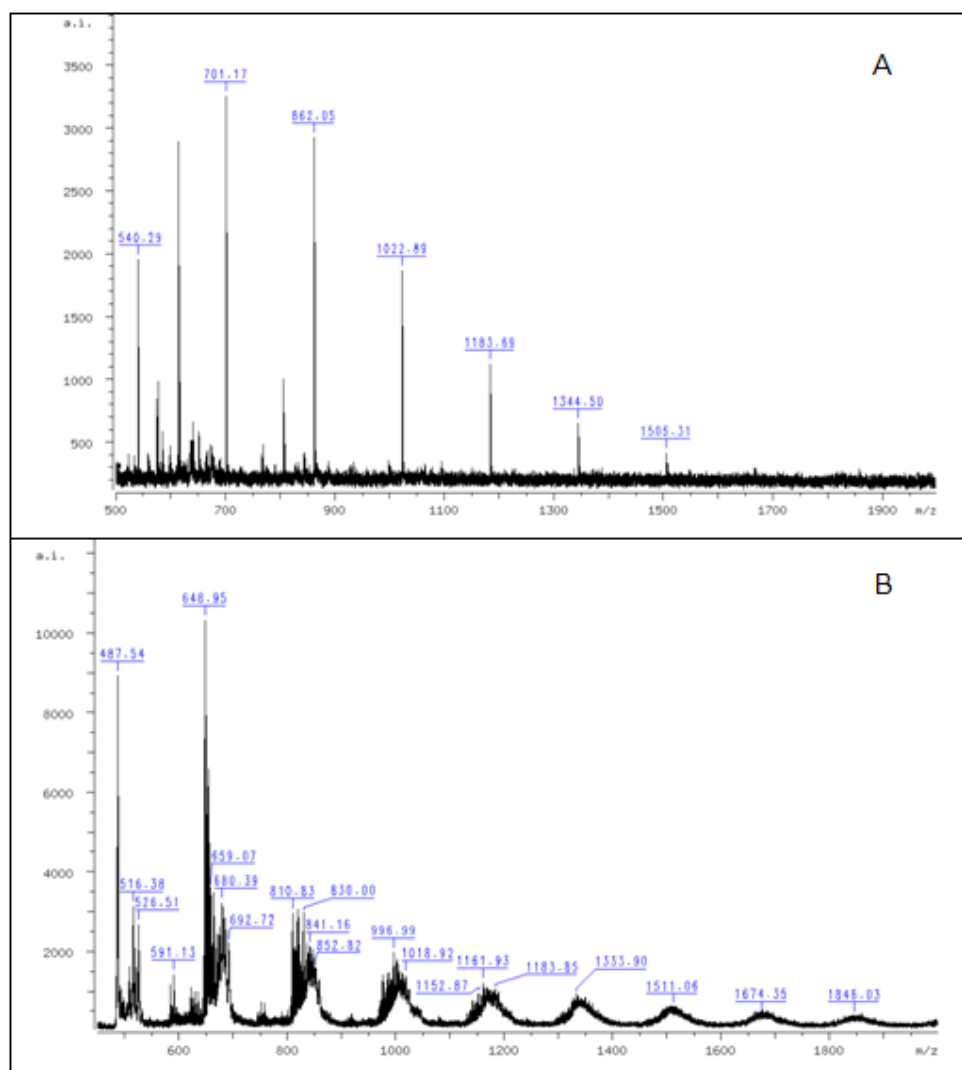


Figure 4.6. Positive ion mode MALDI mass spectrum of COS with 2,5-DHB as matrix prepared in 1:1 MeOH:Milli-Q H_2O solvent system. The sample spot was prepared using VD technique. A. 0.15 M KCl and B. 0.15 M LiCl were added.

There was no sufficient data however to compare which among sodium or potassium can produce more intense signal in the MS. Signal intensity can be subject to many factors that goes beyond simply considering the capabilities of the cation to attach itself to and to ionize the COS molecules. The other factors to consider include crystal structure, energy and size in the presence of both COS and 2,5-DHB as impurities that contribute to crystal defect sites; spot homogeneity; and spot thickness.

For comparison, COS was also analyzed in ESI-Q MS. Figure 4.7 shows the positive ion mode ESI-Q mass spectrum of the COS. Singly-charged COS ions of $n = 2$ to 6 are visible in the mass spectrum. Four differences of ESI-Q mass spectrum from that of MALDI-TOF can be observed. First, ESI produced mainly proton adducts while MALDI produced sodium adducts. Second, COS with $n=3$ is the peak with the most intense signal in ESI-Q while COS with $n=5$ is more prominent in MALDI-TOF. Third, the MWDs are not similar with COS only up to $n = 7$ detected in ESI-Q versus up to $n = 14$ in MALDI-TOF. Fourth, the ESI-Q mass spectrum has singly- and doubly charged ions while MALDI-TOF has only singly charged ions (Figure 4.8). These differences are due to the fact that MALDI and ESI are two very different ionization processes. To investigate further the MWD of COS, SEC was performed.

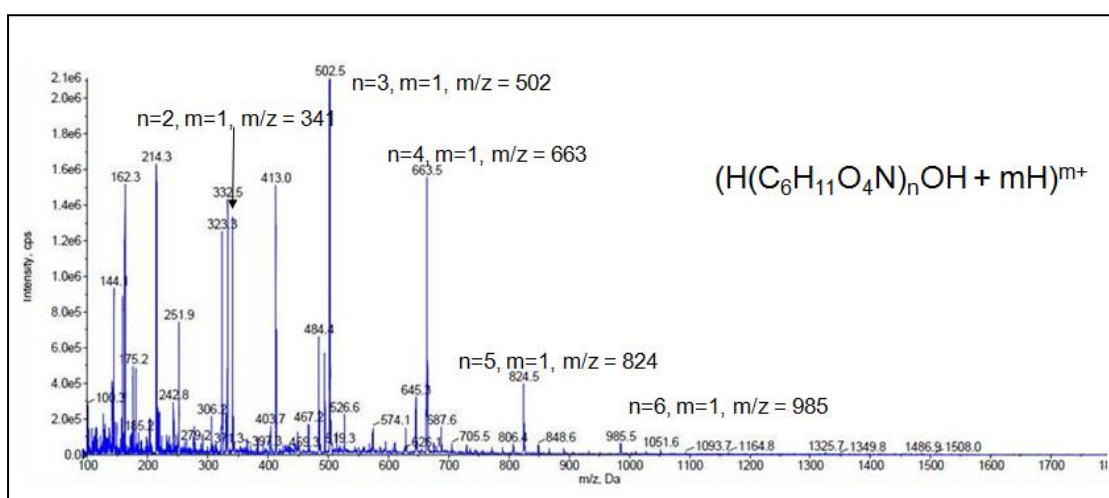


Figure 4.7. Positive ion mode ESI-Q mass spectrum of COS

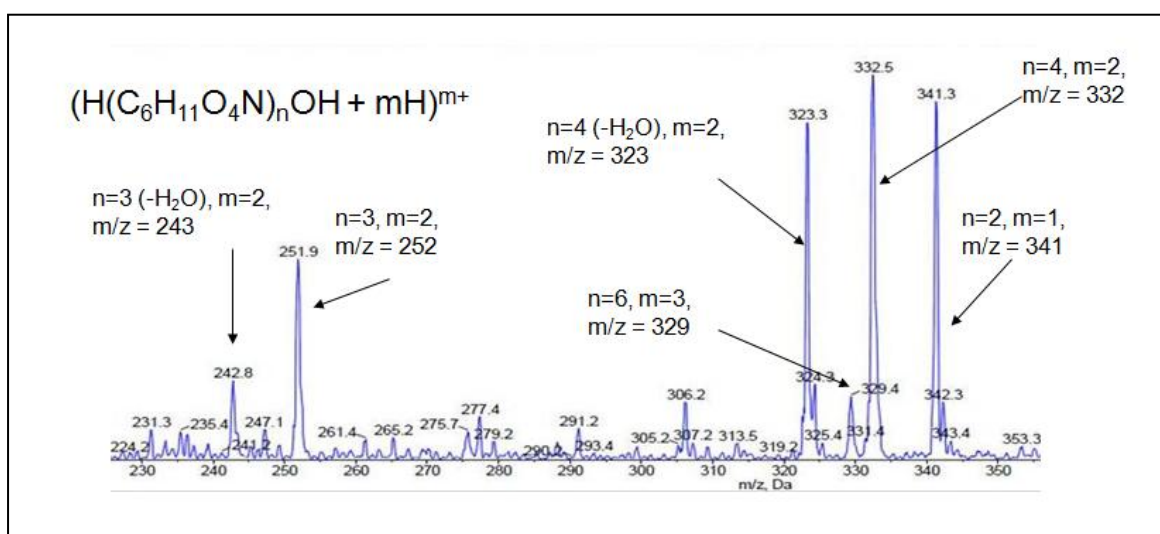


Figure 4.8. Positive ion mode ESI-Q mass spectrum of COS in the region $230 < m/z < 350$

Size-Exclusion Chromatography

Traditionally, SEC is used to obtain molecular weight information about polymers. The molecular weight information from mass spectrometry does not often agree with those from SEC (Jackson, Larsen et al. 1996). The cationic nature of chitosan in weakly acidic eluent makes it difficult to analyze by SEC. A robust SEC method was developed to analyze COS and chitosan in general (Bernhard, Flato et al.). Figure 4.9 shows the chromatogram of COS as it elutes out of the Novema 100 and Novema 1000 dual column. Analysis of the COS peak against poly(vinyl pyridine) molecular weight standard showed that the M_n and M_w are 4210 Da and 7010 Da respectively. These are much higher compared to the MW of the homologues derived from the MALDI-TOF and ESI-Q mass spectrum. Due to the nonavailability of chitosan molecular weight standard, SEC MWs were based on the retention times of the PVP standards. While COS and PVP are cationic in the acidic mobile phase, there could still be differences in their actual conformation in the solution.

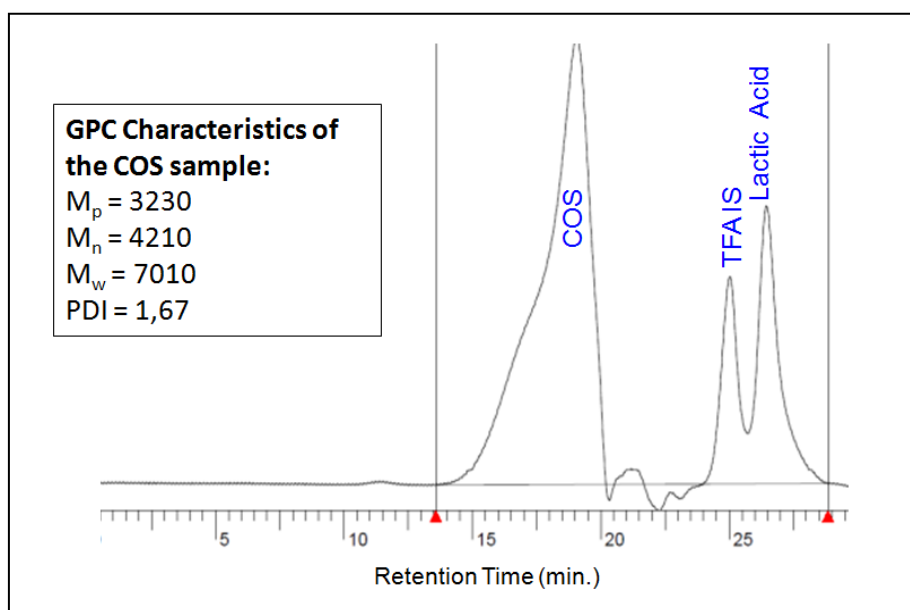


Figure 4.9. Size-exclusion chromatogram of COS in Novema 100 and Novema 1000 dual column with aqueous 0.3 M NaCl, 0.2% trifluoroacetic acid as mobile phase.

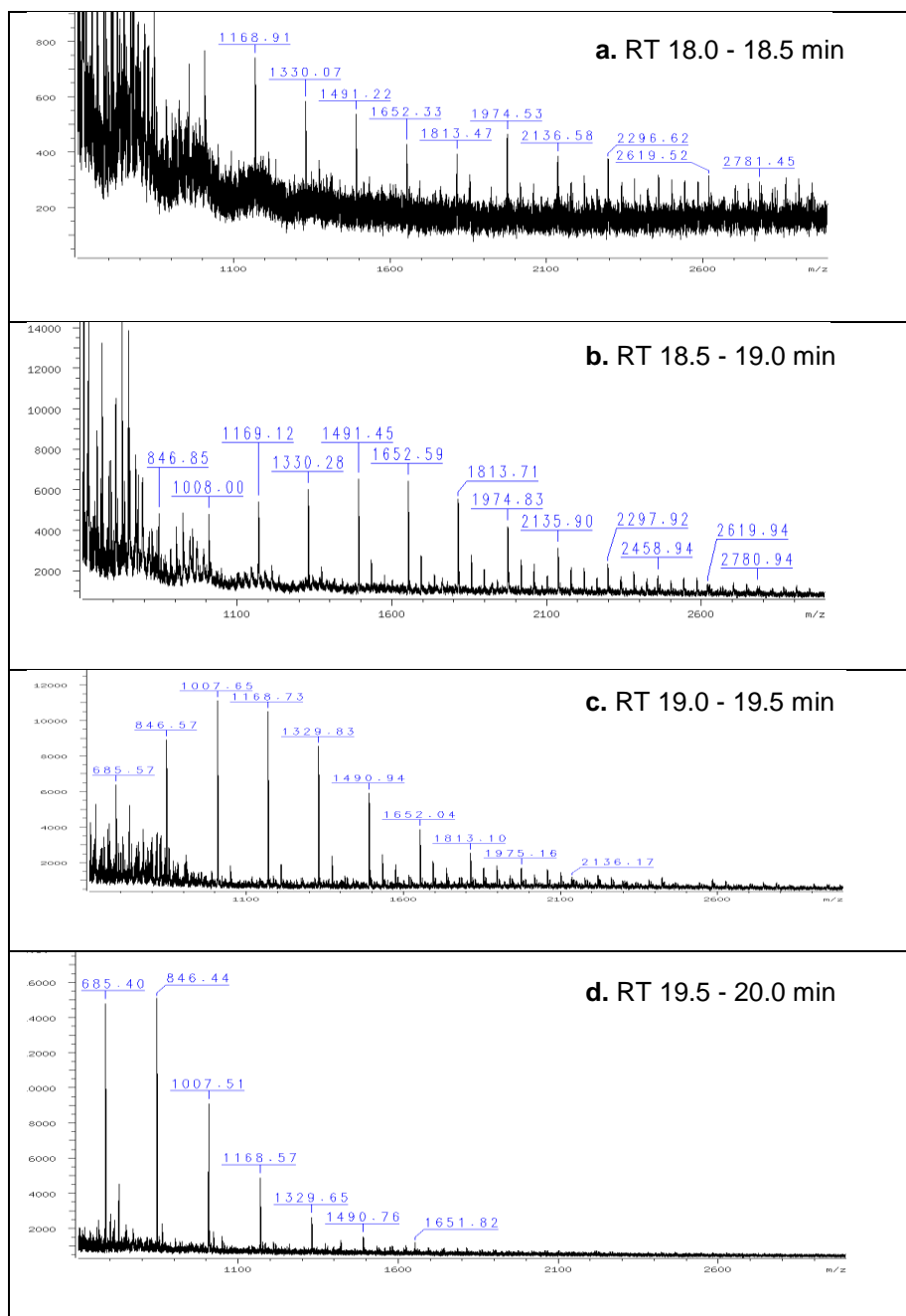


Figure 4.10. MALDI-TOF spectra (positive ion mode) of the collected SEC fractions at specified collection times.

COS was fractionated using the robust SEC method. Figure 4.10 shows the generated MALDI spectra of the fractions collected from retention time 18.0 to 20.0 minutes. The spectrum with most intense signals was generated from the fraction at 19.5-20.0 min (Figure 4.10d). The highest peak in this fraction (m/z 846) can thus be assumed to be the M_n . It must be noted that the M_n of the unfractionated COS is also m/z 846. Contrary to SEC results, no COS greater than 2000 Da was observed.

Conclusion

MALDI-ToF MS has been used in the characterization of polymers. While MALDI-ToF MS offers a fast and robust method in determination of polymer molecular weight distribution, method development often poses a challenge to the researchers. The desorption and ionization process in general is already a complex process. Dealing with large and highly polydispersed polymer molecules adds to the difficulty in producing a MALDI-ToF mass spectrum that accurately describes the polymer composition. In many instances, method development is based on trial-and-error. For well known polymers, published methods or known methods that have “worked” were used. This paper reported a general strategy on developing a MALDI-ToF method for polymer analysis that was divided into four parts namely: choosing the correct matrix, using the most appropriate sample spotting technique, controlling the cation content of the solution and addressing the polydispersity of the sample. In the case of COS, a reproducible mass spectrum with high intensity of the homologue ions and with decreased interference from matrix ions was obtained from a desalted sample that was mixed with 2,5-dihydroxybenzoic acid matrix and was spotted using the vacuum drying technique. Lowering of the COS polydispersity was carried out by fractionation in a size-exclusion chromatographic column.

Chapter 5. CHARACTERIZATION OF 3-AMINOPROPYL OLIGOSILSESQUIOXANE

ABSTRACT

The synthesis routes in the production of polysilsesquioxanes have largely relied upon in situ formations. This perspective often leads to polymers in which their basic structures including molecular weight and functionality are unknown¹. For a better understanding of the polysilsesquioxane properties and applications, there is a need to develop more techniques to enable their chemical characterization. An innovative method was developed to determine the molecular weight distribution (MWD) of an oligosilsesquioxane synthesized in-house from (3-aminopropyl)triethoxysilane. This method which can be applied to other silsesquioxanes, siloxanes and similar oligomers and polymers, involved separation using high performance liquid chromatography (HPLC) and detection using mass spectrometry (MS) with electrospray ionization (ESI). The novelty of the method lies on the unique determination of the absolute concentrations of the individual homologues present in the sample formulation. The use of absolute concentrations is necessary in estimating the MWD of the formulation when relative percentage which is based solely on mass spectral ion intensities becomes irrelevant due to the disproportionate ionization of the homologues and the highly variable fragmentation of the resulting ions. Determination of absolute concentration requires the use of single homologue calibration standards. Because of commercial unavailability, these standards were prepared by efficient fractionation of the original formulation.

Keywords: oligosilsesquioxane, ESI, MALDI, Ion Chromatography

Will be submitted for publication

Dimzon, I.K.D., Frömel, T. and Knepper, T.P., 2014. Characterization of 3-Aminopropyl Oligosilsesquioxane

Introduction

Polysilsesquioxanes refer in general to the polymers whose backbone structure is alternating oxygen and silicon atoms with $[\text{RSiO}_{3/2}]$ as repeat units (Wallace, Guttman et al. 2000; Rahimi and Shokrolahi 2001). These Si-containing polymers can be differentiated from polysiloxanes that have repeat units of $[\text{R}_2\text{SiO}]$ (Wallace, Guttman et al. 2000). Polymeric silsesquioxanes are more thermally stable and have higher chemical resistance compared to polysiloxanes because of the three-fold coordination of Si with O. The additional Si-O-Si bridges create an added stability within a molecule (Wallace, Guttman et al. 1999; Wallace, Guttman et al. 2000). The applications of silsesquioxanes can be wide-ranging and are largely dependent on the attached R groups (Abe and Gunji 2004). Silsesquioxanes are also used as building blocks of ceramics, nanoparticles, hybrid materials and dendrimers (Baney, Itoh et al. 1995; Lichtenhan 1995; Feher and Wyndham 1998; Mori, Lanzendörfer et al. 2004; Hessel, Henderson et al. 2006).

Highly controlled and selective silsesquioxane synthesis can be complex and is dependent on different empirical conditions (Lichtenhan 1995). Synthesis routes have largely relied upon *in situ* formation of silsesquioxanes (Lichtenhan, Vu et al. 1993). This perspective can often lead to polymers in which the basic structures including molecular weight and functionality are unknown (Lichtenhan, Vu et al. 1993). Thus, there is a need to develop some more techniques to enable chemical characterization of silsesquioxanes. This presents an analytical challenge because of the diversity and the uniqueness of the silsesquioxanes.

Aside from molecular weight and the degree of polymerization (n), another important parameter in silsesquioxane characterization is the degree of intramolecular condensation. Intramolecular condensation creates more Si-O-Si bridges within the molecule from the silanol groups (Si-OH) (Wallace, Guttman et al. 2000). High degree of intramolecular condensation leads to the formation of polyhedral oligosilsesquioxanes (Lichtenhan 1995). The silsesquioxanes can be partially or totally condensed. The overall general structure of silsesquioxanes could be random, ladder, cage and partial-cage (Baney, Itoh et al. 1995).

Mass spectrometry, particularly with electrospray ionization (ESI) and matrix-assisted laser desorption ionization (MALDI) techniques, has been used to characterize silsesquioxanes (Wallace, Guttman et al. 1999; Eisenberg, Erra-Balsells et al. 2000; Wallace, Guttman et al. 2000; Williams, Erra-Balsells et al. 2001; Eisenberg, Erra-Balsells et al. 2002). For example, the product from hydrolytic condensation of (3-glycidoxypropyl)trimethoxysilane was characterized using ESI and MALDI with a time-of-flight mass analyzer (TOF) (Williams, Erra-Balsells et al. 2001). ESI-TOF resulted in doubly-charged proton adducts of the

polymer. MALDI-TOF, on the other hand, gave singly charged proton and sodium adducts. Mass discrimination was observed in both ESI and MALDI. In ESI-TOF analysis, only the lower molecular weight compounds (720 to 1500 Da) were observed whereas in the MALDI-TOF analysis, the low and medium molecular weight peak clusters were detected (up to 4000 Da) (Williams, Erra-Balsells et al. 2001). For some homologues, a noticeable pattern of equidistant peaks differing by m/z 18 were observed and were attributed to loss of water. This can be due to the intramolecular condensation (Wallace, Guttman et al. 2000). The loss of water can occur either in-solution or in-MS. For example, ESI and MALDI were used to characterize the polyhedral silsesquioxane product of the hydrolytic condensation of N-(β -aminoethyl)- γ -aminopropyltrimethoxysilane and phenyl glycidyl ester (Fasce, Williams et al. 2001).

There is recent interest on the determination of the molecular weight distribution of polymers (MWD) as well as the molecular weight of every molecule present in a polymer formulation. Aside from being essential in studying the properties of these polymers in relation to their structures, accurate MWD and molecular weight data can be used in studying the impact of these compounds when released into the environment including their degradation (Bernhard, Eubeler et al. 2008). Si-based polymers are not always studied in terms of their biodegradation (Eubeler, Bernhard et al. 2010), fate and the risk they pose to the environment. This can be due to the lack of appropriate techniques that can be used to study them.

In this study, an attempt to determine the MWD of oligosilsesquioxane synthesized by acid-catalyzed hydrolytic condensation of (3-aminopropyl)triethoxy silane is discussed. The method involved the use of a variety of instrumental techniques including high performance liquid chromatography (HPLC), MS and induced-coupled plasma optical emission spectrophotometry (ICP-OES).

Methodology

Silsesquioxane formulation

The silsesquioxane formulation was prepared by dissolving the (3-aminopropyl)triethoxy silane in enough Milli-Q water (Millipore) to produce 10% wt/v %. The mixture was then acidified using nitric acid and was left to react for a period of 24 hours. This mixture was used as the silsesquioxane formulation.

ESI-Q MS of the oligosilsesquioxane formulation

A working solution was prepared by diluting the oligosilsesquioxane formulation to 1/200 in 5+95 (V+V) MilliQ water in methanol (Suprasolv). The working solution was introduced directly to the AB Sciex API 2000 in the ESI mode interfaced to a triple quadrupole mass analyzer, through a syringe pump at the rate of 10 $\mu\text{L}/\text{min}$. The ESI was operated in the positive ion mode with the following parameters: ion spray voltage, 5500 V; cluster gas, 25 psi; ion source gas 1, 10 psi; declustering potential, 160 - 200 V (max); focusing potential, 400 V; and entrance potential, 10 V. The mass spectrum was acquired at the quadrupole 1 (q1), within the m/z 100-1800 mass range and 2 s cycle time.

MALDI-ToF MS of the oligosilsesquioxane formulation

A stock solution was prepared by diluting the oligosilsesquioxane formulation 1/10 using methanol. Equal volumes of the oligosilsesquioxane stock and 20 mg/mL 2,5-dihydroxybenzoic acid (2,5-DHB) in water (matrix solution) were mixed in a separate vial. A 1 μL drop of the mixture was placed on a stainless steel target and was allowed to dry under the normal room condition. The analysis was done in Briflex™ III Bruker Daltonics MALDI-TOF MS with a nitrogen laser emitting at 337 nm in a reflector mode and pulsed for 3 ns. The signals monitored were from positive ions in the $0 \leq m/z \leq 7000$ range. Unless stated differently, the spectra shown were the sum of 150 shots (5 points x 30 shots/point) at 20-40 % laser attenuation. The instrument was externally calibrated using the generated mass spectrum of polyethylene glycol standard ($M_p = 1000$) with 2,5-DHB as matrix at 30% laser attenuation.

Fractionation of the oligosilsesquioxane

Ten microliters of oligosilsesquioxane formulation was injected into an HP1090 LC (HP Agilent; Santa Clara, California, USA) equipped with Kromasil 100-5 C18 column (5 μm particle size, 100 Å pore size, 8 mm internal diameter, 250 mm length) and UV diode array detector. Separation of the oligosilsesquioxane homologues was made possible in a gradient of 5 mM perfluoroheptanoic acid in water (Eluent A) and 5 mM perfluoroheptanoic acid in methanol (Eluent B) at a flow rate maintained at 0.5 mL/min: : Initially, 55% Eluent B for 5 min; increased to 95% Eluent B at a rate of 1%/min; maintained at 95% Eluent B for 15 min; decreased back to 55% Eluent B at rate of 4%/min, maintained at 55% Eluent B for 10 min. The elution of homologues was observed by monitoring the absorbances at 235 and 220

nm. Fractions were collected at retention times that correspond to specific homologues. The composition of each collected fraction was confirmed using ESI-MS.

ICP-OES analysis of the fractions

The homologue concentration in each fraction was quantified indirectly by determining the Si using Spectro Ciros CCD ICP-OES equipped with a cross flow nebulizer and quartz torch (Spectro; Kleve, Germany). Calibration solutions containing 0.1 to 4.0 µg/mL of Si were prepared from (3-aminopropyl)triethoxysilane. All solutions were diluted using Milli-Q water. Quantification was performed by monitoring the 212.41 nm Si emission line after method development with three other emission lines including: 152.67, 251.61 and 288.16 nm. The method limit of quantification was 0.1 µg /mL.

Determination of the MWD of the oligosilsesquioxane formulation

A working solution was prepared by diluting the oligosilsesquioxane formulation to 1/100 in 5+95 (V/V) MilliQ water in methanol. Agilent HPLC with 50 mm Kromasil 100-5 C18 column with 10 mm guard column (5 µm particle size, 100 Å pore size, 2.1 mm diameter). Separation of the oligosilsesquioxane homologues was made possible in the gradient of 5 mM perfluoroheptanoic acid in water (Eluent A) and 5 mM perfluoroheptanoic acid in methanol (Eluent B) at a flow rate maintained at 0.20 mL/min: Initially, 55% Eluent B for 1 min; increased to 95% Eluent B at a rate of 4%/min; maintained at 95% Eluent B for 15 min; decreased back to 55% Eluent B at rate of 8%/min, maintained at 55% Eluent B for 4 min. The analytes were detected in the AB Sciex API 2000 MS with ESI, in the Q1 selected ion monitoring mode. Single-homologue containing fractions that were analyzed in the ICP-OES were used as calibration standards.

Results and Discussion

MS of the 3-aminopropyl oligosilsesquioxane prior to fractionation

The synthesis of silsesquioxane can be done via acid-catalyzed or base-catalyzed reactions. Base-catalysis results to gels and colloidal particles. On the other hand, acid-catalysis produces weakly-branched polymers of various shapes (Brinker 1988; Abe and Gunji 2004). The acid-catalyzed reaction of (3-aminopropyl)triethoxysilane to produce the oligosilsesquioxanes involves two step as shown in Figure 5.1: first is hydrolysis of the monomers producing highly reactive silanols and ethanol; and second is the condensation

reaction producing the oligomers and water. The degree of polymerization, n , of the silsesquioxane formed in the example in Figure 5.1 is four. The reaction mixture, after 24 hrs, was taken and used as the *in situ* oligosilsesquioxane formulation to be characterized. The formulation was found to be stable at normal room conditions. No further polymerization was observed when the formulation was analyzed over several months.

The oligosilsesquioxane formulation was surveyed by direct injection into the ESI-Q MS. Figure 5.2A shows the generated mass spectrum in the positive ion mode. The oligosilsesquioxane homologues present have n in the range from 2 to 12. There are also hydrolyzed but non-polymerized monomers present in the formulation. The expected molecular weights of ions resulting from condensation of the monomers assuming that only polymerization occurred are not present. For example, for $n=6$ (Figure 5.2A insert), the expected m/z of a singly-charged ion (protonated molecule) is 733, accounting for six 3-aminopropyl silsesquioxane repeating units. Instead of m/z 733 one finds lower masses with a difference pattern of 18. The singly charged ions with m/z 661, 643, 625 and 608 are product masses after losses of 4, 5, 6 and 7 more H_2O molecules, respectively. This further loss of H_2O is due to intramolecular condensation in the solution to form the Si-O-Si bridges (in-solution). It is also possible that the intramolecular condensation is triggered further by the ESI process (in-MS). The extent of further H_2O loss after polymerization is described by the degree of intramolecular condensation. The degree of intramolecular condensation described in this paper does not differentiate between the reactions that happened in-solution and in-MS. Figure 5.1 shows two different products of intramolecular condensation. The formation of a fully condensed polyhedral silsesquioxane is favored in-solution as it is catalyzed by the acidic environment (Brinker 1988). On the other hand, the formation of Si=C bonds in silenes in-solution is highly unlikely. The process usually involves high energy conditions or by irreversible elimination of stable salts (Ottosson and Steel 2006). Also, silenes are very unstable although they can be partially stabilized by steric protection and by reversed Si=C bond polarization when there are π -donor substituents in the C atom (Ottosson and Steel 2006).

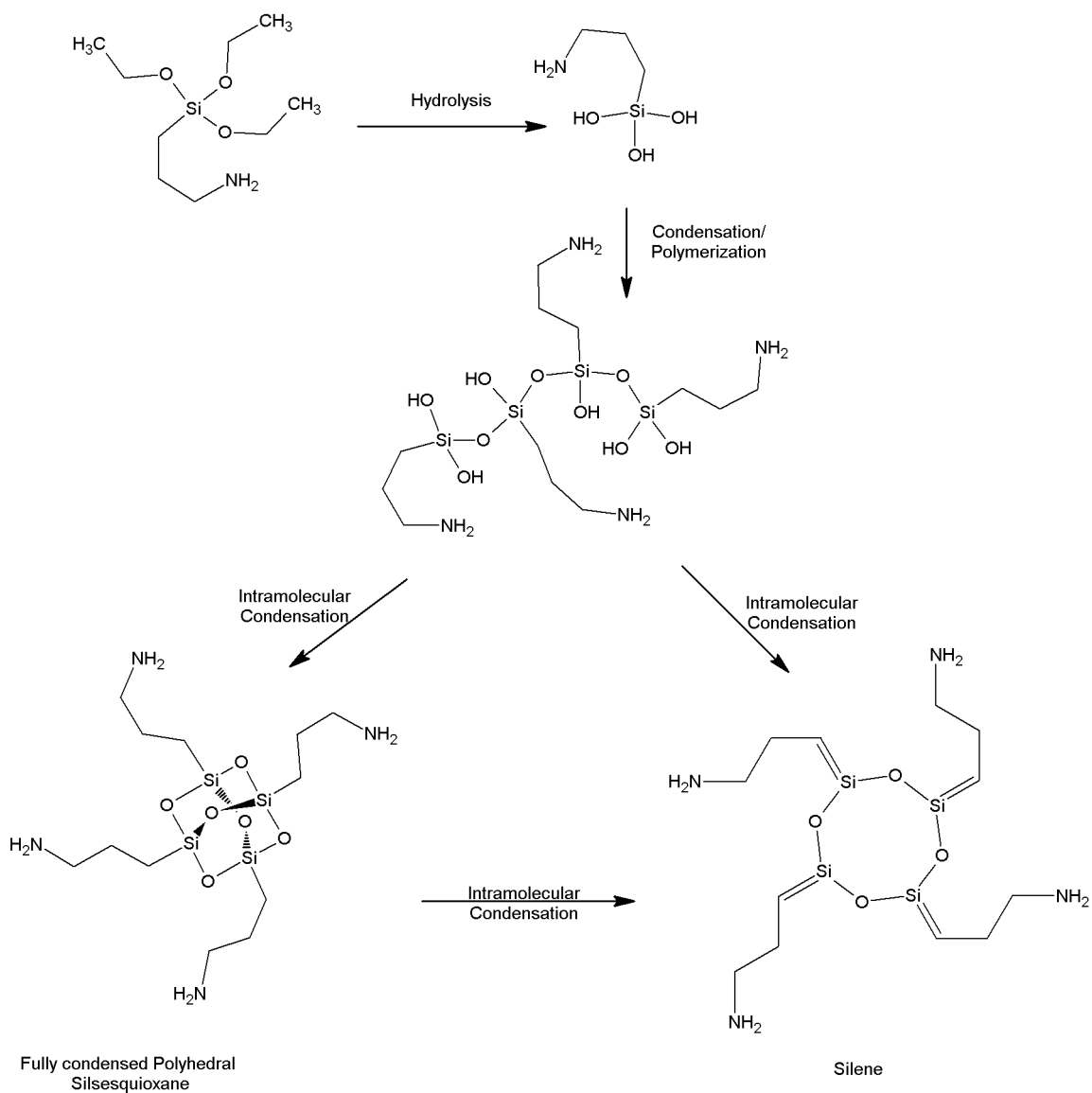


Figure 5.1. General reaction scheme in the formation of oligosilsesquioxane ($n=4$) from (3-aminopropyl)triethoxy silane and the formation of a fully condensed polyhedral silsesquioxane or a silene by intramolecular condensation.

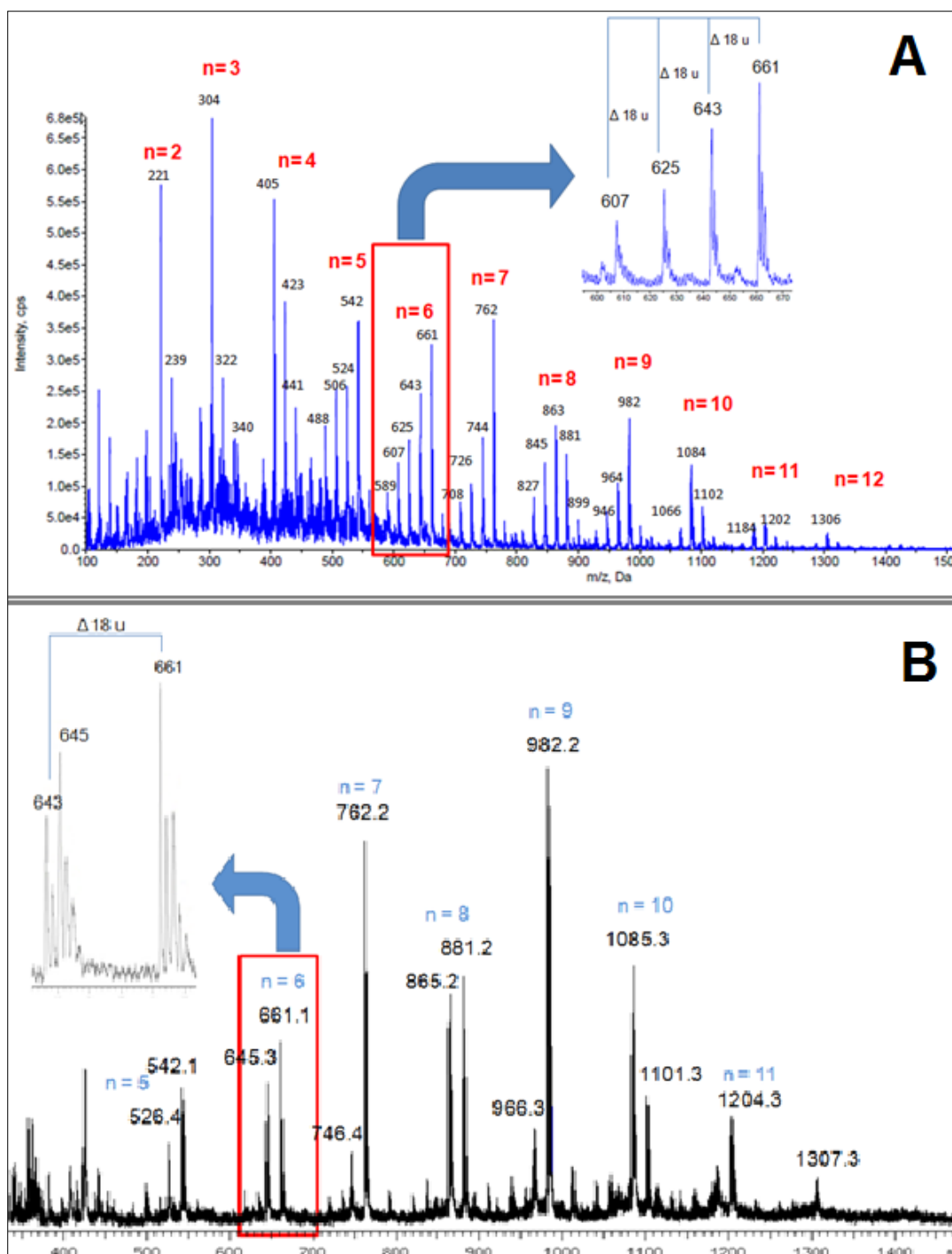


Figure 5.2. Positive-mode mass spectra of 3-aminopropyl oligosilsesquioxane in methanol: A. ESI-Q at declustering potential of 160 V; and B. MALDI-TOF mass spectrum with 2,5-DHB as matrix. Inserts: Zoomed in region showing the ions with $n=6$.

MALDI-TOF MS was also done in addition to the ESI-Q MS analysis. The silsesquioxane formulation was mixed with the solution of 2,5-DHB in water. The mixture was then spotted into a stainless steel target for analysis. The positive ion mode MALDI-TOF mass spectrum

of the sample is shown in Figure 5.2B. The mass range in the reflectron mode was set from 350 to 7000 m/z . The ions formed were protonated molecules. This is different from the generated ions of other silsesquioxanes by MALDI which were cation and proton adducts (Wallace, Guttman et al. 1999; Fasce, Williams et al. 2001; Williams, Erra-Balsells et al. 2001). Moreover, it was noted in a previous study that the degree of intramolecular condensation is proportional to the degree of polymerization (Wallace, Guttman et al. 1999).

The ions generated from both ESI and MALDI are plotted in a graph of the degree of polymerization versus degree of intramolecular condensation in Figure 5.3. Two differences are readily observed. Firstly, the ESI graph showed a wider range of intramolecular condensation than MALDI. And secondly, the mode-average molecular weights (M_m) obtained by ESI-Q MS ($n=3$) is lower than in MALDI-TOF MS ($n=9$). It is difficult to assess the extent that the ESI and MALDI can trigger further intramolecular condensation. It is known that different ionization can result in major differences in the MWD of polymers. Mechanisms of ion formation in ESI and MALDI are entirely different from each other and each will have its own unique limitation (Dimzon and Knepper 2012). In MALDI, the type of matrix used and the manner of spot preparation are optimized so that the polymer molecules are easily desorbed then ionized in the gas phase. In ESI on the other, the solvent buffer and several instrumental parameters are tested to maximize ion intensities. The non-appearance of highly-condensed ions in the MALDI spectrum can be due to either the inability of the MALDI to desorb and ionize the highly-condensed silsesquioxanes in the formulation; or that MALDI is unable to catalyze as in ESI the further condensation of less-condensed silsesquioxanes in the solution. Because of the limitations of each ionization technique, the methods are unable to give accurate information on the relative abundance of the species present in the formulation.

The degree of intramolecular condensation needed to produce a fully-condensed polyhedral silsesquioxane, t , is given by Equations 1 and 2 (Wallace, Guttman et al. 1999).

$$t = 0.5n + 1 \quad (\text{if } n \text{ is even}) \quad \text{Equation 1}$$

$$t = 0.5(n - 1) + 1 \quad (\text{if } n \text{ is odd}) \quad \text{Equation 2}$$

The t is the maximum condensation that can occur to produce the Si-O-Si bridges given a certain n . Equation 1 is drawn in Figure 5.3. This line represents the maximum in-solution intramolecular condensation. It can be observed that most of the points are above the line $t = 0.5n + 1$. Therefore, one can infer that Si-O-Si bridges are not the only products of

intramolecular condensation. One possible reaction that leads to more losses of H₂O could be the formation of Si=C bond or silenes in the gas phase. If this reaction occurs, the maximum degree of intramolecular condensation leading to the formation of Si=C bonds and a single ring, *s*, is given by Equation 3.

$$s = n + 1$$

Equation 3

Equation 3 is also drawn in Figure 5.3. It can be observed that most of the points either in ESI or in MALDI are between the lines $t = 0.5n + 1$ and $s = n + 1$. These points represent molecules that have undergone further condensation beyond the limits if they are to form the fully condensed polyhedral geometry. If these further condensations led to the formation of silenes, then these further condensations must have occurred in the gas phase in the MS. There is no way of differentiating the separate extent of these two different condensation reactions by solely relying on the mass spectral data. Thus, no conclusion can be made as to the extent of the formation of the Si-O-Si bridges in the formulation. The degree of intramolecular condensation as a parameter is dependent on the type of MS being used.

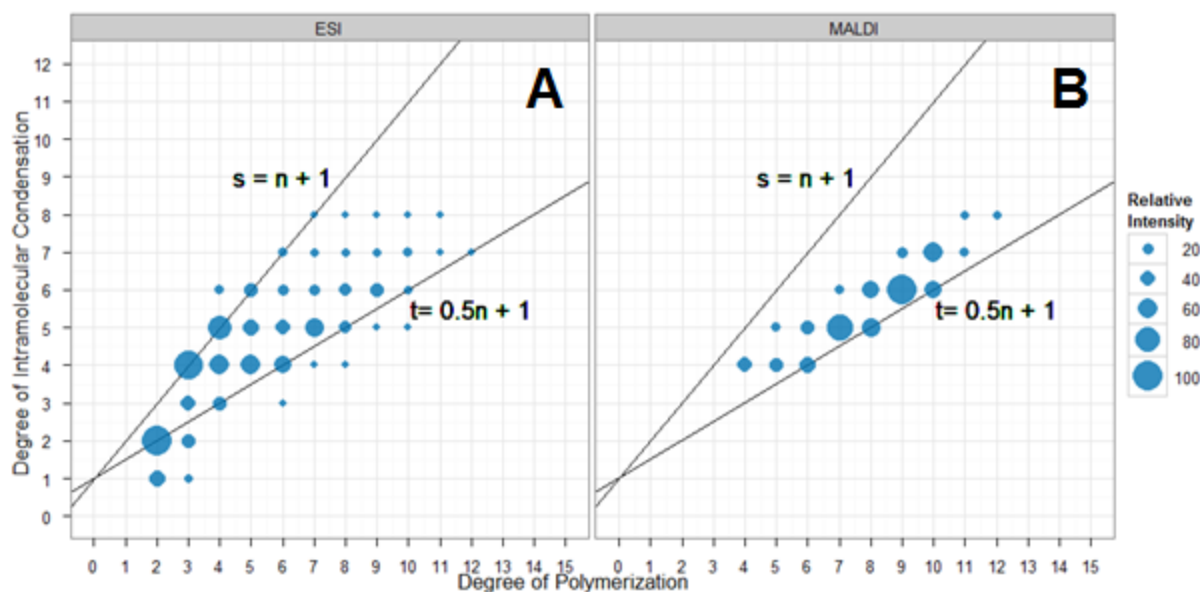


Figure 5.3. Comparison of the degree of polymerization and degree of intramolecular condensation of the ions generated in: A. ESI and B. MALDI.

To gain insight on the oligomer distribution, it would be necessary to do a chromatographic separation and to determine the absolute concentration of the individual homologues in the

formulation. The next sections describe the development of an HPLC method to achieve these goals.

Fractionation of the 3-aminopropyl oligosilsesquioxane formulation

In weakly acidic solution, 3-aminopropyl oligosilsesquioxane compound is ionic and highly polar due to the amino and the hydroxyl groups present in the molecules. Size exclusion chromatography is not suitable to separate the different homologues of the oligosilsesquioxane. Because of their highly polar nature, chromatographic separation of the homologues using the traditional reversed-phase techniques is also not possible. To enable the separation of the homologues, an ion-pair reagent is added into the eluent to enhance the interaction between the compounds to be separated and the stationary phase.

Perfluoroheptanoic acid (PFHpA) was used as an ion-pair reagent to strengthen the interaction of the oligosilsesquioxane homologues and the C18 stationary phase. The number of possible ion-pairing for an oligosilsesquioxane homologue is proportional to its degree of polymerization. The higher the n , the more amine group is available where the perfluoroheptanoic acid can attach to. Consequently, this results to more interaction with the C18 stationary phase and to a slower migration rate. Fractionation was achieved in the gradient of water and methanol with 5 mM PFHpA in a semi-preparative C18 column with DAD detector. The fraction corresponding to a homologue was collected at a retention time set after a thorough optimization. The composition of each fraction was confirmed using ESI-Q MS.

The fractionation process allowed the separation of homologues making the resulting fractions less polydispersed and less complex to be analyzed in the ESI-Q MS. The mass spectra of fractions containing homologues with $n=5, 7$ and 11 are shown in Figure 5.4- A, B and C respectively. It can be observed that at higher n , multiply-charged ions are favored by the ESI process. For example, at $n=7$, two patterns of the same compounds appear in the mass spectrum. One form results from the singly charged species while the other form originates from doubly-charged species. The mass differences of 18 and 9 for these forms reflect the intramolecular condensation of the singly- and doubly- charged ions, respectively. For $n=11$, the singly-charged form occurred minimally while the doubly- and triply-charged forms are more pronounced. Multiple-charging is highly probable at higher n since the number of amine groups that can accept extra protons is proportional to n . Doubly-charged ions with even-numbered n can have m/z that are almost equal to the m/z of singly charged ions with $n/2$ degree of polymerization. Multiple charging was not observed in the ESI mass spectrum of unfractionated formulation. This highlights the need to study thoroughly and

optimize the ESI process before a conclusion can be made regarding the relative amount of the homologues present in the formulation.

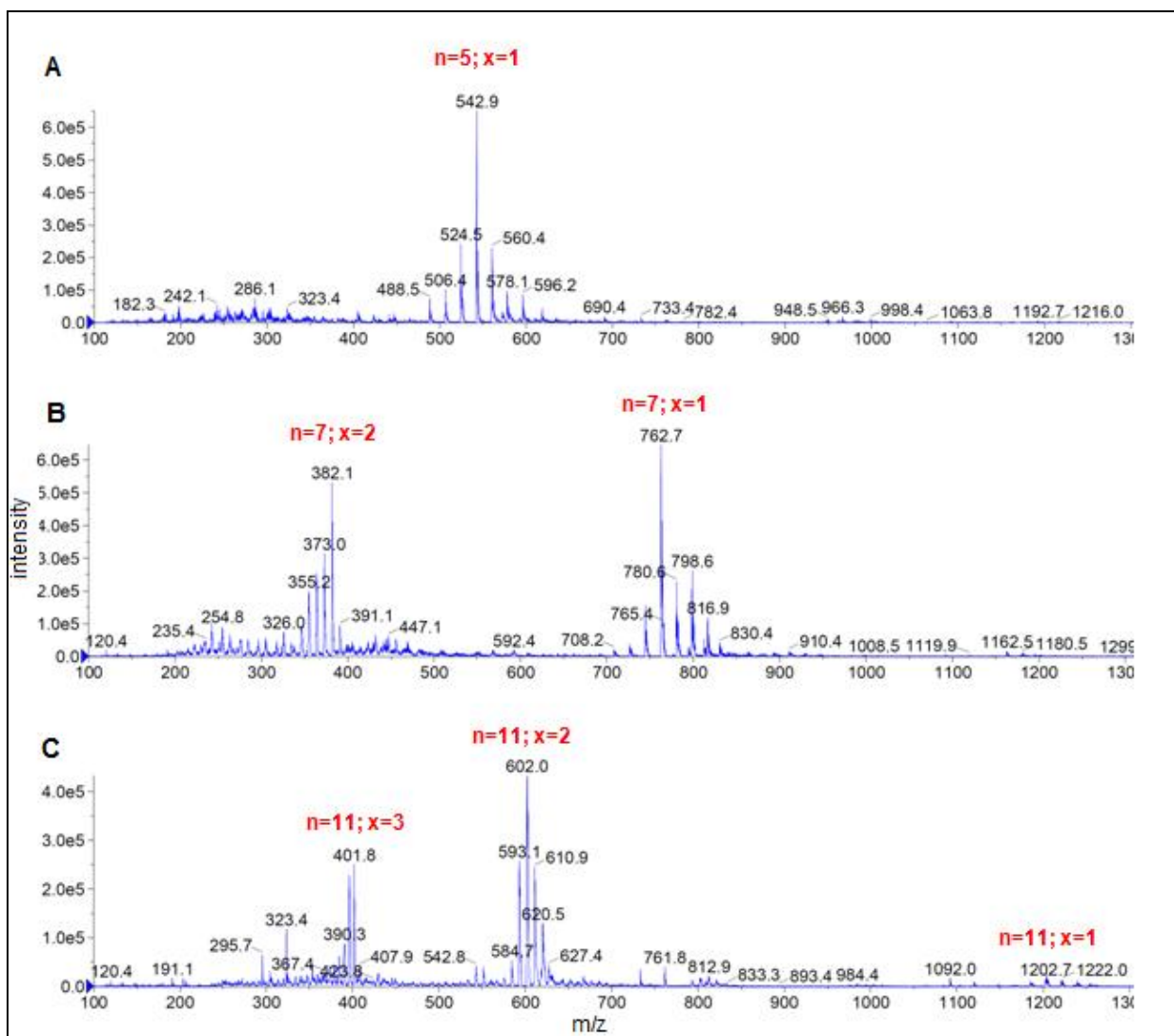


Figure 5.4. Positive-mode ESI-Q mass spectra of fractions containing oligosilsesquioxanes of $n = 5$, 7 and 11 (A-C) respectively. The x represents the charge of the ions.

Determination of the silsesquioxane molar concentration by ICP-OES

Single-homologue containing fractions can be used as calibration standards in the LC-ESI-Q MS determination of the absolute and relative molar concentration of the individual homologues as well as the MWD of the 3-aminopropyl oligosilsesquioxane formulation. Fraction collection was repeated several times to gather a significant amount for use as

calibration standard. The purity of the fractions was checked by ESI-Q MS. For some homologues, it was difficult to obtain a fraction that is free of other homologues. These cannot be used as standards. The molar concentration of the silsesquioxane in single-homologue containing fractions was estimated using the Si emission lines in the ICP-OES. Four Si emission lines were initially tested: 152.7, 212.4, 251.6 and 288.2 nm. The emission at 212.4 nm gave a low baseline and was free from matrix interferences. This emission line was used in the quantification Si in the fractions. The (3-aminopropyl) triethoxysilane was used as Si calibration standard. The calibration curve was set to linear and had a coefficient of determination (R^2) of 0.9991. Another silane, the dichlorodimethylsilane was used as quality control standard. A dilute solution of this was prepared in Milli-Q water at concentration of 0.25 and 0.50 $\mu\text{g Si/mL}$. Analysis of these two solutions against the (3-aminopropyl) triethoxysilane calibration curve gave a result of 120% and 104% recoveries respectively. Fractions containing single homologues of $n=3, 4, 5$ and 6 were analyzed in ICP-OES. The obtained Si concentration value in each fraction was reexpressed so that the final unit was in nmol Si/mL . To calculate the final concentration in terms of $\text{nmol polymer molecule/mL}$, the concentrations in nmol Si/mL were divided by the degree of polymerization. The fractions with the known homologue concentration were used as standards in HPLC ESI-Q MS analysis of the formulation.

Determination of the MWD of the oligosilsesquioxane by HPLC ESI-Q MS

The oligosilsesquioxane formulation was introduced into an HPLC with analytical C18 column and interfaced to ESI QqQ MS. The mobile phases used were water and methanol with 5mM PFHpA as ion pair reagent. Selected ions were monitored in the Q1. Table 1 lists the m/z monitored for each homologue from $n=3$ to $n=12$. The different m/z per homologue were results of varying degree of intramolecular condensation and charging. The main criterion in the selection of ions to be included in the list is their appearance or detection in the scan mass spectra of the fractions. Figure 5.5 shows the elution of the different homologues of the oligosilsesquioxane. Some m/z represent two different homologues. For example, m/z 405 and 423 can either be the doubly-charged ions of homologues with $n=8$ or the singly-charged ions of homologues with $n=4$. Nonetheless, they are well separated in the C18 column and will not be a problem in the analysis.

For quantification, the sum of the chromatographic areas of all the selected m/z per homologue was calculated. Three to four levels of calibration standards were prepared from the single-homologue containing fractions ($n= 3, 4, 5$ and 6) to generate the calibration curves. The reciprocal of the slopes of the calibration curves can be used as response

factors to quantify the homologues in the formulation. Figure 5.6 shows that the slope of the calibration curve is linearly proportional to n . This highly empirical correspondence can be used to extrapolate the slopes and the response factors for the homologues with $n= 7$ to 12.

Table 5.1. Selected ions monitored in the HPLC ESI-Q MS. Aso shown in parenthesis are the degrees of charging (x).

Degree of Polymerization (n)	of m/z monitored
3	($x=1$) 304, 322, 340, 358
4	($x=1$) 405, 423, 441, 459, 477
5	($x=1$) 506, 524, 542, 560, 578, 596
6	($x=1$) 625, 643, 661, 679, 697
7	($x=1$) 744, 762, 780, 798, 816, ($x=2$) 355, 364, 373, 382,
8	($x=1$) 845, 863, 881, 899, ($x=2$) 405, 414, 423, 432
9	($x=1$) 982, 1000 ($x=2$) 465, 474, 483, 492
10	($x=2$) 524, 533, 542, 551, 560
11	($x=2$) 602, 611, 620 ($x=3$) 401
12	($x=2$) 652, 661, 670, 679 ($x=3$) 429, 435

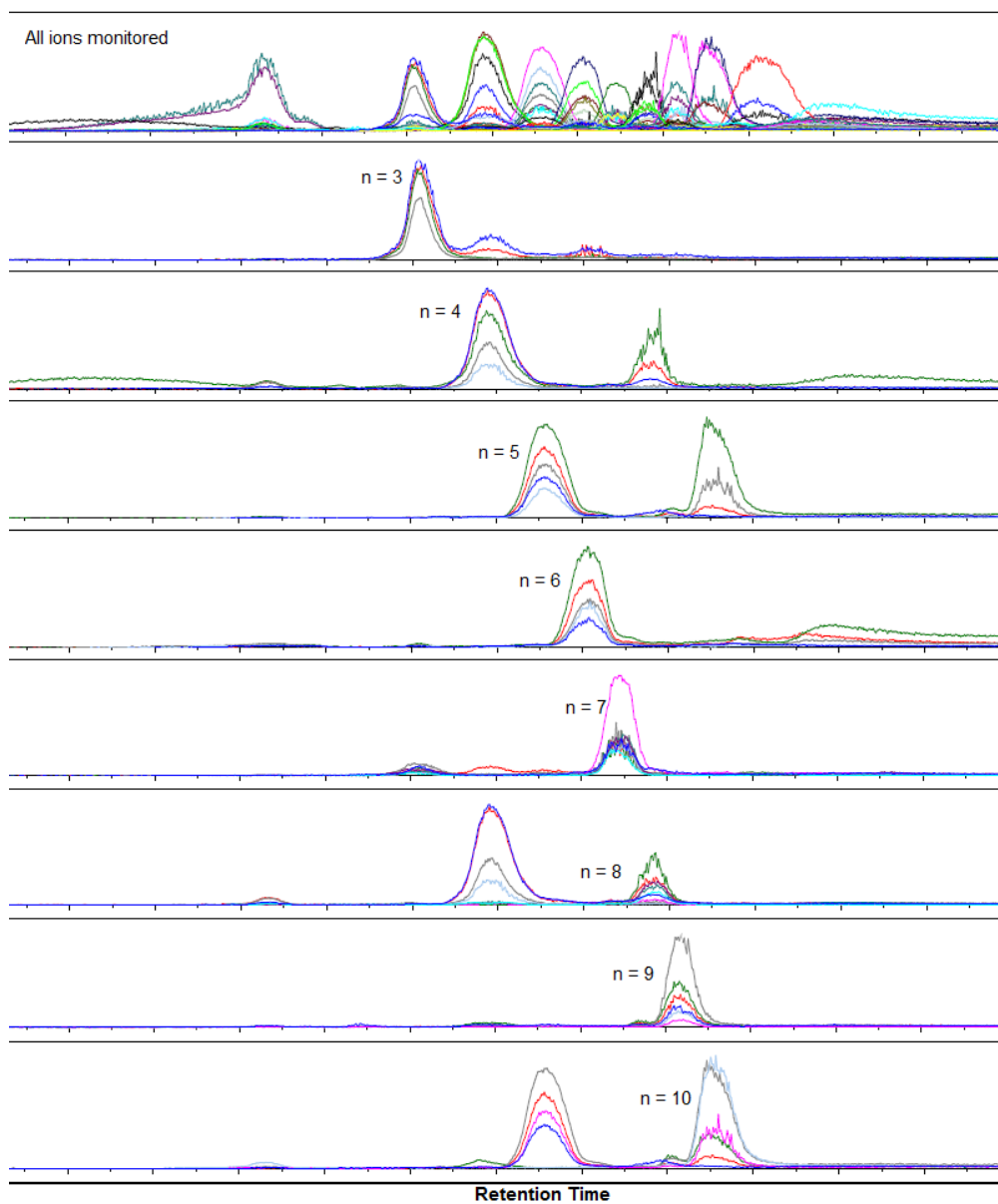


Figure 5.5. Elution of the oligosilsesquioxane homologues in the C18 column and in the gradient of water and methanol with 5 mM PFHpA.

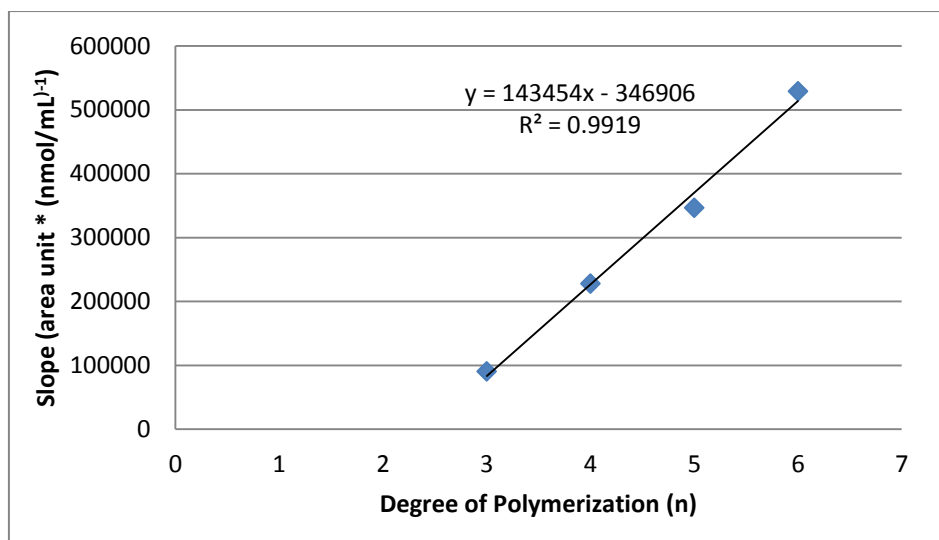


Figure 5.6. Degree of polymerization versus the slope of the calibration curve

The response factors (experimental response factors for $n=3$ to 6 and empirical response factors for $n=7$ to 14) were used to determine the concentration of the homologues in the fraction. The final MWD was obtained after normalization relative to the homologue with highest molar concentration (Figure 5.7). It is a bimodal distribution with $n=3$ and $n=10$ having the highest relative abundance. The absolute molecular weights of the individual homologue in the solution cannot be determined from MS because of the problem of further condensation in the gas phase. Thus, an accurate calculation of the polydispersity index will not be possible. The MWD shown in Figure 5.7 is better expressed as a degree of polymerization distribution instead.

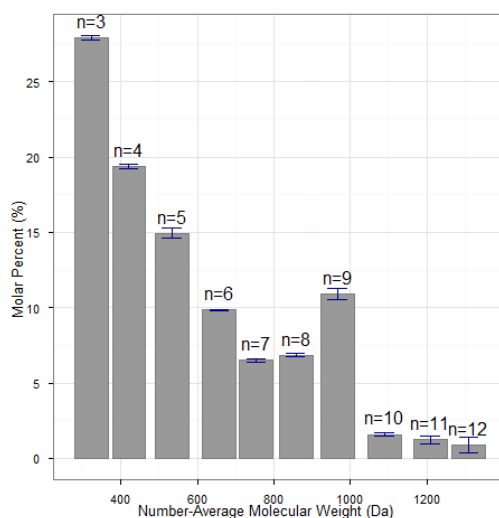


Figure 5.7. MWD of oligosilsesquioxane obtained by HPLC-ESI-Q MS

Conclusion

The use and applications of oligomers and polymers are dependent on the base structure of the monomer, the average MW and the polydispersity index. For oligosilsesquioxanes, the amount of Si-O-Si is additionally studied to determine the stability of the structure. The same physico-chemical properties dictate the behavior of these substances when released into the environment, for example, toxicity, fate and degradation.

The determination of the MWD of highly complex oligomers and polymers like the silsesquioxanes will not be possible using MS alone. In this paper, direct MS analysis using soft ionization techniques like ESI and MALDI gave contrasting MWD for the 3-aminopropyl oligosilsesquioxane formulation. ESI and MALDI are two different ionization processes; and the relative intensities of ions in the ESI and MALDI mass spectra are not directly translatable to MWD. The extent of ionization is affected by the functionality and the degree of polymerization of the polymers. This necessitated the development of a method with LC separation prior to MS detection and with absolute determination of concentration using single-homologue standards. The method used in this research can also be applied to other complex polymer formulation provided: 1. There is an efficient fractionation method to separate the different unique molecules in the formulation; and 2. There is a way of quantifying the molecule. Efficient fractionation can be done by using specialized columns, addition of ion-pairs, and optimization of mobile phase and the eluent gradient. Quantification of the unique fractions to be used as calibration standards can include spectroscopic techniques like uv-vis and nuclear magnetic resonance as well as another chromatographic technique.

With this method, the absolute and relative concentrations and the absolute molecular weights of each homologue were easily determined. These are vital information to be able to correlate the structure of the silsesquioxane with its properties and activity. The applicability of the method can be extended to other polysilsesquioxanes and polysiloxanes.

Chapter 6. HIGH RESOLUTION MASS SPECTROMETRY OF POLYFLUORINATED POLYETHER – BASED FORMULATION

ABSTRACT

High resolution mass spectrometry (HRMS) was successfully applied to elucidate the structure of a polyfluorinated polyether (PFPE)-based formulation. The mass spectrum generated from direct injection into MS was examined by identifying the different repeating units manually and with aid of the instrument data processor. Highly accurate mass spectral data enables the calculation of nth order mass defects. The different plots of MW and the nth order mass defects can aid in assessing the structure of the different repeating units and estimating their absolute and relative number per molecule. The three major repeating units were $-C_2H_4O-$, $-C_2F_4O-$, and $-CF_2O-$. Tandem MS was used to identify the end groups that appeared to be phosphates, as well as the possible distribution of the repeating units. Reversed-phase HPLC enabled the separation of the polymer molecules on the basis of number of nonpolar repeating units. The elucidated structure has resemblance with the structure in the published manufacturer technical data.

This analytical approach to the characterization of a PFPE-based formulation can serve as a guide in analyzing not just other PFPE-based formulations but also other fluorinated and non-fluorinated polymers. The information from MS is essential in studying the physico-chemical properties of PFPEs and can help in assessing the risks they pose to the environment and to human health.

Keywords: PFPE, ESI, Q-TOF, Orbitrap, mass defect

Submitted to the Journal of The American Society for Mass Spectrometry

Dimzon, I.K.D., Trier, X., Helmus, R., Knepper, T.P. and de Voogt, P. 2014. High Resolution Mass Spectrometry of Polyfluorinated Polyether – based Formulation

Introduction

Perfluoropolyalkylether (PFPE) represents a very diverse group of enduring polymers with unique applications. Generally, PFPEs have high thermal and chemical stabilities and low surface energies, dielectric constants and vapor pressures (Karis and Jhon 1998; Howell, Shtarov et al. 2011). Consequently, PFPEs provide low wettabilities and coefficients of friction (Pilati, Toselli et al. 1992). As such, these polymers have found variety of uses as high performance lubricating oils and greases. These include lubricants for food processing equipment (Solvay Solexis 2012). Another important use is for making food paper and paper products oleo-repellent in packaging of fats (e.g. butter or margarine), dry foods such as coffee and chocolate, and foods having a high fat content as meats, chips, hamburgers, popcorns, food to be cooked in microwave oven, crisps for cats or dogs and in general pet food (Iengo 2007; Solvay Solexis 2012). They have previously been found present in popcorn bag paper by ^{19}F NMR (Trier 2011). PFPEs are thus listed as materials that can be used in materials intended to contact with food by both the US FDA (Food and Drug Administration 2010; Food and Drug Administration 2010), the EU Plastics Regulation (European Commission 2011) and in the German BfR recommendations (Bundesinstitut für Risikobewertung 2014), and is to some extent used to replace long-chain fluorosurfactants with perfluoroalkyl chains longer than seven $-\text{CF}_2-$ units (Scheringer, Trier et al. 2014). Other uses include biomedical applications (Krafft and Riess 2009), as ultrathin film of liquid lubricant in magnetic recording devices to reduce friction and to prevent early deteriorations due to the slider-disk contact (Gellman 1998; Spada and Basov 2000; Li, Jones et al. 2004). The surface properties of PFPEs including their tribology are dependent on their viscosity, molecular structure and degree of polymerization (Karis and Jhon 1998).

The different PFPE formulations in the market today have their backbone structures synthesized using manufacturer-specific processes based on a combination of techniques like anionic polymerization, hydrolysis, exhaustive fluorination and photo-induced oxidation polymerization from raw materials such as 2,2,3-trifluoro-3-(trifluoromethyl)oxirane, 2,2,3,3-tetrafluorooxetane, tetrafluoroethene and/or hexafluoropropene (Howell, Friesen et al. 2007; Howell, Shtarov et al. 2011), and ref Solvay solexis 2007, Fomblin) Some commercially-available PFPE bases are known by their trade names such as Krytox® , Fomblin® and Demnum® (Howell, Shtarov et al. 2011). The PFPE bases can have $-\text{CF}_2\text{O}-$, $-\text{C}_2\text{F}_4\text{O}-$, $-\text{C}_3\text{F}_6\text{O}-$ or a random combination of these repeating units with molecular weights ranging from 500 to 15,000 Da (Howell, Shtarov et al. 2011). For specific final applications, the physico-chemical properties of PFPE bases are enhanced by further modifications. Another polymer block (for example polyethylene glycol) (Pilati, Toselli et al. 1992); and/or some end groups (for example, perfluorinated alkyl chains, or carboxylic or phosphate polar heads) can

be added to the PFPE during or after polymerization (Howell, Friesen et al. 2007). Modified PFPEs are also synthesized by addition of new reactants before halting the polymerization process producing copolymers, like in the case of synthesizing PFPE with tetrafluoroethene (TFE) and 2,2,4-trifluoro-5-trifluoromethoxy-1,3-dioxole blocks (Avataneo, Navarrini et al. 2009; Avataneo, De Patto et al. 2011).

The complexity in the chemical composition presents an analytical challenge in elucidating the structures of the individual species present in a PFPE formulation. In general, studying polymeric structures includes understanding of the different features that contribute to their diversity. These features include: a) molecular weight distribution; b) nature of the repeating units; c) presence of end groups, side chains and other functionalities (Van Krevelen and Te Nijenhuis 2009). Other structural attributes include the degree of branching and cross-linking; and the nature of defects in the natural sequence of these polymers (Van Krevelen and Te Nijenhuis 2009). Mass spectrometry (MS), in recent years, has been widely used in the characterization of polymers. Soft ionization techniques like matrix-assisted laser desorption ionization (MALDI) and electrospray ionization (ESI) make possible to perform MS analysis of large, intact molecules with minimum fragmentation. Ultra high performance liquid chromatography can easily be interfaced to the ESI source to analyze complex polymer formulations (Dimzon and Knepper 2012). Accurate masses derived using high resolution mass spectrometry (HRMS) in combination with fragmentation information makes possible the elucidation of molecular structures.

Recently, the use of mass defects has become increasingly popular as a way of screening compounds in processing of high resolution mass spectra in non-target analyses. The mass defect is the difference between the exact mass of a molecule and its nominal integer mass. Mass defects arise from the fact that each nuclide has slightly different nuclear binding energy relative to carbon-12 (Sleno 2012). In some nuclides, a tiny portion of the mass is converted into energy to keep the nuclei together. Since ^1H does not have a neutron in the nucleus, it does not need extra nuclear energy. As a result, the proton has a positive mass defect (1.0078 u). The mass defect of a molecule is the sum total of the mass defects of the individual nuclides. In a homologous hydrocarbon series, the mass defect increases proportionally with the number of H. On the other hand, F (18.9984 u) has a negative mass defect (NMD) such that when it is present in a molecule, the overall mass defect of the molecule is lower compared to the corresponding hydrocarbon molecule with H bound to carbon. A molecule consisting of C, H and F atoms will have negative mass defect if the proportion of F to H nuclides is greater than 4.9. If a molecule contains other hetero atoms, such as oxygen (15.9976), then this will add to the NMD of the molecule. Mass defect analysis has been successfully applied as a data mining tool in the identification of the

different components of very complex mixtures like crude oil and extracts from biological matrices (Hughey, Hendrickson et al. 2001; Zhang, Zhang et al. 2009). PFASs, being dominated by F nuclide are usually characterized by NMDs. NMDs, therefore can serve as an important screening tool for these substances (Trier, Granby et al. 2011). However, using only the mass defect has the disadvantage that it changes with the m/z of the molecule, which cannot be corrected for with current MS softwares, which only can set the mass defect filters in a specific region from e.g. 0.8 to 0.99 u.

However, this can be solved by 'normalising' the mass defects, by dividing the measured m/z with the nominal mass of the repeating unit. This is called the Kendrick mass defect scale. In polymers this method can be used to determine the presence of some repeating units as in the case of homologous series (Hughey, Hendrickson et al. 2001). For example, in the case of the $-CH_2-$ repeating unit in a homologous series, the Kendrick scale converts the repeating mass of 14.01565 u to 14.00000 u (Hughey, Hendrickson et al. 2001). Thus, when a repeating unit is normalized, the mass defect of the scaled mass is only due to the other un-normalized units. Caution must be exercised however in using the mass scaling since the effectivity of Kendrick mass defect calculations is diminished with the decrease in mass accuracy. This is especially true in the case of PFASs where the single F nuclide has an absolute mass defect of only 0.0016 u.

The information regarding chemical structure of polymers provides vital insights as to the properties these substances exhibit. This knowledge enables the manufacturers to fine-tune the production processes towards a specific application through quantitative structure-property relationship studies. Chemical data of polymers can also aid in studying the fate, behavior and degradability (Frömel and Knepper 2008) of these substances in the environment. This is particularly important for poly/perfluorinated polymers like the PFPE as they can be precursors to highly persistent and/or toxic perfluorinated pollutants, in e.g. landfills (Eschauzier, Raat et al. 2013; Wang, Huang et al. 2013).

In this research work, the composition of an unknown PFPE-based formulation was characterized by high resolution MS, specifically using ESI with quadrupole-time-of-flight (QqTOF) and Orbitrap mass analyzers. Mass spectral data interpretation was improved by employing first-, second- and third-order mass defect (MD) analyses. Tandem MS up to the fourth order was done on the most abundant ion in to acquire information on the structural features of the ion including its end group. The elution order of the different components of the formulation in a C18 chromatographic column provided some complementary information regarding the repeating units the formulation and the influence of these features on the overall polarity of the polymeric species.

Materials and Methods

Unknown PFPE-based formulation and chemicals

The PFPE-based formulation was Solvera PT5045 from Solvay Solexis, Italy. For the experiments done at the University of Amsterdam, Institute of Biodiversity and Ecosystem Dynamics (UvA-IBED), the following reagents were used: methanol (ULC/MS grade, absolute) and formic acid (ULC/MS grade, 99%) purchased from Biosolve; sub-boiled purified water prepared in-house. For the experiments done at the Hochschule Fresenius (HSF), the following reagents were used: methanol, formic acid purchased from Karl Roth; Milli-Q water.

High resolution MS

Two different mass spectrometers were used in this research study. The maXis 4G™ QTOF (QqTOF) (Bruker Daltonics) was used. The working solution was prepared by diluting the PFPE-based formulation by a factor of 10000 with 0.2 % formic acid in methanol. The working solution was then introduced into the ESI source via a syringe pump at a 3 µL/min flow rate. The positive and negative mode TOF mass spectra were taken after instrumental parameter optimization in the range from 500 to 3000 u. The following were the optimized ESI parameter values: Capillary, 5 kV; nebulizer gas, 0.4 bar; dry gas, 4.0 L/min; and dry temperature, 180 °C. The mass analyzer settings were: funnel RF, 400 Vpp (peak-to-peak voltage); multipole RF, 400; quadrupole ion energy, 4.0 eV; collision energy, 8.0 eV; collision RF, 3500 Vpp; transfer time, 75 µs; and pre-pulse storage, 35 µs. Mass calibration was performed using polypropylene glycol standard.

Chromatographic separation was done using Shimadzu Nexera UPLC equipped with LC-30 AD pumps and IL-30 AC autosampler. The stationary phase was Phenomenex Luna C18 (II), 150 mm length, 3.0 mm internal diameter, 3 µm particle size and 100 Å pore size. Gradient elution was performed using 0.2% formic acid in 95:5 water:methanol (Eluent A) and 0.2% formic acid in methanol (Eluent B). Eluent ratio was varied from 40% Eluent B to 100% Eluent B in a total run time of 20 min: gradient was first increased to 80% Eluent B at a rate of 20% /min; then, gradient was increased to 100% Eluent B at a rate of 2% /min; the gradient was maintained at 100% Eluent B for 11 min; the gradient was put back to 40% Eluent B and was re-equilibrated. The mobile phase flow rate was maintained constant at 0.20 mL/min. The injection volume was 5 µL.

Also the Orbitrap VelosPro, Hybrid linear ion trap/orbitrap MS (Thermo Scientific) was used. The working solution was prepared by diluting the PFPE-based formulation by a factor of 1000 with 0.2 % formic acid in methanol. This was introduced into the MS via a syringe pump at 3 $\mu\text{L}/\text{min}$. The following were the optimized ESI parameter values: sheath gas flow rate, 30 (arbitrary unit, arb); aux gas flow rate, 20 (arb); spray voltage, 3.5 kV; and capillary temperature, 320 $^{\circ}\text{C}$. The lenses were tuned prior to use.

MS data processing and Kendrick mass defect analysis

Data were processed using the accompanying software for each instrument. The Data Analysis 4.2 (Bruker Daltonics) and the Thermo Xcalibur 2.2 Qual browser (Thermo Scientific) were used for the QqTOF and Orbitrap data respectively. Additionally, the ChemCalc molecular formula finder (Patinay 2013) was used aside from the equivalent built-in functions in the software.

The processed mass spectral data from the Orbitrap were extracted into a Microsoft Excel 2007 sheet and was saved as comma delimited files. The raw Excel file was then processed by sorting the data according to decreasing relative intensity. The peaks with relative intensities less than 5% were not included in the Kendrick mass defect calculations.

The free software 'R' (The R Foundation for Statistical Computing) was used in the Kendrick mass defect calculations and in the generation of the Kendrick plot. An R source code, 'MassDef', was developed in-house for this purpose. The 'MassDef' code makes use of several user-defined functions to generate different plots – e.g. molecular weight vs. first-order mass defect. The plotting was made possible using the 'ggplot2' package. The algorithm developed for the source code was based on the calculation of n^{th} -order mass defects as described in details in the works of Roach, *et al.* (Roach, Laskin *et al.* 2011) .

Tandem Mass Spectrometry

Two fragmentation modes in the Orbitrap Velos-Pro MS were used in the MS^n experiments: Higher energy C-trap dissociation (HCD) and collision-induced dissociation (CID). The ion with m/z 1176.999 was studied under different fragmentation parameters. The resulting fragment ions were then analyzed in the Orbitrap and in the linear ion trap. Initially, the ion with m/z 1176.999 was fragmented in the HCD cell at an increasing normalized energy of from 20% to 35%. The optimum normalized energy was found to be around 20%. Then, MS^n analysis up to the 4th order was performed using stepwise CID starting from m/z 1176.999.

The following precursor ions were fragmented using normalized collision energy of 20%: m/z 1079; 1035 and 991.

Results and Discussion

MS Analysis of PFPE-based formulation

A survey of the molecular weight distribution and the possible components of the PFPE-based formulation was initially done using ESI with Orbitrap and QqTOF mass analyzers. The QqTOF was calibrated using polypropylene glycol standard in the m/z range from 500 to 2000. The mass errors after calibration (residuals) were all below 1 ppm. The QqTOF provides a mass resolution of up to 50,000. The mean value of 10 determinations for m/z 1176.9991 has an expanded uncertainty of ± 0.0050 (95% confidence interval). The Orbitrap on the other hand, was calibrated as specified by the manufacturer. The mass errors after calibration (residuals) were all below 1 ppm. It has a mass resolution of up to 100,000 at m/z 400. The mean of 10 determinations has an expanded uncertainty of ± 0.0005 (95% confidence interval) for m/z 1176.9996 .

The generated average QqTOF positive-mode mass spectrum is shown in Figure 6.1. Most of the observed positive ions are in the m/z range between 900 and 1500. The base peak had an m/z of 1176.999 (Figure 6.1, insert). This m/z has an expanded uncertainty of ± 0.020 ($n=10$, $CI=95\%$). The nearby low-intensity peak with m/z of 1177.079 can easily be mistaken as an isotopolog. It will be shown in section 3.3, however, that the species with m/z of 1177.079 is not an isotopolog of m/z 1176.999 but a chemically distinct moiety because it has a different retention time in the HPLC. The generated positive ions are singly charged. Using the Data Analysis 4.2 software, the mass spectrum was screened for patterns of m/z differences. Patterns identified were consistent with $-C_2H_4O-$ (44.026 u), $-C_2F_4O-$ (115.989 u), $-CF_2-$ (49.997 u) and $-CF_2O-$ (65.992 u) moieties. These identified differences can be the possible repeating units of the multiblock co-polymer.

The obtained positive-mode Orbitrap mass spectrum has a comparable mass distribution to that obtained using the QqTOF. The peak with highest intensity has an m/z of 1176.9994. This m/z has an expanded uncertainty of ± 0.002 ($n=10$, $CI=95\%$).

ChemCalc Molecular Formula Finder (Patiny 2013) was used to predict the most likely chemical formula of the most intense ion in the QqTOF mass spectrum. Filter parameters were applied on the basis of prior observations regarding the possible repeating units and on the assumption that the molecules will not be too complex. Thus, it was preselected that the search will include the following: C: 0-50; H: 0-100; F: 0-100; O: 0-50 and P: 0-3. Degree of

unsaturation was set to be between -2 and 2. The upper limit of the degree of unsaturation was set to a low value based on the information that the identified repeating units were saturated.

The most likely chemical formulae of the ion with m/z 1176.999 are $[C_{25}O_{10}F_{37}H_{13} + H]^+$ or $[C_{23}H_{24}O_{20}F_{26}P_2 + H]^+$ and the calculated differences of their corresponding exact masses to the obtained mass are 0.44 ppm and 0.68 ppm, respectively. The other m/z values can subsequently be assigned with the corresponding chemical formula on the basis of the difference pattern. Protonation is the primary ionization mode for this type of polymers, having oxygen atoms with lone pairs that donate electrons to the protons. Sodium adducts were not observed in substantial amounts. A molecular dynamic simulation study by Jonkers et al. suggests that the ethoxylate groups can wrap themselves around the sodium ion in such a way that the electron density of oxygen has optimum interaction with the cation (Jonkers, Govers et al. 2005). In perfluorinated polyethers, the oxygen electron density can be diminished by the fluorine atoms. Therefore, formation of sodium adducts will only be possible when there is a substantial number of $-C_2H_4O-$ units in a molecule.

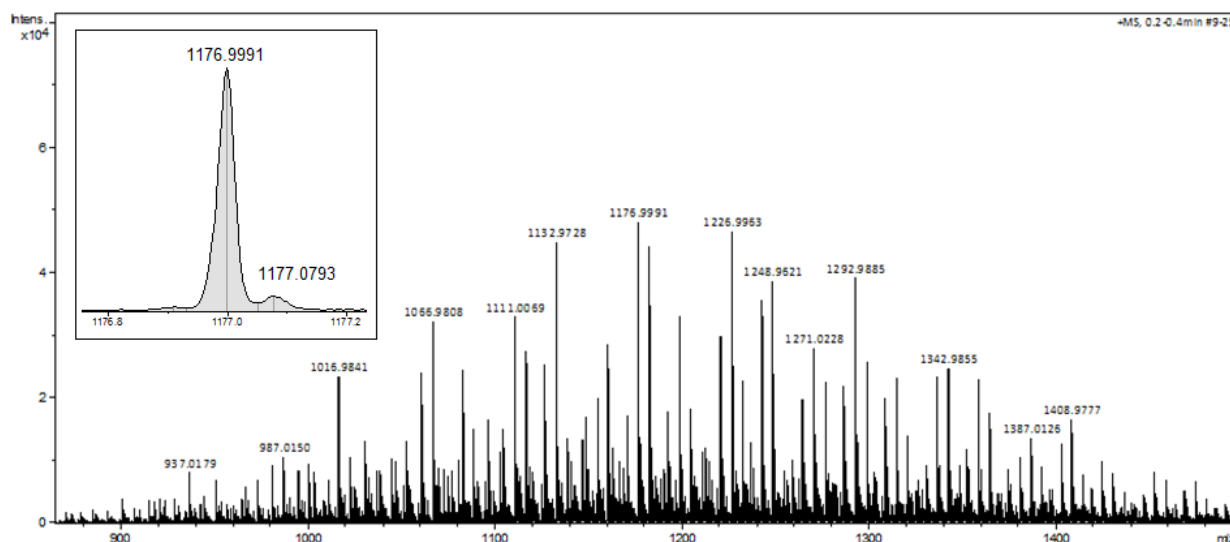


Figure 6.1. Positive-mode QqTOF mass spectrum of the PFPE-based formulation. Insert: Magnified view of the peak with highest intensity

Analysis of Mass Defects

The positive-mode ESI-Orbitrap MS data of the PFPE-based formulation was used in the analysis of mass defects because these have lower uncertainty. The acquired molecular weights were first converted to the Kendrick scale relative to the $-C_2H_4O-$ repeating unit. The

Kendrick mass defect was then obtained by subtracting the nominal mass from the Kendrick mass. In this case, the nominal mass was taken as the lowest integer value next to the Kendrick mass (can be derived using the “round” function of the basic R code). Figure 6.2 shows the plot of the acquired molecular weights versus the first-order Kendrick mass defect (MD1). The mass defect was calculated in absolute value to eliminate the negative sign. The “first-order” qualifier is used to denote the first cycle of Kendrick mass calculation. The size of the points is proportional to the corresponding relative ion intensity. To visualize what happens during the Kendrick mass defect calculation, m/z 1176.999 and the masses related to it by some repeating units were monitored. The repeating units monitored included: 115.989 (-C₂F₄O-); 44.026 (-C₂H₄O-), 65.992 (-CF₂O-) and 49.997 (-CF₂-) These m/z values were shown in different shapes in Figure 6.2. It can be observed that all the m/z of $1176.999 \pm n * 44.026$ are aligned horizontally indicating that they have equal MD1. This is consistent with the fact that the Kendrick mass was scaled with respect to -C₂H₄O- unit. The molecules with equal MD1 values vary only in the number of the -C₂H₄O- units. All the other atoms in those molecules are exactly the same. The other m/z monitored e.g. those varying by 115.989, 65.992 and 49.997 repeating units from 1176.999, follow a decreasing trend in MD1 with increasing molecular weight. The increase in the number of F and O nuclei caused the overall decrease in MD1.

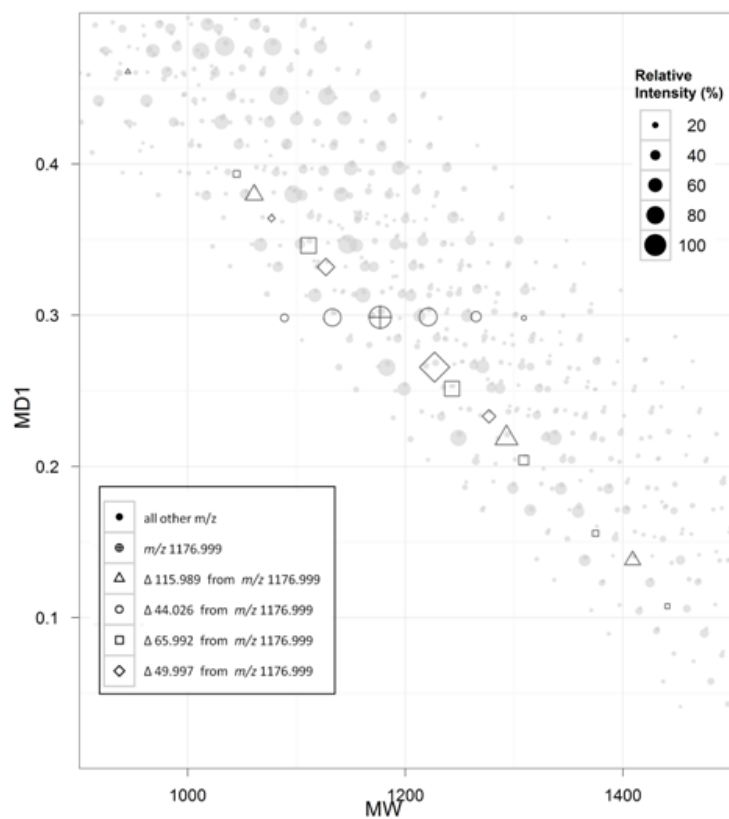


Figure 6.2. Molecular weight versus first-order Kendrick mass defect, MD1 (Generated using 'MassDef,' an R source code). The first-order mass transformation was done relative to the $-C_2H_4O-$ repeating units. The values of the molecular weight used were from the positive-mode ESI-Orbitrap mass spectrum with relative intensities greater than 5%

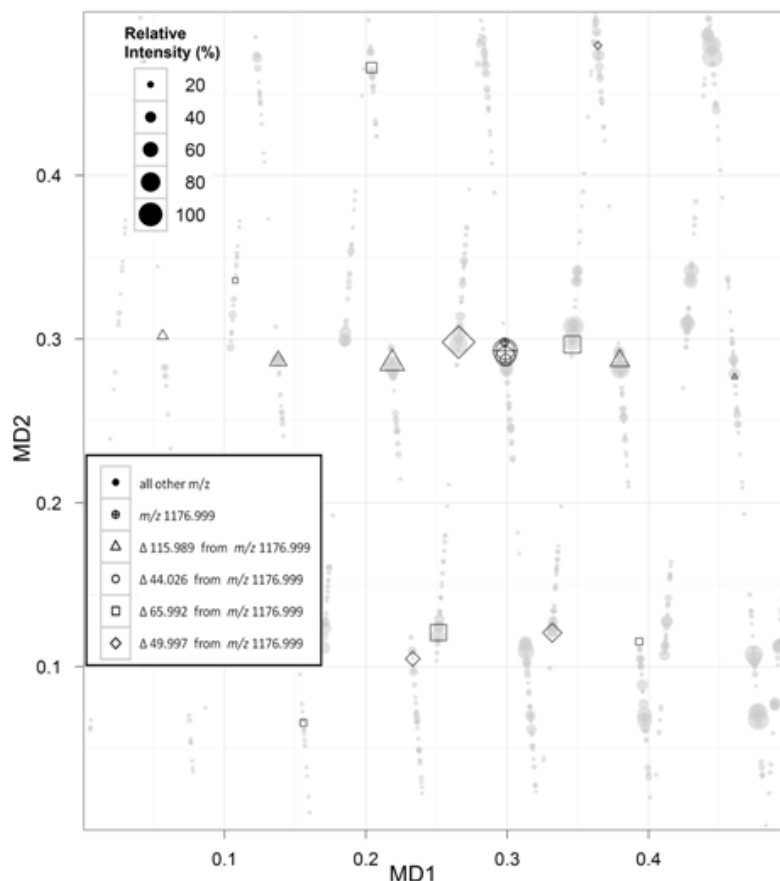


Figure 6.3. First-order (MD1) versus second-order (MD2) Kendrick mass defect (Generated using 'MassDef,' an R source code). The second-order mass transformation was done relative to the $-C_2F_4O-$ repeating units

Another cycle of mass scaling and mass defect calculations can be employed (Roach, Laskin et al. 2011) to detect other patterns present in a complex mixture. The so-called second-order mass transformation was done with respect to the $-C_2F_4O-$ repeating unit. The plot of MD1 versus the second-order (MD2) Kendrick mass defects is shown in Figure 6.3. It can be observed that the points with equal MD1 in Figure 6.2 clustered together into just a single point in Figure 6.3. All points with equal MD1 will always have equal MD2. After the second-order transformation, all the points with m/z varying by 115.989 from 1176.999 have equal MD2 as m/z 1176.999. The molecules with equal MD2s vary in the number of both the $-C_2H_4O-$ and $-C_2F_4O-$ units. All the other atoms in those molecules are exactly the same.

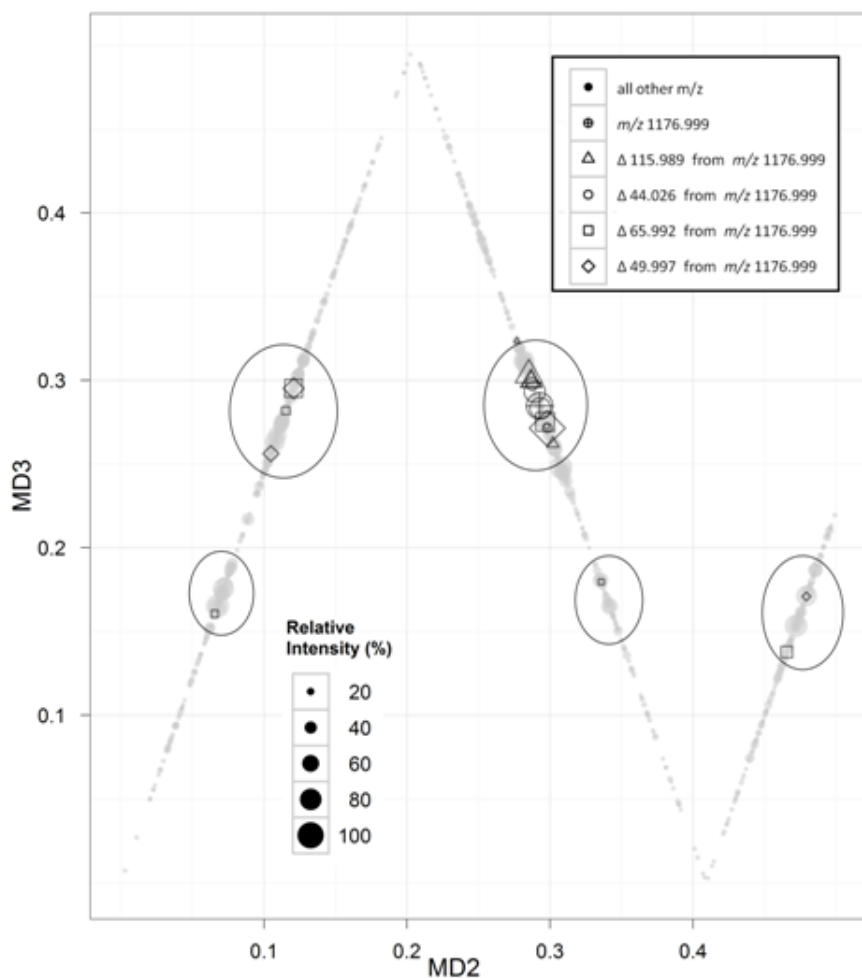
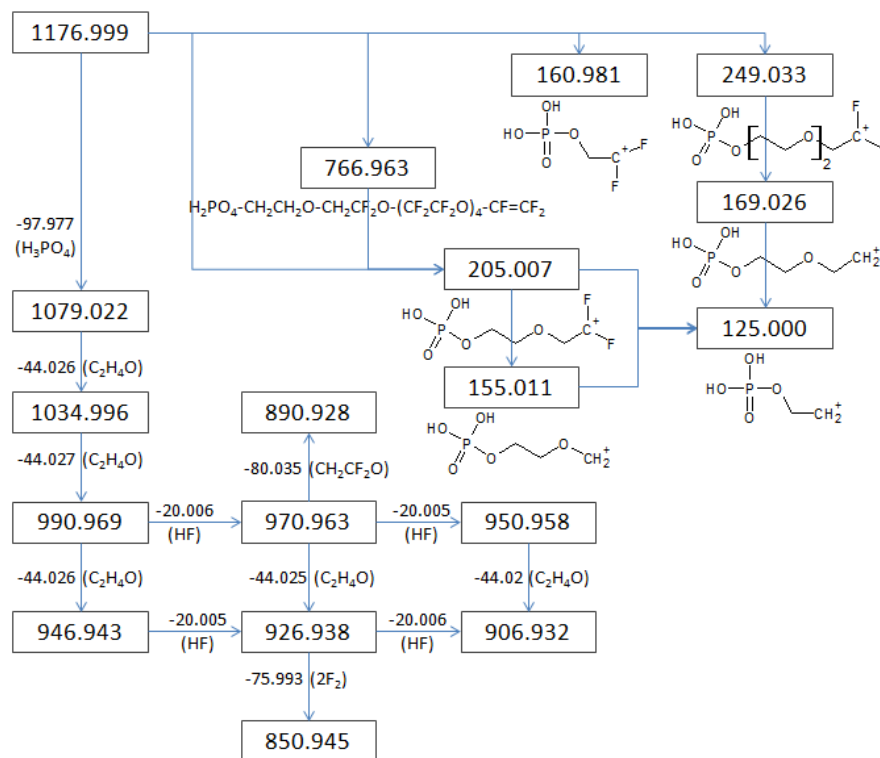


Figure 6.4. Second-order (MD2) versus third-order (MD3) Kendrick mass defect (Generated using the 'MassDef,' an R source code). The third-order mass transformation was done relative to the CF_2O repeating units

Third-order mass transformation was done relative to $-\text{CF}_2\text{O}-$ unit and the plot of MD2 versus the third-order (MD3) Kendrick mass defects is shown in Figure 6.4. In this plot, five clusters of points can be observed: 2 large clusters and 3 small clusters. The large clusters are in the same range of MD3 (2.3 – 3.3). Likewise, the small clusters are all in another MD3 range (1.4 – 2.0). Ideally, it is expected that all the m/z that vary only in the number of $-\text{CF}_2\text{O}-$ from 1176.999 units will have equal MD3. In Figure 6.4, the points are in a certain range instead of being in a single horizontal line that denote equal MD3. The precision of MS data is a limiting factor on how far one can perform n^{th} -order mass transformation for mass defect calculations. The spreading of the MD3 values within a certain range, therefore, can be attributed to enlarged effect of noise and the low value of the mass defect of the CF_2O repeating unit.

It is shown in this section that n^{th} -order mass defect is a powerful tool that can be used not just in screening the perfluorinated polymers but also in surveying the different repeating units and the extent of their variability in a given polymer mixture.

Tandem Mass Spectrometry



Scheme 1

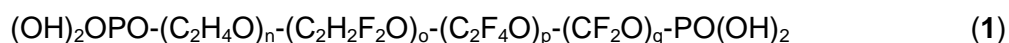
The MS^n fragmentation of the ion with m/z 1176.999 is summarized in Scheme 1. The high-MW principal product ions of m/z 1176.999 result from the loss of H_3PO_4 (97.977 u) and the successive losses of C_2H_4O (44.026 u). The other high-MW product ions result from the loss of HF (20.006 u) of the main fragments. On the other hand, most of the low mass product ions contain phosphate functional groups. MS^3 was performed on the product ions of m/z 1176.999: m/z 1079.022, 1034.996 and 990.969. The mass spectra obtained showed successive losses of 44.026 u as was previously observed. This also confirms the linear nature of the polymer molecule. The product ion of m/z 1177.0 with m/z of 991.0 was further fragmented in the CID. The main product ions have m/z of 970.963 and 946.943. These correspond to the losses of HF and C_2H_4O respectively. MS_4 was done on the product ion with m/z 971.0 following the transition: $1177.0 \rightarrow 991.0 \rightarrow 971.0$. The product ions have m/z values of 951.0 and 926.9. These ions correspond to the losses of HF and C_2H_4O ,

respectively. The product ion with m/z 906.9 results from the successive losses of HF and C_2H_4O . Interestingly, not all the ions produced in the fragmentation of m/z 991.0 are also generated in the fragmentation of m/z 970.9, particularly m/z 946.9. The ions with m/z of 970.9 and 946.9 can be generated from either different positional isomers or from the same but asymmetric polymer molecule. The product ion with m/z 890.9 was also observed. This is the result of the loss of $C_2H_2F_2O$ from m/z 970.9.

Reversed-phase HPLC

Reversed-phase HPLC was to separate the different components of the formulation based on polarity. Shown in Figure 6.5A is the base peak chromatogram of PFPE formulation obtained with the QTOF-MS. Superimposed in the same figure are the 'Dissect' chromatogram traces resulting from the deconvolution process. The dissect algorithm of the Data Analysis software combines all ions from molecules with similar chromatographic elution profile into one chromatographic trace. At a certain time window, if two or more ions have the same retention times and peak widths, and if they have similar shapes; then they are combined together as one chromatographic trace. In Figure 6.5A, the 90 software-derived chromatographic traces represent 90 groups of compounds with different elution properties in a C18 stationary phase. An inspection of the mass spectrum of a chromatogram trace reveals that the molecules with the same elution properties showed a pattern of 44.026 u mass differences. This pattern can be attributed to $-C_2H_4O-$ repeating units. This implies that species varying only in the number of $-C_2H_4O-$ repeating units are not separated by this particular C18 HPLC column, though separation of such oligomers previously has been obtained on an UHPLC column (Acquity C18, 150 mm, 2.1 mm, 1.7 μ m) (Trier 2011).

Based on the results of the previous HRMS experiments and mass defect analyses, a major component of the polymer formulation will have the general formula (1):



The elution order of selected species having this general chemical formula was monitored as shown in Figure 6.5B. In general, the retention in C18 column of the polymer molecule is proportional to the total number of CF_2 units given by the formula $2p+q$. If the number of CF_2 units are equal, the higher the sum of C_2F_4O and CF_2O ($p+q$), the longer is the retention time.

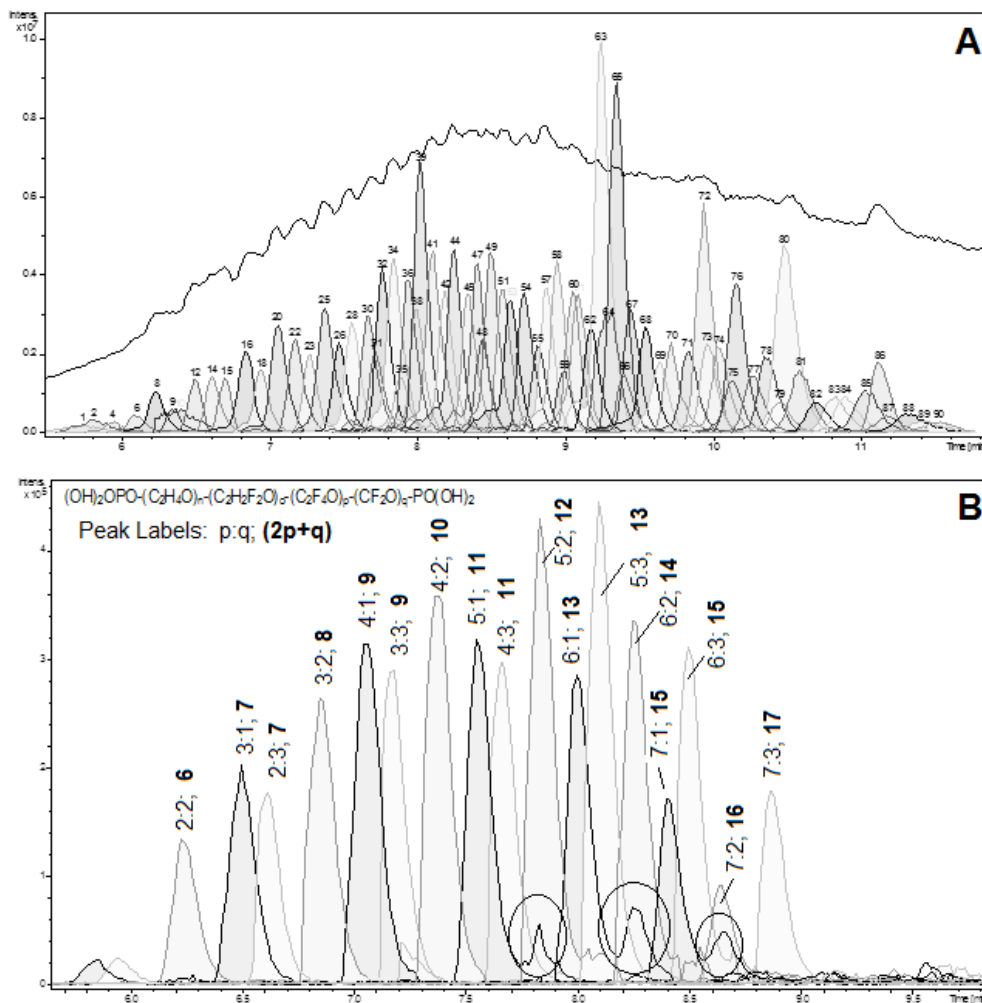
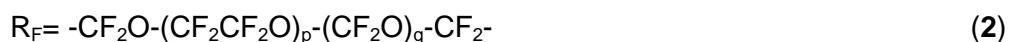
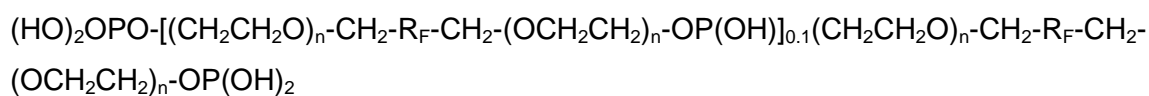


Figure 6.5. A) Base peak chromatogram of the PFPE formulation and the Dissect chromatogram traces; and B) Chromatograms of selected ions that correspond to the indicated chemical formula

Some shoulders were observed in the chromatogram as shown in Figure 5B. These shoulders are in reality a set of masses different from the ones being monitored. The m/z values that caused the shoulders were 0.095 different from the m/z values being monitored. For example, the m/z values of 1248.9619 and 1249.0571 have chemical formulas $C_{23}H_{21}F_{30}O_{20}P_2$ ($n=3$; $p:q = 5:3$) and $C_{27}H_{33}F_{26}O_{21}P_2$ ($n=6$; $p:q = 5:1$) respectively. These two will have different retention times. The software settings to generate the chromatograms were not discriminating enough between these two sets of masses with less than 0.1 m/z differences.

Comparison of the derived chemical structure to the published technical data

The chemical structure is not given on the technical datasheet for the PT 5045, produced by Solvay Solexis. They do however mention that it is a perfluoropolyether-phosphate derivative, used for paper and board. In a 2013 patent application from the same company and where PT 5045 is a raw material, the average structure of the polymer is given as (2):



The patent specifies that p:q is between 2 and 3 and that n is 1.8 (Tonelli, Sergio et al. 2013). The structure suggests that a molecule can contain two or three P atoms. Ninety percent of the molecules contain only two P atoms that are at both ends of the molecules as phosphate esters.

The results of the present study suggest a structure similar to the one proposed by Solvay Solexis for PT5045, although the ratio p:q is more variable and ranges from 1:3 to 7:1 as shown in Figure 6.5B. Also, the distribution of n s not always symmetric. Positional isomers can exist and the number of -CH₂CH₂O- repeating units on both ends of the molecule beside the phosphate groups adds up to 4 as can be deduced from Figure 6.2.

Chemical structure and physico-chemical properties of PFPE-based formulations

In the past years, fluorinated polymeric coatings have become increasingly popular as a way to decrease the potential migration from food packaging in contrast to smaller PFASs, for example the fluorotelomer alcohols (FTOHs). First of all the polymer is coated only at the surface, and secondly the polymer is cross-bound to itself so it is less amenable to migrate. Engineering the endgroups and the number of each monomer units in a PFPE molecule is a way to adjust their solubility to certain solvents and to enable their binding to a variety of polar to nonpolar surfaces. The presence of ether groups makes the polymer more water soluble by the ability of the oxygen lone pairs to donate electrons for hydrogen bonding. Water solubility can be further enhanced by addition of an ionic terminal endgroup, called the polar head of the surfactant, which typically could be phosphates, carboxylates or quaternary amines.

As surfactants PFPEs may elicit significant physicochemical differences depending on the hydrocarbon segments (blocks) they contain. The hydrocarbon block enables them to make hydrophobic bonds to hydrocarbon surfaces. This increases the abrasion strength of other

layers, such as printing inks, lacquers or glue which are to be tied onto the PFPE layer at the surface. On the other hand perfluorinated ethers without the hydrocarbon block would repel the hydrocarbon chemicals. If these PFPEs are to be used in food packaging, the size of the hydrocarbon block must be controlled because of the increased risk to humans upon intake brought about by increased binding to lipids (Krafft and Riess 2009).

Currently, PFPE-based polymers are considered alternatives to persistent long-chain perfluoroalkyl carboxylic acids and sulfonates and their precursors. However several questions arise regarding their degradability, persistence and toxicity (Wang, Cousins et al. 2013). These polymers can most likely be also precursors to persistent and slowly degrading compounds. For, example, Galden ®, a PFPE with $-\text{OCF}_2(\text{CF}_3)\text{CF}-$ repeating units, was shown to degrade very slowly at atmospheric conditions (Young, Hurley et al. 2006; Wang, Cousins et al. 2013). These data gaps can only be addressed properly beginning with accurate information regarding the chemical structures of the polymers derived from mass spectrometry studies. Lack of information of specific chemical substances, technical blends cannot be assessed by *in-silico* methods, such as quantitative structure property relations (QSPR) and quantitative structure activity relations (QSAR) which require knowledge of the specific molecular structure (Duchowicz, Fioressi et al. 2015). For the same reason technical mixtures are also often omitted from evaluation of toxicity also for *in-vitro* and *in-vivo* studies (Nordic Report on PFAS 2013). This is of concern as it means that whole groups of chemicals bypass critical evaluation. Introduction of tools to facilitate the identification and quantification of mixtures of chemicals is therefore highly needed, and in this respect this research paper provides an HRMS based approach to the characterization of not only PFPE-based formulations, but also other fluorinated and nonfluorinated polymers. The use of Kendrick's Mass Defects is furthermore of interest to other fields studying blends of chemicals, such as fracking liquids (Thurman, Ferrer et al. 2014), petroleum, cosmetics and more, and will in the future be facilitated since Kendrick's mass defect calculations and plots will be included in the upcoming software updates of various MS products for HRMS screening.

Conclusion

Industrial chemicals often come as mixtures of substances, as in the case of petroleum (Thurman, Ferrer et al. 2014), detergents (Jonkers, Laane et al. 2002) or as polymers used in food contact materials. The complexity of the mixtures makes it time consuming and challenging both to identify and quantify the individual substances in the blends and in real samples. In this study we demonstrated how the use of the Kendrick's Mass Defect can help

to reduce the complexity of a PFPE-based formulation, by extraction of the most relevant data from high accuracy mass spectra, acquired by HRMS. Initially, a survey of the formulation was made by direct injection into the HRMS (Orbitrap). During this step, the repeating units were identified such as: $-C_2H_4O-$, C_2F_4O , and CF_2O . Tandem MS was used to identify the end groups and the possible distribution of the repeating units. Reversed phase HPLC enabled the separation of the homologues series of individual polymer molecules on the basis of increasing numbers of the nonpolar repeating units. The structure was consistent with the structure supplied in the manufacturer's technical data sheet, albeit containing more information on the individual polymer molecules and not just average data. The analytical approach presented in this research paper can be applied to other polymers as well. MS data as well as the mass defect graphs can be useful tools that can provide essential starting information. Eventually, the data gaps that hamper the assessment of the risks that these complex mixtures pose to the environment can be narrowed down.

Chapter 7. SYNTHESIS AND OUTLOOK

Synthesis

Modern polymer substances and formulations are complex and pose a challenge to analytical chemists. The complexity of polymer substances comes from the diversity of the polymer molecules present in every formulation or mixture. In this research work, multi-technique but polymer-specific approaches were used instead of the standard single-technique approaches in characterizing polymers. To that end three modern polymers were characterized: chitosan, 3-aminopropyl oligosilsesquioxanes and PFPE. Table 7.1 highlights their key properties and the notable structural features that influence their behaviour, activity and applications. The MWD as well as the monomeric composition of the three polymers were studied using a combination of different instrumental and computational methods: liquid chromatography (reversed-phase and size-exclusion), molecular and atomic spectroscopy, mass spectrometry and chemometrics.

Rather than proposing that the traditional methods be replaced by the contemporary ones, the works presented here showed how the traditional methods can be improved and can be complemented by other techniques so that more reliable information can be obtained. This main theme is consistently repeated in every research work presented in this thesis. To further illustrate this theme, in the following text five questions will be addressed:

- 1. How can the IR determination of the degree of deacetylation of chitosan be improved? What is the effect of the degree of deacetylation on the oil-binding property of chitosan?*
- 2. How is MS used in polymer characterization? What are the main differences in the molecular weights obtained by MS to that by SEC?*
- 3. How can the accuracy of the MS determination of the MWD of oligomeric silsesquioxanes be improved?*
- 4. How can the high resolution MS information be used to study the chemical composition of the PFPE-based formulation?*
- 5. How can MS be a tool to study the environmental fate and degradation of polymers?*

Table 7.1. *Polymers used in this research work.*

Polymer	Solubility	Notable Structural Feature	Characterization Tool
Chitosan and COS	Acidic aqueous solution	Polycationic in acidic aqueous solutions Amine group can be acetylated	Chitosan: IR, PLS, SEC COS: MALDI-TOF MS; ESI-Q MS; SEC
Oligosilsesquioxane	Water, methanol, acetonitrile	Polycationic in acidic solution Undergoes intramolecular condensation	LC ESI-Q MS, MALDI-TOF MS, ICP-OES
PFPE	Water, methanol	Perfluorinated and Non perfluorinated blocks Very diverse and complex composition in a mixture	LC ESI-Q-TOF; Orbitrap; IR

The methods of polymer characterization have evolved strongly over the past years. Polymers have become more complex as newer technologies are being developed to synthesize them. Traditional methods have become limited or even unfit for certain characterization purposes. Currently, there are many studies being done to improve the traditional methods like SEC (Bro 2003; Armenta, Garrigues et al. 2008). Aware of the limitations of SEC, researchers and manufacturers focus on developing special columns and special molecular weight standards that can be used to analyze unique polymers. Some work also focuses on interfacing SEC to detectors like MS, IR and NMR to boost its capability.

IR spectroscopy has a unique contribution in studying the structures of polymers. IR methods are not as powerful as NMR in identifying and confirming the structure of polymers. However, because IR methods are fast, robust and way cheaper, they are useful screening tools. In polymer characterization, IR can be used to determine the relative monomer composition of polymers. IR methods are always affected by the high and often noisy baseline. Also, the absorbance at a specific bond is affected by the neighbouring bands due to poor resolution. One tool that has become closely linked to IR is PLS chemometric analysis (Booksh and Kowalski 1994). PLS is a robust multivariate technique that can be used to process the IR data and do an improved quantitative IR analysis. While PLS is

based mostly on empirical calculations, the soundness of a PLS model can be strengthened if it can be explained by the existing scientific principles.

Aside from improving the traditional techniques like SEC and IR, non-conventional methods of polymer characterization have become emergent, for example MS. It was noted that while MS had been one of driving tools in the analysis of biomacromolecules and in the growth of *omics* sciences in biochemistry, MS is underutilized in the analysis of polymers (Hart-Smith and Barner-Kowollik 2010). MS has an advantage over other techniques because it gives information on both the absolute molecular weights and chemical structures of the polymer including the nature of the repeating units. The literature review in Chapter 3 notes that the advent of soft ionization techniques like the MALDI and ESI, makes possible the analysis of intact molecules. MALDI produces mainly singly-charged polymer cations while ESI produces singly- and multiply-charged, predominantly protonated polymer ions. In this regard, MALDI has an advantage over ESI because the mass spectrum is simpler with only singly-charged ions present. The TOF mass analyzer fits perfectly the MALDI instrumentation because both are pulsed techniques. Moreover, the wider mass range of the TOF mass analyzer makes possible the separation of up to m/z 100,000. ESI is a continuous ionization technique and can easily be interfaced to a liquid chromatographic instrument as sample entry and to different mass analyzers including quadrupole, Orbitrap, ion-cyclotron resonance. The ability of the ESI to produce multiply-charged ions can offset the limitation of the quadrupole mass analyzer's narrow mass range (m/z 3000 max). With the advancements in instrumentation, interfacing an ionization technique to any mass analyzer is no longer a problem. MS can be used to determine the molecular weight and the MWD of the polymers. The average molecular weights M_n and M_w can be calculated from the individual molecular weights and their corresponding intensities.

The illustrations using chitosan oligosaccharide (COS) in Chapter 4 and the oligosilsesquioxanes in Chapter 5 highlight the main differences between the MALDI and ESI methods. The obtained molecular weights of COS and the oligosilsesquioxanes using MALDI and ESI were not comparable. MS methods, both in the ionization and in detection, have bias against larger polymer homologues. The biases against large homologues of the two ionization techniques are not congruent. This causes the large differences in the MWD derived using MALDI versus ESI as was observed in the mass spectra of COS and oligosilsesquioxane. Additionally, MALDI produced singly-charged COS ions while ESI generated multiply-charged COS ions. The degree of fragmentation in the MS is different in both MALDI and ESI. For example, MALDI showed oligosilsesquioxane ions with less degree of intramolecular condensation than in ESI. Given these limitations, can an accurate picture of the molecular weight distribution be arrived at using MS?

For a limited number of simple polymers like polyethylene glycol/polyethylene oxide, polystyrene and polyvinyl propylidone, direct MALDI analysis using a suitable matrix can give average MWs and polydispersity indices that are comparable to the data obtained by SEC. However, for most polymers, obtaining an accurate MWD by direct MS analysis remains elusive. A strategy to determine more accurately the MWD was developed for 3-aminopropyl oligosilsesquioxane. This strategy can also be applied to other cationic silsesquioxanes and siloxanes. The technique involves preparing in-house by fractionation some standard solutions containing only single homologues. Efficient separation can be achieved by ion pair chromatography and the quantification of the standard solutions can be done by ICP-OES. With these in-house prepared standards, the absolute and relative concentrations of the individual homologues present in the formulation as well as the MWD are easily determined. The use of chromatographic separation reduces the bias caused by polymer polydispersity and allows a better determination of concentration based on calibration standards.

Aside from molecular weight information, MS also can give hints on the chemical structure of the polymer. The constant m/z differences in the mass spectrum are directly related to the monomer units present. The identity of the polymer is linked to the nature of its repeating units. The elucidation becomes more complex for copolymers and for functionalized polymers (with side chains and end groups added). High resolution mass spectrometry is a promising tool in the chemical characterization of complex polymer formulation. Chapter 6 describes in detail the elucidation of the structures of polymers in a PFPE-based formulation. The technique itself can be applied to other polymers that are ionizable in the MS. The first step is to assign a chemical formula on the most abundant ions detected. In general, accurate molecular weights are necessary in assigning a chemical formula to an ion because it limits the number of possible structure an ion can have. For polymers, the number of "hits" can be narrowed down based on knowledge of the possible repeating units. The second step is to do an n^{th} -order mass defect analysis. The mass defects provide a way of sorting out the different ions detected. The third step is to do tandem MS experiments. MS^n in an MS with high resolution mass analyzers is a powerful tool in structure elucidation.

MS is indeed a promising tool in polymer characterization. However, will it be replacing SEC as the standard method of polymer characterization? As already pointed out, SEC remains to be the most important tool in determining the average MW, the MWD and the polydispersity index of polymers. It will remain to be the case in the future as the technique is continuously improved in order to overcome its limitations and to make it more applicable to a wider range of polymer products. The processes of determination of MWD by SEC and MS are very different from each other giving them unique advantages and disadvantages. First,

SEC-derived MWs are average values and are relative to the MW standards used while MS-derived MWs are absolute MWs that pertain to a specific polymer molecule. In SEC, only samples with the same monomer composition as the MW standards will have accurate MWs. If the sample has different monomer type and composition from that of the MW standards, then the SEC method needs to be optimized in terms of the column and mobile phase so that the sample and the MW standards will have similar hydrodynamic properties. On the other hand, the accuracy of the MS-derived MWs are based on instrument calibration that is independent of the nature of the calibrant and the sample. Second, in SEC the detector response can be easily transformed to molar distributions of the polymer molecules in solution. On the other hand, MS ion intensity is not necessarily translatable to the molar distribution of the polymer molecules in solution due to unknown and varying ionization and detector biases especially with large MW. Therefore, MS is not meant to replace SEC or vice versa. The two techniques are very different and must be used complementary to each other.

In this research work, the capability of MS as a modern tool of polymer characterization was highlighted. Indeed, MS is a very powerful tool that the polymer analytical chemists must exploit.

As already pointed out, the purpose of polymer characterization is not just about product development and quality control. Characterization has been a way for authorities to regulate polymer production and distribution – establish toxicity and chemical properties; study their biodegradability and know their behavior when released into the environment. MS is a tool in the implementation of the European regulation on REACH. In the guideline set by the ECHA, SEC is the preferred method to determine the M_n following the OECD TG 118 (1996) (ECHA 2012). This should allow a decision on whether a substance falls under the definition of polymer. MALDI-TOF-MS is an alternative tool, however it must be used with caution and awareness of its limitations. These limitations were thoroughly discussed in this thesis work. The role of MS can be exploited and widely expanded, especially if the other ionization methods in combination with other mass separation techniques are considered. It was shown in the examples of the silsesquioxanes and PFPEs how ESI interfaced to different mass analyzers like QqQ, Q-TOF and Orbitrap are able to give more information than just about molecular weights. The ECHA guideline lists MS as a method to determine the unreacted monomers and other reactants but the MS characterization of the polymer itself will provide an added value.

Outlook

A multi-technique but polymer-specific approach is the new way to go in polymer characterization. MS will surely find its right place in the polymer characterization lingo as a complementary method to the existing ones. MS will also be a tool for environmental scientists to explore the “mysterious” fate of polymer substances when released into the environment. One particular family of polymers that is of interest to environmental scientists is the poly- and perfluorinated polymers. Little is known about these substances (Kannan 2011). MS can be used to study the behavior of these polymer substances in the environment.

MS allows the identification and quantification of the unreacted monomers, residues and additives in polymer formulation and in the final products. When they are leached into the environment, either these molecules themselves pose environmental risk or they can be transformed into products with high environmental risk (Muir and Howard 2006). For example, fluorotelomer alcohols (FTOH) and sulfonamides (PFOSA) were detected from a polymeric fluoromaterial formulation prior to their application to consumer and industrial products (Dinglasan-Panlilio and Mabury 2006). FTOHs and PFOSAs are starting materials in the synthesis of the fluoropolymers. When in the environment, FTOHs and PFOSAs can degrade to the much more persistent perfluorooctanoic acid (PFOA) and perfluorosulfonic acid (PFOS). On the other hand, the composition and the relative distribution of the residuals can be used as a chemical characterization tool of the polymer itself (Washington, Naile et al. 2014) especially if the polymer is nonionizable in the MS.

Detection and quantification of poly and perfluorinated polymers themselves and not just the residuals and the smaller molecule products would be useful in studying the environmental fate of the persistent perfluorocarboxylic acids and perfluorosulfonic acids in water. For instance, it was previously observed in many wastewater treatment plant (WWTP) studies that the concentrations of PFOA and PFOS in effluents are significantly higher than in influents (Heidler and Halden 2008; Yu, Hu et al. 2009). One possible source of the additional PFOA and PFOS in the WWTP is the degradation of unaccounted poly and perfluorinated polymers that are suspended in the wastewater or that have settled in the sludge. In the future, if an MS method (in combination with a chromatographic technique) is developed to identify and characterize polymeric materials in complex matrices such as wastewater, then some answers can be provided.

MS allows the monitoring of the polymer before and after degradation tests. It will also enable the identification of the degradation products. For example, the shifting of the MWD towards lower molecular weight is an indication of degradation (Trimpin, Eichhorn et al.

2001; Bernhard, Eubeler et al. 2008). In another study, a quadrupole mass analyzer was coupled to a thermogravimetric analyzer to study the thermal degradation of an irradiated perfluoropolyethylene (Lappan, Häußler et al. 1997). Degradation products can be identified using high resolution MS (Yamamoto, Hisatomi et al. 2014).

MS of polymers can also impact other fields – for example food science. Polymers are used as coating materials in food packaging. Some of these are poly and perfluorinated polymers (Trier, Granby et al. 2011). Some residuals and/or degradation products of these materials are polyfluoroalkyl phosphate surfactants which were found to inhibit male sex hormone production (Rosenmai, Nielsen et al. 2013). In the same way as in the environmental science, MS can be used to analyze the residuals, the polymer formulation and the degradation products to study the risks they pose to human health.

MS information can be used as a predictor of property or activity in quantitative structure-property (QSPR) and structure-activity (QSAR) relations. QSPR and QSAR of small molecules have exciting developments. The main aim of these studies is to develop in-silico techniques to predict the activities and properties based on structural information. In the future, this can be extended to polymer substances. In one study, the high resolution m/z values and intensities of blood proteomes were used to generate molecular graph parameters and new topological indices that can be used to model early detection of disease (Cruz-Monteagudo, Munteanu et al. 2008). In a similar manner, future QSPR and QSAR methods can be used to study very complex synthetic polymers. A set of QSAR descriptors can be formulated based on information derived from MS data like mass defects, repeating units and the individual absolute MWs. For example, in chitosan, the degree of deacetylation is a basic chemical property that influences other physico-chemical properties including solubility and viscosity. The oil-binding capacity of chitosan is shown to be largely dependent on its degree of deacetylation and to a smaller extent on its degree of polymerization. Here, it was demonstrated that studies on structure-property and structure-activity relations are only made possible with high quality data (high precision, low uncertainties) on the chemical structures. Modern chemometric techniques like PLS can improve data processing by eliminating the effects of noise and correlated variables.

Aside from QSPR and QSAR, other in-silico/chemometric techniques will play a greater role in polymer characterization. For one, highly advanced software will be needed to process large full scan data. Many of the instrument data processing software are already available with many interesting chemometric function. For example, the Data Analysis software (Bruker Daltonics) proved to be useful in studying the different repeating units through its 'ruler' and 'dissect' functions. Some of these functions are too specialized and are only applicable to biological molecules or to smaller molecules. Functions that are specifically

designed for polymer and similar molecules can be added to these softwares. To visualize the different polymer molecules in the PFPE-based formulation (Chapter 6), the free Statistical Computing software, R, was used to create a special function that can generate different graphs of mass defects and MW. A similar function can be added to the existing instrument software.

SUMMARY

Polymers are large molecules composed of repeating units called monomers. Polymers vary in terms of the monomer/s used; the number, distribution and type of linkage of monomers per molecule; and the side chains and end groups attached. Given this diversity, traditional single-technique approaches to characterization often give limited and inadequate information about a given polymer. Multi-technique but polymer-specific approach was found to be an appropriate alternative. This strategy was applied in characterizing polymers of a wide range of properties from simple polyethylene glycol, to polycationic chitosan and aminopropyl based oligosiloxanes, and to polydiverse polyfluorinated polyethoxylates.

The molecular weight distribution of polycationic chitosan oligosaccharide was studied using size-exclusion chromatography (SEC) and mass spectrometry. The average molecular weights obtained by matrix-assisted laser desorption ionization mass spectrometry (MALDI-MS) and electrospray mass spectrometry (ESI-MS) were significantly different from those obtained by SEC with poly(2-vinyl pyridine) molecular weight standards.

The polycationic nature of chitosan depends on the degree of deacetylation (DD). This single most important property dictates the behaviour of chitosans in aqueous solutions. Partial least squares (PLS) chemometric technique was successfully applied to improve the determination of DD using infrared spectroscopy. The values obtained for chitosan samples with unknown DD using IR-PLS were comparable to the values obtained by standard potentiometric titrations. In a separate study, the combined effects of DD and degree of polymerization (DP) on the ability of chitosan to bind with oil, was elucidated. PLS was used to correlate the oil-binding activity to DD and DP.

Siloxane-based and silsesquioxane-based polymers have been difficult to analyze using traditional techniques. Liquid chromatography with electrospray ionization mass spectrometry (LC-ESI-MS) was effectively utilized to determine the molecular weight distribution of in-house synthesized 3-aminopropyl oligosilsesquioxane. Single homologue siloxane standards were prepared by fractionating the sample in an octadecyl column by ion pair chromatography. The molar concentration of siloxane homologues in each collected fraction was assigned using induced coupled plasma – optical emission spectroscopy (ICP-OES).

Polyfluorinated polymers represent a contemporary class of materials with unique properties. One important group comprises of random copolymers of fluorinated ether monomers

(methoxy, ethoxy and propoxy). High resolution mass spectrometry techniques like linear quadrupole – time of flight and orbitrap coupled to electrospray ionization were used to determine the molecular formulas of the different species present in an unknown formulation composed mainly of polyfluorinated polyethoxylate. Separation in a C18 column and analysis of retention times gave additional insights as to the monomer composition of the polymer. The use of Kendrick's plot highlights the different ways in which the different species in the polymer formulation vary.

The research works included in this thesis have demonstrated that polymer characterization can be accomplished with the use of a combination of different instrumental and statistical techniques. This strategy allows the researcher to explore additional information about the polymer formulation and correlate these to some observed behaviors or activities.

SAMENVATTING

Polymeren zijn grote moleculen die zijn opgebouwd uit een reeks van zogenaamde monomeren, moleculaire eenheden die zich in het grote molecuul herhalen. Er is een grote variëteit aan polymeren die door het type monomeer, de verdeling ervan en de manier waarop de monomeren aan elkaar vast zitten, wordt bepaald. Ook de zijketens en de eindgroepen zijn van belang. Traditionele technieken die gebruikt worden om polymeren te karakteriseren en die op één enkel meetprincipe zijn gebaseerd geven vanwege deze grote diversiteit meestal maar beperkte of niet adequate informatie over de polymeer. Een geschikte alternatief hiervoor zijn benaderingen die gebaseerd zijn op meerdere - en polymeer-specifieke technieken. Een dergelijke strategie is in dit proefschrift gebruikt voor het karakteriseren van enkele polymeren met een uiteenlopende reeks van eigenschappen: van het eenvoudige polyethyleenglycol tot polycationisch chitosan en aminopropyl oligosiloxanen en tot meervoudig polygefluorideerde polyethoxylaten.

De moleculegewichtverdeling van polycationisch chitosan oligosaccharide is onderzocht met size-exclusion chromatografie (SEC) en massaspectrometrie (MS). Het gemiddelde moleculegewicht dat is gevonden met matrix-ondersteunde laser desorptie ionisatie MS (MALDI-MS) en met electrospray MS (ESI-MS) verschilde significant van de waarde die is bepaald aan de hand van SEC met gebruik van poly(2-vinyl pyridine) standaarden.

De meervoudig cationische aard van chitosan hangt af van de deacetyleringsgraad (DD). Het is specifiek deze ene en belangrijkste eigenschap die het gedrag van chitosan in oplossing bepaalt. De chemometrische methode Partial least squares (PLS) is met succes gebruikt om de DD te bepalen met behulp van infrarood spectroscopie (IR). De DD waarden van chitosanmonsters met onbekende DD die zijn gemeten met IR-PLS blijken overeen te komen met waarden die via de standaard potentiometrische titraties zijn bepaald. In een vervolgonderzoek zijn met PLS de gecombineerde effecten van DD en de polymerisatiegraad (DP) bepaald op de mate waarin chitosan kan binden aan olie.

Eigenschappen van polymeren met een siloxaan- en silsesquioxaanstructuur zijn lastig te bepalen met traditionele polymeerkarakteriseringstechnieken. Vloeistofchromatografie (LC) gekoppeld aan ESI-MS bleek een effectieve methode om de moleculegewichtverdeling van in het laboratorium gesynthetiseerd 3-aminopropyl oligosilsesquioxaan te bepalen. Homologe standaarden van siloxaan zijn gemaakt door fractionering van een monster met behulp van ionpaarchromatografie over een octadecyl (C18) kolom. De molaire concentratie van de siloxaan homologen in iedere fractie is toegekend met behulp van inductief gekoppeld plasma – optische emissiespectroscopie.

De polygefluorideerde polymeren vormen een klasse van moderne kunststofmaterialen met unieke eigenschappen. Een van de belangrijke representanten van deze klasse is de groep van zogenaamde random copolymeren die opgebouwd zijn uit gefluorideerde ethers (methoxy, ethoxy, propoxy). In dit promotieonderzoek zijn hoge resolutie MS technieken zoals lineaire quadrapool – time of flight en Orbitrap® MS gekoppeld aan ESI gebruikt om de moleculeformules van de verschillende monomeren te bepalen die in een onbekende formulering bestaande uit voornamelijk polygefluorideerd polyethoxylaate voorkwamen. De monomere samenstelling van de polymeer is aan de hand van scheiding op een C18 kolom en de resulterende retentietijden vastgesteld. Het gebruik hierbij van Kendrick's plots, gebaseerd op massadefecten, stelt ons in staat de verschillende manieren waarop de diverse monomeren variëren in de polymeer aan te geven.

Het onderzoek in dit proefschrift heeft laten zien dat de karakterisering van polymeren kan worden gedaan met een combinatie van verschillende moderne instrumentele en statistische technieken. Een dergelijke strategie biedt de onderzoeker de mogelijkheid om extra informatie over de compositie van de polymeer te vergaren en deze te relateren aan het gedrag ervan en aan wat er met de polymeer gebeurt (bijvoorbeeld wanneer deze in het afvalstadium of in het milieu terechtkomt).

REFERENCE LIST

- Abdi, H. (2010). "Partial least squares regression and projection on latent structure regression (PLS Regression)." Wiley Interdisciplinary Reviews: Computational Statistics **2**(1): 97-106.
- Abe, Y. and T. Gunji (2004). "Oligo- and polysiloxanes." Progress in Polymer Science **29**(3): 149-182.
- Aiba, S.-i. (1992). "Studies on chitosan: 4. Lysozymic hydrolysis of partially N-acetylated chitosans." International Journal of Biological Macromolecules **14**(4): 225-228.
- Allan, G. G. and M. Peyron (1995). "Molecular weight manipulation of chitosan I: kinetics of depolymerization by nitrous acid." Carbohydrate Research **277**(2): 257-272.
- Alves, N. M. and J. F. Mano (2008). "Chitosan derivatives obtained by chemical modifications for biomedical and environmental applications." International Journal of Biological Macromolecules **43**(5): 401-414.
- Applied Biosystems (2005). Operator's Manual: 3200 Q Trap. Canada, Applied Biosystems.
- Aranaz, I., M. Mengibar, et al. (2009). "Functional Characterization of Chitin and Chitosan." Current Chemical Biology **3**(2): 203-230.
- Armenta, S., S. Garrigues, et al. (2008). "Green Analytical Chemistry." TrAC Trends in Analytical Chemistry **27**(6): 497-511.
- Avataneo, M., U. De Patta, et al. (2011). "Perfluoropolyether-tetrafluoroethylene (PFPE-TFE) block copolymers: An innovative family of fluorinated materials." Journal of Fluorine Chemistry **132**(11): 885-891.
- Avataneo, M., W. Navarrini, et al. (2009). "Novel perfluoropolyethers containing 2,2,4-trifluoro-5-trifluoromethoxy-1,3-dioxole blocks: synthesis and characterization." Journal of Fluorine Chemistry **130**(10): 933-937.
- Azzouz, T., A. Puigdoménech, et al. (2003). "Comparison between different data pre-treatment methods in the analysis of forage samples using near-infrared diffuse reflectance spectroscopy and partial least-squares multivariate calibration method." Analytica Chimica Acta **484**(1): 121-134.
- Bahr, U., A. Deppe, et al. (1992). "Mass spectrometry of synthetic polymers by UV-matrix-assisted laser desorption/ionization." Analytical Chemistry **64**(22): 2866-2869.
- Baney, R. H., M. Itoh, et al. (1995). "Silsesquioxanes." Chemical Reviews **95**(5): 1409-1430.
- Baxter, A., M. Dillon, et al. (1992). "Improved method for i.r. determination of the degree of N-acetylation of chitosan." International Journal of Biological Macromolecules **14**(3): 166-169.
- Belu, A. M., J. M. DeSimone, et al. (1996). "Evaluation of matrix-assisted laser desorption ionization mass spectrometry for polymer characterization." Journal of the American Society for Mass Spectrometry **7**(1): 11-24.
- Bernhard, M., J. P. Eubeler, et al. (2008). "Aerobic biodegradation of polyethylene glycols of different molecular weights in wastewater and seawater." Water Research **42**(19): 4791-4801.
- Bernhard, M., H. Flato, et al. "Robust molecular weight determination of chitosan and low-molecular chitosan oligosaccharide by size exclusion chromatography." to be submitted for publication.

- Bjorn-Helge, M. and R. Wehrens (2007). "The pls package: principal component and partial least squares regression in R." Journal of Statistical Software **18**(2): 1-24.
- Bloor, D. M., J. F. Holzwarth, et al. (1995). "Polymer/Surfactant Interactions. The Use of Isothermal Titration Calorimetry and emf Measurements in the Sodium Dodecyl Sulfate/Poly(N-vinylpyrrolidone) System." Langmuir **11**(6): 2312-2313.
- Bokura, H. and S. Kobayashi (2003). "Chitosan decreases total cholesterol in women: a randomized, double-blind, placebo-controlled trial." European Journal of Clinical Nutrition **57**(5): 721-725.
- Booksh, K. S. and B. R. Kowalski (1994). "Theory of analytical chemistry." Analytical Chemistry **66**(15): 782A-791A.
- Braun, D., H. Cherdrón, M. Rehahn, H. Ritter, B. Voit (2005). Polymer Synthesis: Theory and Practice: Fundamentals, Methods, Experiments. Berlin, Springer.
- Brinker, C. J. (1988). "Hydrolysis and condensation of silicates: Effects on structure." Journal of Non-Crystalline Solids **100**(1-3): 31-50.
- Bro, R. (2003). "Multivariate calibration: What is in chemometrics for the analytical chemist?" Analytica Chimica Acta **500**(1-2): 185-194.
- Brugnerotto, J., J. Lizardi, et al. (2001). "An infrared investigation in relation with chitin and chitosan characterization." Polymer **42**(8): 3569-3580.
- Bundesinstitut für Risikobewertung. (2014). "XXXVI. Paper and board for food contact (Unofficial Translation)." Retrieved 2014, from <http://bfr.zadi.de/kse/faces/DBEmpfehlung.jsp>.
- Cabrera, J. C. and P. Van Cutsem (2005). "Preparation of chitooligosaccharides with degree of polymerization higher than 6 by acid or enzymatic degradation of chitosan." Biochemical Engineering Journal **25**(2): 165-172.
- Cammas, S., K. Suzuki, et al. (1997). "Thermo-responsive polymer nanoparticles with a core-shell micelle structure as site-specific drug carriers." Journal of Controlled Release **48**(2-3): 157-164.
- Chen, M., X. Zhu, et al. (2010). "Application of matrix-assisted laser desorption/ionization time-of-flight mass spectrometry (MALDI-TOF-MS) in preparation of chitosan oligosaccharides (COS) with degree of polymerization (DP) 5-12 containing well-distributed acetyl groups." International Journal of Mass Spectrometry **290**(2-3): 94-99.
- Cho, Y. I., H. K. No, et al. (1998). "Physicochemical Characteristics and Functional Properties of Various Commercial Chitin and Chitosan Products." Journal of Agricultural and Food Chemistry **46**(9): 3839-3843.
- CODEX Alimentarius (1981). CODEX standards for olive oils and olive pomace oils CODEX STAN 33-1981, CODEX Alimentarius.
- Coles, J. and M. Guilhaus (1993). "Orthogonal acceleration — a new direction for time-of-flight mass spectrometry: Fast, sensitive mass analysis for continuous ion sources." TrAC Trends in Analytical Chemistry **12**(5): 203-213.
- Cotter, R. J. (1992). "Time-of-Flight Mass Spectrometry for the Structural Analysis of Biological Molecules." Analytical Chemistry **64**(21): 1027A-1039A.
- Cruz-Monteaudo, M., C. R. Munteanu, et al. (2008). "Stochastic molecular descriptors for polymers. 4. Study of complex mixtures with topological indices of mass spectra spiral and star networks: The blood proteome case." Polymer **49**(25): 5575-5587.
- Dawson, J. H. J. and M. Guilhaus (1989). "Orthogonal-acceleration time-of-flight mass spectrometer." Rapid Communications in Mass Spectrometry **3**(5): 155-159.

- Deuchi, K., O. Kanauchi, et al. (1995). "Effect of the viscosity or deacetylation degree of chitosan on fecal fat excreted from rats fed on a high-fat diet." Bioscience, Biotechnology and Biochemistry **59**(5): 781-785.
- Deuchi, K., O. Kanauchi, et al. (1994). "Decreasing effect of chitosan on the apparent fat digestibility by rats fed on a high-fat diet." Bioscience, Biotechnology and Biochemistry **58**9: 1616-1613.
- Dimzon, I. K. D., J. Ebert, et al. (2013). "The interaction of chitosan and olive oil: Effects of degree of deacetylation and degree of polymerization." Carbohydrate Polymers **92**(1): 564-570.
- Dimzon, I. K. D. and T. P. Knepper (2012). MALDI-TOF MS for characterization of synthetic polymers in aqueous environment. Amsterdam, Elsevier.
- Dinglasan-Panlilio, M. J. A. and S. A. Mabury (2006). "Significant Residual Fluorinated Alcohols Present in Various Fluorinated Materials." Environmental Science & Technology **40**(5): 1447-1453.
- Domszy, J. G. and G. A. F. Roberts (1985). "Evaluation of infrared spectroscopic techniques for analysing chitosan." Die Makromolekulare Chemie **186**(8): 1671-1677.
- Duarte, M. L., M. C. Ferreira, et al. (2002). "An optimised method to determine the degree of acetylation of chitin and chitosan by FTIR spectroscopy." International Journal of Biological Macromolecules **31**(1-3): 1-8.
- Dubin, P. L. and J. M. Principi (1989). "Failure of universal calibration for size-exclusion chromatography of rodlike macromolecules vs. random coils and globular proteins." Macromolecules **22**(4): 1891-1896.
- Dubois, F. d. r., R. Knochenmuss, et al. (1996). "On the mechanism and control of salt-induced resolution loss in matrix-assisted laser desorption/ionization." European Journal of Mass Spectrometry **2**: 167-172.
- Duchowicz, P. R., S. E. Fiorelli, et al. (2015). "QSPR studies on refractive indices of structurally heterogeneous polymers." Chemometrics and Intelligent Laboratory Systems **140**(0): 86-91.
- Easterling, M. L., T. H. Mize, et al. (1998). "Routine Part-per-Million Mass Accuracy for High-Mass Ions: Space-Charge Effects in MALDI FT-ICR." Analytical Chemistry **71**(3): 624-632.
- ECHA. "REACH." Retrieved September 2014, from <http://echa.europa.eu/regulations/reach>.
- ECHA (2012). Guidance for monomers and polymers: Guidance for the implementation of REACH, European Chemicals Agency.
- Eisenberg, P., R. Erra-Balsells, et al. (2000). "Cagelike Precursors of High-Molar-Mass Silsesquioxanes Formed by the Hydrolytic Condensation of Trialkoxysilanes." Macromolecules **33**(6): 1940-1947.
- Eisenberg, P., R. Erra-Balsells, et al. (2002). "Silsesquioxanes Derived from the Bulk Polycondensation of [3-(Methacryloxy)propyl]trimethoxysilane with Concentrated Formic Acid: Evolution of Molar Mass Distributions and Fraction of Intramolecular Cycles." Macromolecules **35**(4): 1160-1174.
- Eschauzier, C., K. J. Raat, et al. (2013). "Perfluorinated alkylated acids in groundwater and drinking water: Identification, origin and mobility." Science of The Total Environment **458-460**(0): 477-485.

- Eubeler, J. P., M. Bernhard, et al. (2010). "Environmental biodegradation of synthetic polymers II. Biodegradation of different polymer groups." TrAC Trends in Analytical Chemistry **29**(1): 84-100.
- European Commission (2011). Plastics Implementing Measures (PIM): 2011/10/EC Commission Regulation of 14th January 2011 on plastic materials and articles intended to come into contact with foodstuffs.
- Fasce, D. P., R. J. J. Williams, et al. (2001). "One-Step Synthesis of Polyhedral Silsesquioxanes Bearing Bulky Substituents: UV-MALDI-TOF and ESI-TOF Mass Spectrometry Characterization of Reaction Products." Macromolecules **34**(11): 3534-3539.
- Feher, F. J. and K. D. Wyndham (1998). "Amine and ester-substituted silsesquioxanes: synthesis, characterization and use as a core for starburst dendrimers." Chemical Communications(3): 323-324.
- Fenn, J., M. Mann, et al. (1989). "Electrospray ionization for mass spectrometry of large biomolecules." Science **246**(4926): 64-71.
- Fenn, J. B., M. Mann, et al. (1990). "Electrospray ionization—principles and practice." Mass Spectrometry Reviews **9**(1): 37-70.
- Fischer, S. G. and J. Chiu (1983). "Analysis of polymer blends and copolymers by coupled thermogravimetry and automatic titration." Thermochimica Acta **65**(1): 9-17.
- Food and Drug Administration (2010). 21CFR § 176.170 'Components of paper and paperboard in contact with aqueous and fatty foods' and §176.180 'Components of paper and paperboard in contact with dry food. United States.
- Food and Drug Administration (2010). Regulations 176.160 and 176.170 and effective food contact-notifications (FCN's) United States.
- Frömel, T. and T. P. Knepper (2008). "Mass spectrometry as an indispensable tool for studies of biodegradation of surfactants." TrAC Trends in Analytical Chemistry **27**(11): 1091-1106.
- Gallaher, C. M., J. Munion, et al. (2000). "Cholesterol Reduction by Glucomannan and Chitosan Is Mediated by Changes in Cholesterol Absorption and Bile Acid and Fat Excretion in Rats." The Journal of Nutrition **130**(11): 2753-2759.
- Gellman, A. J. (1998). "Lubricants and overcoats for magnetic storage media." Current Opinion in Colloid & Interface Science **3**(4): 368-372.
- Goedhart, D. and A. Opschoor (1970). "Polymer characterization by coupling gel-permeation chromatography and automatic viscometry." Journal of Polymer Science Part A-2: Polymer Physics **8**(7): 1227-1233.
- Golbraikh, A. and A. Tropsha (2002). "Beware of q2!" Journal of Molecular Graphics and Modelling **20**(4): 269-276.
- Gross, J. (2004). Mass Spectrometry: A Textbook. Heidelberg, Springer.
- Gruending, T., S. Weidner, et al. (2010). "Mass spectrometry in polymer chemistry: a state-of-the-art up-date." Polymer Chemistry **1**(5): 599-617.
- Han, L. K., Y. Kimura, et al. (1999). "Reduction in fat storage during chitin-chitosan treatment in mice fed a high-fat diet." International Journal of Obesity **23**: 174-179.
- Hanton, S., I. Hyder, et al. (2004). "Investigations of electrospray sample deposition for polymer MALDI mass spectrometry." Journal of the American Society for Mass Spectrometry **15**(2): 168-179.

- Hanton, S. D. and X. M. Liu (2000). "GPC Separation of Polymer Samples for MALDI Analysis." Analytical Chemistry **72**(19): 4550-4554.
- Hart-Smith, G. and C. Barner-Kowollik (2010). "Contemporary Mass Spectrometry and the Analysis of Synthetic Polymers: Trends, Techniques and Untapped Potential." Macromolecular Chemistry and Physics **211**(14): 1507-1529.
- Heidler, J. and R. U. Halden (2008). "Meta-Analysis of Mass Balances Examining Chemical Fate during Wastewater Treatment." Environmental Science & Technology **42**(17): 6324-6332.
- Hessel, C. M., E. J. Henderson, et al. (2006). "Hydrogen Silsesquioxane: A Molecular Precursor for Nanocrystalline Si-SiO₂ Composites and Freestanding Hydride-Surface-Terminated Silicon Nanoparticles." Chemistry of Materials **18**(26): 6139-6146.
- Hobert, A.-M. and D. Haddleton (1997). "Letter: Evidence for cationization of polymers in the gas phase during matrix-assisted laser desorption/ionization." European Journal of Mass Spectrometry **3**(6): 471-473.
- Hoteling, A. J., W. J. Erb, et al. (2004). "Exploring the Importance of the Relative Solubility of Matrix and Analyte in MALDI Sample Preparation Using HPLC." Analytical Chemistry **76**(17): 5157-5164.
- Howell, J. L., C. M. Friesen, et al. (2007). "Improved thermal stability of perfluoropolyalkylethers (PFPAEs)." Journal of Synthetic Lubrication **24**(4): 227-234.
- Howell, J. L., A. B. Shtarov, et al. (2011). "Synthesis of new linear perfluoroalkyl polyethers starting from diols and tetrafluoroethylene." Lubrication Science **23**(2): 61-80.
- Hughey, C. A., C. L. Hendrickson, et al. (2001). "Kendrick Mass Defect Spectrum: A Compact Visual Analysis for Ultrahigh-Resolution Broadband Mass Spectra." Analytical Chemistry **73**(19): 4676-4681.
- Hutmacher, D. W. (2000). "Scaffolds in tissue engineering bone and cartilage." Biomaterials **21**(24): 2529-2543.
- Iengo, P., Gavezotti, P (2007). Use of carboxylic perfluoropolyethers for the oleo-repellent paper sizing, Solvay Solexis S.p.A.
- Jackson, C., B. Larsen, et al. (1996). "Comparison of Most Probable Peak Values As Measured for Polymer Distributions by MALDI Mass Spectrometry and by Size Exclusion Chromatography." Analytical Chemistry **68**(8): 1303-1308.
- Jia, Z. and D. Shen (2002). "Effect of reaction temperature and reaction time on the preparation of low-molecular-weight chitosan using phosphoric acid." Carbohydrate Polymers **49**(4): 393-396.
- Jonkers, N., H. Govers, et al. (2005). "Adduct formation in LC-ESI-MS of nonylphenol ethoxylates: mass spectrometrical, theoretical and quantitative analytical aspects." Analytica Chimica Acta **531**(2): 217-228.
- Jonkers, N., R. W. P. M. Laane, et al. (2002). "Fate of Nonylphenol Ethoxylates and Their Metabolites in Two Dutch Estuaries: Evidence of Biodegradation in the Field." Environmental Science & Technology **37**(2): 321-327.
- Kanauchi, O., K. Deuchi, et al. (1995). "Mechanism for the inhibition of fat digestion by chitosan and for the synergistic effect of ascorbate." Bioscience, Biotechnology and Biochemistry **59**(5): 786-790.
- Kannan, K. (2011). "Perfluoroalkyl and polyfluoroalkyl substances: current and future perspectives." Environmental Chemistry **8**(4): 333-338.

- Karas, M., D. Bachmann, et al. (1987). "Matrix-assisted ultraviolet laser desorption of non-volatile compounds." International Journal of Mass Spectrometry and Ion Processes **78**(0): 53-68.
- Karas, M., D. Bachmann, et al. (1985). "Influence of the wavelength in high-irradiance ultraviolet laser desorption mass spectrometry of organic molecules." Analytical Chemistry **57**(14): 2935-2939.
- Karas, M., U. Bahr, et al. (1995). "Matrix Dependence of Metastable Fragmentation of Glycoproteins in MALDI TOF Mass Spectrometry." Analytical Chemistry **67**(3): 675-679.
- Karas, M. and F. Hillenkamp (1988). "Laser desorption ionization of proteins with molecular masses exceeding 10,000 daltons." Analytical Chemistry **60**(20): 2299-2301.
- Karas, M. and R. Krüger (2003). "Ion Formation in MALDI: The Cluster Ionization Mechanism." Chemical Reviews **103**(2): 427-440.
- Karis, T. E. and M. S. Jhon (1998). "The relationship between PFPE molecular rheology and tribology." Tribology Letters **5**(4): 283-286.
- Kasaai, M. R. (2008). "A review of several reported procedures to determine the degree of N-acetylation for chitin and chitosan using infrared spectroscopy." Carbohydrate Polymers **71**(4): 497-508.
- Kasaai, M. R. (2009). "Various Methods for Determination of the Degree of N-Acetylation of Chitin and Chitosan: A Review." Journal of Agricultural and Food Chemistry **57**(5): 1667-1676.
- Kebarle, P. and U. H. Verkerk (2009). "Electrospray: From ions in solution to ions in the gas phase, what we know now." Mass Spectrometry Reviews **28**(6): 898-917.
- Khan, R., A. Kaushik, et al. (2008). "Zinc oxide nanoparticles-chitosan composite film for cholesterol biosensor." Analytica Chimica Acta **616**(2): 207-213.
- Kietzke, T., D. Neher, et al. (2003). "Novel approaches to polymer blends based on polymer nanoparticles." Nature Materials **2**(6): 408-412.
- Kim, S.-K. and N. Rajapakse (2005). "Enzymatic production and biological activities of chitosan oligosaccharides (COS): A review." Carbohydrate Polymers **62**(4): 357-368.
- Knochenmuss, R., E. Lehmann, et al. (1998). "Polymer cationization in matrix-assisted laser desorption/ionization." European Journal of Mass Spectrometry **4**(6): 421-426.
- Kononikhin, A., E. Nikolaev, et al. (2005). "Letter: Multiply charged ions in matrix-assisted laser desorption/ionization generated from electrosprayed sample layers." European Journal of Mass Spectrometry **11**(3): 257-260.
- Krafft, M. P. and J. G. Riess (2009). "Chemistry, Physical Chemistry, and Uses of Molecular Fluorocarbon– Hydrocarbon Diblocks, Triblocks, and Related Compounds□ Unique "Apolar" Components for Self-Assembled Colloid and Interface Engineering." Chemical Reviews **109**(5): 1714-1792.
- Krutchinsky, A. N. and B. T. Chait (2002). "On the nature of the chemical noise in MALDI mass spectra." Journal of the American Society for Mass Spectrometry **13**(2): 129-134.
- Kumar, M. N., R. A. Muzzarelli, et al. (2004). "Chitosan chemistry and pharmaceutical perspectives." Chemical Reviews **104**(12): 6017-6084.
- Lappan, U., L. Häußler, et al. (1997). "Thermal stability of electron beam-irradiated polytetrafluoroethylene." Journal of Applied Polymer Science **66**(12): 2287-2291.

- Larsen, B., W. Simonsick, et al. (1996). "Fundamentals of the application of matrix-assisted laser desorption-ionization mass spectrometry to low mass poly(methylmethacrylate) polymers." Journal of the American Society for Mass Spectrometry **7**(3): 287-292.
- Lavine, B. K. (2000). "Chemometrics." Analytical Chemistry **72**(12): 91-98.
- Lee, D., S. Rumbelow, et al. (2009). "Identification and quantitation of trace impurities in fatty alcohol ethoxylates using HPLC and MALDI-TOF mass spectrometry." Analytica Chimica Acta **654**(1): 59-63.
- Li, L., P. M. Jones, et al. (2004). "Effect of Chemical Structure and Molecular Weight on High-Temperature Stability of Some Fomblin Z-Type Lubricants." Tribology Letters **16**(1-2): 21-27.
- Lichtenhan, J. D. (1995). "Polyhedral Oligomeric Silsesquioxanes: Building Blocks for Silsesquioxane-Based Polymers and Hybrid Materials." Comments on Inorganic Chemistry **17**(2): 115-130.
- Lichtenhan, J. D., N. Q. Vu, et al. (1993). "Silsesquioxane-siloxane copolymers from polyhedral silsesquioxanes." Macromolecules **26**(8): 2141-2142.
- Liu, J., J. Zhang, et al. (2008). "Hypocholesterolaemic effects of different chitosan samples in vitro and in vivo." Food Chemistry **107**(1): 419-425.
- Macha, S. F. and P. A. Limbach (2002). "Matrix-assisted laser desorption/ionization (MALDI) mass spectrometry of polymers." Current Opinion in Solid State and Materials Science **6**(3): 213-220.
- Maezaki, Y., K. Tsuji, et al. (1993). "Hypocholesterolemic Effect of Chitosan in Adult Males." Bioscience, Biotechnology and Biochemistry **57**(9): 1439-1444.
- Maggio, R. M., T. S. Kaufman, et al. (2009). "Monitoring of fatty acid composition in virgin olive oil by Fourier transformed infrared spectroscopy coupled with partial least squares." Food Chemistry **114**(4): 1549-1554.
- Mann, M. and N. L. Kelleher (2008). "Precision proteomics: The case for high resolution and high mass accuracy." Proceedings of the National Academy of Sciences **105**(47): 18132-18138.
- Mao, S., X. Shuai, et al. (2004). "The depolymerization of chitosan: effects on physicochemical and biological properties." International Journal of Pharmaceutics **281**(1-2): 45-54.
- Marshall, A. G. and C. L. Hendrickson (2008). "High-Resolution Mass Spectrometers." Annual Review of Analytical Chemistry **1**(1): 579-599.
- Marshall, A. G., C. L. Hendrickson, et al. (1998). "Fourier transform ion cyclotron resonance mass spectrometry: A primer." Mass Spectrometry Reviews **17**(1): 1-35.
- Massart, D. L., B. G. M. Vandeginste, et al. (1998). Handbook of Chemometrics and Qualimetrics: Part A, Elsevier.
- Meier, M. A. R., N. Adams, et al. (2006). "Statistical Approach To Understand MALDI-TOFMS Matrices: Discovery and Evaluation of New MALDI Matrices." Analytical Chemistry **79**(3): 863-869.
- Miretzky, P. and A. F. Cirelli (2009). "Hg(II) removal from water by chitosan and chitosan derivatives: A review." Journal of Hazardous Materials **167**(1-3): 10-23.
- Mohr, M. D., K. OlafBörnsen, et al. (1995). "Matrix-assisted laser desorption/ionization mass spectrometry: Improved matrix for oligosaccharides." Rapid Communications in Mass Spectrometry **9**(9): 809-814.

- Montaudo, G., M. S. Montaudo, et al. (1994). "2-(4-hydroxyphenylazo)-benzoic acid: A solid matrix for matrix-assisted laser desorption/ionization of polystyrene." Rapid Communications in Mass Spectrometry **8**(12): 1011-1015.
- Montaudo, G., F. Samperi, et al. (2006). "Characterization of synthetic polymers by MALDI-MS." Progress in Polymer Science **31**(3): 277-357.
- Moon, J.-S., H.-K. Kim, et al. (2007). "The antibacterial and immunostimulative effect of chitosan-oligosaccharides against infection by *Staphylococcus aureus* isolated from bovine mastitis." Applied Microbiology and Biotechnology **75**(5): 989-998.
- Moon, J.-S., H.-K. Kim, et al. (2007). "The antibacterial and immunostimulative effect of chitosan-oligosaccharides against infection by *Staphylococcus aureus* isolated from bovine mastitis." Applied Microbiology and Biotechnology **75**(5): 989-998.
- Mori, H., M. G. Lanzendörfer, et al. (2004). "Silsequioxane-Based Nanoparticles Formed via Hydrolytic Condensation of Organotriethoxysilane Containing Hydroxy Groups." Macromolecules **37**(14): 5228-5238.
- Morris, G. A., J. Castile, et al. (2009). "Macromolecular conformation of chitosan in dilute solution: A new global hydrodynamic approach." Carbohydrate Polymers **76**(4): 616-621.
- Muir, D. C. G. and P. H. Howard (2006). "Are There Other Persistent Organic Pollutants? A Challenge for Environmental Chemists†." Environmental Science & Technology **40**(23): 7157-7166.
- Murgasova, R. and D. Hercules (2002). "Polymer characterization by combining liquid chromatography with MALDI and ESI mass spectrometry." Analytical and Bioanalytical Chemistry **373**(6): 481-489.
- Muzzarelli, R. A. A. (2012). 10.06 - Nanochitins and Nanochitosans, Paving the Way to Eco-Friendly and Energy-Saving Exploitation of Marine Resources. Polymer Science: A Comprehensive Reference. M. Editors-in-Chief: Krzysztof and M. Martin. Amsterdam, Elsevier: 153-164.
- Muzzarelli, R. A. A., N. Frega, et al. (2000). "Interactions of chitin, chitosan, N-lauryl chitosan and N-dimethylaminopropyl chitosan with olive oil." Carbohydrate Polymers **43**(3): 263-268.
- Muzzarelli, R. A. A., F. Orlandini, et al. (2006). "Chitosan taurocholate capacity to bind lipids and to undergo enzymatic hydrolysis: An in vitro model." Carbohydrate Polymers **66**(3): 363-371.
- Neves, A. C. d. O., A. A. de Araújo, et al. (2012). "Near infrared spectroscopy and multivariate calibration for simultaneous determination of glucose, triglycerides and high-density lipoprotein in animal plasma." Journal of Pharmaceutical and Biomedical Analysis **66**(0): 252-257.
- No, H. K., S. H. Lee, et al. (2003). "Comparison of Physicochemical, Binding, and Antibacterial Properties of Chitosans Prepared without and with Deproteinization Process." Journal of Agricultural and Food Chemistry **51**(26): 7659-7663.
- Novoa-Carballal, R., R. Riguera, et al. (2013). "Chitosan hydrophobic domains are favoured at low degree of acetylation and molecular weight." Polymer **54**(8): 2081-2087.
- Ottosson, H. and P. G. Steel (2006). "Silylenes, Silenes, and Disilenes: Novel Silicon-Based Reagents for Organic Synthesis?" Chemistry – A European Journal **12**(6): 1576-1585.
- Parra-Barraza, H., M. G. Burboa, et al. (2005). "Chitosan–Cholesterol and Chitosan–Stearic Acid Interactions at the Air–Water Interface†." Biomacromolecules **6**(5): 2416-2426.

- Patiny, L. (2013). "ChemCalc." Retrieved August 2013, from <http://www.chemcalc.org/>.
- Payet, L. and E. M. Terentjev (2008). "Emulsification and Stabilization Mechanisms of O/W Emulsions in the Presence of Chitosan." Langmuir **24**(21): 12247-12252.
- Pearson, F. G., R. H. Marchessault, et al. (1960). "Infrared spectra of crystalline polysaccharides. V. Chitin." Journal of Polymer Science **43**(141): 101-116.
- Pereda, M., G. Amica, et al. (2012). "Development and characterization of edible chitosan/olive oil emulsion films." Carbohydrate Polymers **87**(2): 1318-1325.
- Philippova, O. E., E. V. Korchagina, et al. (2012). "Aggregation of some water-soluble derivatives of chitin in aqueous solutions: Role of the degree of acetylation and effect of hydrogen bond breaker." Carbohydrate Polymers **87**(1): 687-694.
- Pilati, F., M. Toselli, et al. (1992). "Synthesis of polyesters-perfluoropolyethers block copolymers." Polymer Bulletin **28**(2): 151-157.
- Podzimek, S. (1994). "The use of GPC coupled with a multiangle laser light scattering photometer for the characterization of polymers. On the determination of molecular weight, size and branching." Journal of Applied Polymer Science **54**(1): 91-103.
- Podzimek, S., T. Vlcek, et al. (2001). "Characterization of branched polymers by size exclusion chromatography coupled with multiangle light scattering detector. I. Size exclusion chromatography elution behavior of branched polymers." Journal of Applied Polymer Science **81**(7): 1588-1594.
- Prabaharan, M. (2008). "Review Paper: Chitosan Derivatives as Promising Materials for Controlled Drug Delivery." Journal of Biomaterials Applications **23**(1): 5-36.
- Puretzky, A. A. and D. B. Geohegan (1998). "Gas-phase diagnostics and LIF-imaging of 3-hydroxypicolinic acid maldi-matrix plumes." Chemical Physics Letters **286**(5-6): 425-432.
- Qin, C., H. Li, et al. (2006). "Water-solubility of chitosan and its antimicrobial activity." Carbohydrate Polymers **63**(3): 367-374.
- Rabea, E. I., M. E. T. Badawy, et al. (2003). "Chitosan as Antimicrobial Agent: Applications and Mode of Action." Biomacromolecules **4**(6): 1457-1465.
- Rahimi, A. and P. Shokrolahi (2001). "Application of inorganic polymeric materials: I. Polysiloxanes." International Journal of Inorganic Materials **3**(7): 843-847.
- Rao, J. P. and K. E. Geckeler (2011). "Polymer nanoparticles: Preparation techniques and size-control parameters." Progress in Polymer Science **36**(7): 887-913.
- Ravi Kumar, M. N. V. (2000). "A review of chitin and chitosan applications." Reactive and Functional Polymers **46**(1): 1-27.
- Reinhold, M., R. J. Meier, et al. (1998). "How feasible is matrix-assisted laser desorption/ionisation time-of-flight mass spectrometry analysis of polyolefins?" Rapid Communications in Mass Spectrometry **12**(23): 1962-1966.
- Rinaudo, M. (2006). "Chitin and chitosan: Properties and applications." Progress in Polymer Science **31**(7): 603-632.
- Riva, R., H. Ragelle, et al. (2011). Chitosan and Chitosan Derivatives in Drug Delivery and Tissue Engineering. Chitosan for Biomaterials II. R. Jayakumar, M. Prabaharan and R. A. A. Muzzarelli, Springer Berlin Heidelberg. **244**: 19-44.
- Roach, P. J., J. Laskin, et al. (2011). "Higher-Order Mass Defect Analysis for Mass Spectra of Complex Organic Mixtures." Analytical Chemistry **83**(12): 4924-4929.

- Rosenmaj, A. K., F. K. Nielsen, et al. (2013). "Fluorochemicals used in food packaging inhibit male sex hormone synthesis." Toxicology and Applied Pharmacology **266**(1): 132-142.
- Roy, P. P. and K. Roy (2008). "On Some Aspects of Variable Selection for Partial Least Squares Regression Models." QSAR & Combinatorial Science **27**(3): 302-313.
- Sabnis, S. and L. Block (1997). "Improved infrared spectroscopic method for the analysis of degree of N-deacetylation of chitosan." Polymer Bulletin **39**(1): 67-71.
- Sannan, T., K. Kurita, et al. (1976). "Studies on chitin, 2. Effect of deacetylation on solubility." Die Makromolekulare Chemie **177**(12): 3589-3600.
- Schatz, C., C. Viton, et al. (2003). "Typical Physicochemical Behaviors of Chitosan in Aqueous Solution." Biomacromolecules **4**(3): 641-648.
- Scheringer, M., X. Trier, et al. (2014). "Helsingør Statement on poly- and perfluorinated alkyl substances (PFASs)." Chemosphere **114**(0): 337-339.
- Schmaucks, G., G. Sonnek, et al. (1992). "Effect of siloxanyl groups on the interfacial behavior of quaternary ammonium compounds." Langmuir **8**(7): 1724-1730.
- Schriemer, D. C. and L. Li (1996). "Detection of High Molecular Weight Narrow Polydisperse Polymers up to 1.5 Million Daltons by MALDI Mass Spectrometry." Analytical Chemistry **68**(17): 2721-2725.
- Schulz, P. C., M. S. Rodríguez, et al. (1998). "Emulsification properties of chitosan." Colloid & Polymer Science **276**(12): 1159-1165.
- Senak, L., C. S. Wu, et al. (1987). "Size Exclusion Chromatography of Poly(vinylpyrrolidone)." Journal of Liquid Chromatography **10**(6): 1127-1150.
- Seyfarth, F., S. Schliemann, et al. (2008). "Antifungal effect of high- and low-molecular-weight chitosan hydrochloride, carboxymethyl chitosan, chitosan oligosaccharide and N-acetyl-d-glucosamine against *Candida albicans*, *Candida krusei* and *Candida glabrata*." International Journal of Pharmaceutics **353**(1-2): 139-148.
- Shigemasa, Y., H. Matsuura, et al. (1996). "Evaluation of different absorbance ratios from infrared spectroscopy for analyzing the degree of deacetylation in chitin." International Journal of Biological Macromolecules **18**(3): 237-242.
- Sigma-Aldrich (2001). Analytix: Advances in analytical chemistry. MALDI-Mass Spectrometry, Sigma-Aldrich.
- Sleno, L. (2012). "The use of mass defect in modern mass spectrometry." Journal of Mass Spectrometry **47**(2): 226-236.
- Smith, I. O., X. H. Liu, et al. (2009). "Nanostructured polymer scaffolds for tissue engineering and regenerative medicine." Wiley Interdisciplinary Reviews: Nanomedicine and Nanobiotechnology **1**(2): 226-236.
- Solvay Solexis. (2012). "Solvay Plastics." Retrieved 23 October 2014, 2014, from <http://www.solvayplastics.com/sites/solvayplastics/EN/Pages/SolvayPlastics.aspx>.
- Spada, F. and D. Basov (2000). "Fourier transform infrared investigation of thin perfluoropolyether films exposed to electric fields." Tribology Letters **8**(2-3): 179-186.
- Stevens, M. (1990). Polymer Chemistry: An Introduction. New York, Oxford University Press.
- Tan, S. C., E. Khor, et al. (1998). "The degree of deacetylation of chitosan: advocating the first derivative UV-spectrophotometry method of determination." Talanta **45**(4): 713-719.

- Tanaka, K., H. Waki, et al. (1988). "Protein and polymer analyses up to m/z 100 000 by laser ionization time-of-flight mass spectrometry." Rapid Communications in Mass Spectrometry **2**(8): 151-153.
- Tanaka, K., Yutaka, I., Akita, S. (1987). Detection of high mass molecules by laser desorption time-of-flight mass spectrometry. 2nd Japan-China Joint Symposium on Mass Spectrometry.
- Tetko, I. V., K.-W. Schramm, et al. (2014). "Experimental and Theoretical Studies in the EU FP7 Marie Curie Initial Training Network Project, Environmental ChemOinformatics (ECO)." Alternatives to Laboratory Animals **42**(1): 7-11.
- The European Parliament and the Council of the European Union (2006). Registration, Evaluation, Authorisation and Restriction of Chemicals (REACH). EC No. 1907/, The European Parliament and the Council of the European Union. **1907/**.
- The Royal Swedish Academy of Sciences. "Advanced information on the Nobel Prize in chemistry 2002." from nobelprize.org.
- Thongngam, M. and D. J. McClements (2004). "Characterization of Interactions between Chitosan and an Anionic Surfactant." Journal of Agricultural and Food Chemistry **52**(4): 987-991.
- Thurman, E. M., I. Ferrer, et al. (2014). "Analysis of Hydraulic Fracturing Flowback and Produced Waters Using Accurate Mass: Identification of Ethoxylated Surfactants." Analytical Chemistry **86**(19): 9653-9661.
- Tôei, K. and T. Kohara (1976). "A conductometric method for colloid titrations." Analytica Chimica Acta **83**(0): 59-65.
- Tonelli, C. A. P., A. Sergio, et al. (2013). Fluoropolyether phosphate derivatives, Google Patents.
- Trier, X. (2011). Polyfluorinated surfactants in food packaging of paper and board PhD, University of Copenhagen.
- Trier, X., K. Granby, et al. (2011). "Polyfluorinated surfactants (PFS) in paper and board coatings for food packaging." Environmental Science and Pollution Research **18**(7): 1108-1120.
- Trier, X., K. Granby, et al. (2011). "Tools to discover anionic and nonionic polyfluorinated alkyl surfactants by liquid chromatography electrospray ionisation mass spectrometry." Journal of Chromatography A **1218**(40): 7094-7104.
- Trimpin, S., P. Eichhorn, et al. (2001). "Recalcitrance of poly(vinylpyrrolidone): evidence through matrix-assisted laser desorption–ionization time-of-flight mass spectrometry." Journal of Chromatography A **938**(1–2): 67-77.
- Trombotto, S. p., C. Ladavière, et al. (2008). "Chemical Preparation and Structural Characterization of a Homogeneous Series of Chitin/Chitosan Oligomers." Biomacromolecules **9**(7): 1731-1738.
- Vadillo, D. C., A. Soucemarianadin, et al. (2009). "Dynamic contact angle effects onto the maximum drop impact spreading on solid surfaces." Physics of Fluids (1994-present) **21**(12): -.
- van den Hul, H. J. and J. W. Vanderhoff (1970). "Inferences on the mechanism of emulsion polymerisation of styrene from characterisation of the polymer end-groups." British Polymer Journal **2**(2): 121-127.
- Van Krevelen, D. W. and K. Te Nijenhuis (2009). Properties of polymers: Their correlation with chemical structure; their numerical estimation and prediction from additive group contribution Amsterdam, Elsevier.

- Vandeginste, B. G. M., D. L. Massart, et al. (1998). Handbook of Chemometrics and Qualimetrics: Part B, Elsevier.
- Vårum, K. M., M. H. Ottøy, et al. (1994). "Water-solubility of partially N-acetylated chitosans as a function of pH: effect of chemical composition and depolymerisation." Carbohydrate Polymers **25**(2): 65-70.
- Vishu Kumar, A. B. and R. N. Tharanathan (2004). "A comparative study on depolymerization of chitosan by proteolytic enzymes." Carbohydrate Polymers **58**(3): 275-283.
- Wallace, W. E., C. M. Guttman, et al. (1999). "Molecular structure of silsesquioxanes determined by matrix-assisted laser desorption/ionization time-of-flight mass spectrometry." Journal of the American Society for Mass Spectrometry **10**(3): 224-230.
- Wallace, W. E., C. M. Guttman, et al. (2000). "Polymeric silsesquioxanes: degree-of-intramolecular-condensation measured by mass spectrometry." Polymer **41**(6): 2219-2226.
- Wang, C., P. Ravi, et al. (2004). "Self-Assembly Behavior of Poly(methacrylic acid-block-ethyl acrylate) Polymer in Aqueous Medium: Potentiometric Titration and Laser Light Scattering Studies." The Journal of Physical Chemistry B **108**(5): 1621-1627.
- Wang, S., J. Huang, et al. (2013). "First Report of a Chinese PFOS Alternative Overlooked for 30 Years: Its Toxicity, Persistence, and Presence in the Environment." Environmental Science & Technology **47**(18): 10163-10170.
- Wang, W., S. Bo, et al. (1991). "Determination of the Mark-Houwink equation for chitosans with different degrees of deacetylation." International Journal of Biological Macromolecules **13**(5): 281-285.
- Wang, W. and D. Xu (1994). "Viscosity and flow properties of concentrated solutions of chitosan with different degrees of deacetylation." International Journal of Biological Macromolecules **16**(3): 149-152.
- Wang, Z., I. T. Cousins, et al. (2013). "Fluorinated alternatives to long-chain perfluoroalkyl carboxylic acids (PFCAs), perfluoroalkane sulfonic acids (PFSA) and their potential precursors." Environment International **60**(0): 242-248.
- Washington, J. W., J. E. Naile, et al. (2014). "Characterizing Fluorotelomer and Polyfluoroalkyl Substances in New and Aged Fluorotelomer-Based Polymers for Degradation Studies with GC/MS and LC/MS/MS." Environmental Science & Technology **48**(10): 5762-5769.
- Wei, H., K. Nolkrantz, et al. (2004). "Electrospray sample deposition for matrix-assisted laser desorption/ionization (MALDI) and atmospheric pressure MALDI mass spectrometry with attomole detection limits." Rapid Communications in Mass Spectrometry **18**(11): 1193-1200.
- Wetzel, S. J., C. M. Guttman, et al. (2004). "The influence of matrix and laser energy on the molecular mass distribution of synthetic polymers obtained by MALDI-TOF-MS." International Journal of Mass Spectrometry **238**(3): 215-225.
- Williams, J. B., A. I. Gusev, et al. (1997). "Characterization of Polyesters by Matrix-Assisted Laser Desorption Ionization Mass Spectrometry." Macromolecules **30**(13): 3781-3787.
- Williams, R. J. J., R. Erra-Balsells, et al. (2001). "UV-MALDI-TOF and ESI-TOF Mass Spectrometry Characterization of Silsesquioxanes Obtained by the Hydrolytic Condensation of (3-Glycidoxypropyl)- trimethoxysilane in an Epoxidized Solvent." Macromolecular Chemistry and Physics **202**(11): 2425-2433.

- Wold, S., M. Sjöström, et al. (2001). "PLS-regression: a basic tool of chemometrics." Chemometrics and Intelligent Laboratory Systems **58**(2): 109-130.
- Wong, C., M. P. So, et al. (1998). "Origins of the proton in the generation of protonated polymers and peptides in matrix-assisted laser desorption/ionization." European Journal of Mass Spectrometry **4**(3): 223-232.
- Woodgate, D. E. and J. A. Conquer (2003). "Effects of a Stimulant-Free Dietary Supplement on Body Weight and Fat Loss in Obese Adults: A Six-Week Exploratory Study." Current Therapeutic Research **64**(4): 248-262.
- Wydro, P., B. Krajewska, et al. (2007). "Chitosan as a Lipid Binder: A Langmuir Monolayer Study of Chitosan-Lipid Interactions." Biomacromolecules **8**(8): 2611-2617.
- Xia, W., P. Liu, et al. (2011). "Biological activities of chitosan and chitooligosaccharides." Food Hydrocolloids **25**(2): 170-179.
- Yalcin, T., Y. Dai, et al. (1998). "Matrix-assisted laser desorption/ionization time-of-flight mass spectrometry for polymer analysis: solvent effect in sample preparation." Journal of the American Society for Mass Spectrometry **9**(12): 1303-1310.
- Yalcin, T., D. Schriemer, et al. (1997). "Matrix-assisted laser desorption ionization time-of-flight mass spectrometry for the analysis of polydienes." Journal of the American Society for Mass Spectrometry **8**(12): 1220-1229.
- Yamamoto, A., H. Hisatomi, et al. (2014). "Use of high-resolution mass spectrometry to identify precursors and biodegradation products of perfluorinated and polyfluorinated compounds in end-user products." Analytical and Bioanalytical Chemistry **406**(19): 4745-4755.
- Yau, W. W. and S. W. Rementer (1990). "Polymer Characterization by SEC-Viscometry: Molecular Weight (MW), Size (Rg) and Intrinsic Viscosity (IV) Distribution." Journal of Liquid Chromatography **13**(4): 627-675.
- Yoon, H. J., M. E. Moon, et al. (2007). "Chitosan oligosaccharide (COS) inhibits LPS-induced inflammatory effects in RAW 264.7 macrophage cells." Biochemical and Biophysical Research Communications **358**(3): 954-959.
- Young, C. J., M. D. Hurley, et al. (2006). "Atmospheric Lifetime and Global Warming Potential of a Perfluoropolyether." Environmental Science & Technology **40**(7): 2242-2246.
- Yu, J., J. Hu, et al. (2009). "Perfluorooctane sulfonate (PFOS) and perfluorooctanoic acid (PFOA) in sewage treatment plants." Water Research **43**(9): 2399-2408.
- Zenobi, R. and R. Knochenmuss (1998). "Ion formation in MALDI mass spectrometry." Mass Spectrometry Reviews **17**(5): 337-366.
- Zhang, H., D. Zhang, et al. (2009). "Mass defect filter technique and its applications to drug metabolite identification by high-resolution mass spectrometry." Journal of Mass Spectrometry **44**(7): 999-1016.
- Zhou, K., W. Xia, et al. (2006). "In vitro binding of bile acids and triglycerides by selected chitosan preparations and their physico-chemical properties." LWT - Food Science and Technology **39**(10): 1087-1092.

ACKNOWLEDGEMENTS

First and foremost, I would like to extend my deepest gratitude to my dear supervisors and promoters, **Thomas P. Knepper** and **Pim de Voogt**, for trusting in my capabilities; for fully supporting me in my research tasks; and for continually inspiring me to do my best.

I whole-heartedly acknowledge the **European Commission** who supported and funded my doctoral works under the project Environmental Chemoinformatics. I am thankful to **Heike Weil** and **Eva Schlosser** for their full assistance.

I am grateful to my colleagues in IFAR - **Tobias Frömel, Marco Bernhard, Jutta Müller, Christoph Gremmel, Inge van Driezum** and **Sascha Klein**, for the technical support they have provided.

I appreciate the warm reception and the technical assistance extended to me by my colleagues and by the laboratory personnel of IBED, most especially **Christian Eschauzier, Chiara Cerli, Joke Westerveld, Rick Helmus, Frans van der Wielen, Peter Serne** and **Leo Hoitinga**.

I am thankful to my very good friends **Geoffrey Tan** and **Elliard Yanza** whom I can always rely on and who have been my travel companions in Germany and in Europe. Thank you too, to **Oui Buenafe** for always welcoming me in Leuven.

I greatly value the warmth and the hospitality of my relatives, *kasimanwa, kababayan* and friends in Germany: **Ritchie, Michael** and **Alex Fischer**; **Norma** and **Phil Aliberto**; **Patricia** and **Eberhard Kalb**; **Florida Weise, Flory Kowarzik, Jane Parma** and **Norma Usinger**; and my housemaster **Erich Kamann**.

I dedicate this research work (in part) in memory of the late **Ang Shiong An** whose generosity have enabled many students like me to dream bigger and bolder.

Finally, I extend a profound message of gratitude to **My Family and Loved Ones** who constantly prayed for my success and patiently waited for this wonderful moment.